

DDTime: Dataset Distillation with Spectral Alignment and Information Bottleneck for Time-Series Forecasting

Yuqi Li^{1*} Kuiye Ding^{1*} Chuanguang Yang^{2†} Hao Wang³
 Haoxuan Wang⁴ Huiran Duan¹ Junming Liu⁵ Yingli Tian^{1†}

¹The City University of New York, CUNY

²Institute of Computing Technology, Chinese Academy of Sciences

³Zhejiang University

⁴University of Illinois at Chicago

⁵Tongji University

Abstract

Time-series forecasting is fundamental across many domains, yet training accurate models often requires large-scale datasets and substantial computational resources. Dataset distillation offers a promising alternative by synthesizing compact datasets that preserve the learning behavior of full data. However, extending dataset distillation to time-series forecasting is non-trivial due to two fundamental challenges: ❶ temporal bias from strong autocorrelation, which leads to distorted value-term alignment between teacher and student models; and ❷ insufficient diversity among synthetic samples, arising from the absence of explicit categorical priors to regularize trajectory variety.

In this work, we propose DDTime, a lightweight and plug-in distillation framework built upon first-order condensation decomposition. To tackle **Challenge ❶**, it revisits value-term alignment through temporal statistics and introduces a frequency-domain alignment mechanism to mitigate autocorrelation-induced bias, ensuring spectral consistency and temporal fidelity. To address **Challenge ❷**, we further design an inter-sample regularization inspired by the information bottleneck principle, which enhances diversity and maximizes information density across synthetic trajectories. The combined objective is theoretically compatible with a wide range of condensation paradigms and supports stable first-order optimization. Extensive experiments on 20 benchmark datasets and diverse forecasting architectures demonstrate that DDTime consistently outperforms existing distillation methods, achieving about 30% relative accuracy gains while introducing about 2.49% computational overhead. All code and distilled datasets will be released.

*Equal Contribution.

†Corresponding Author.

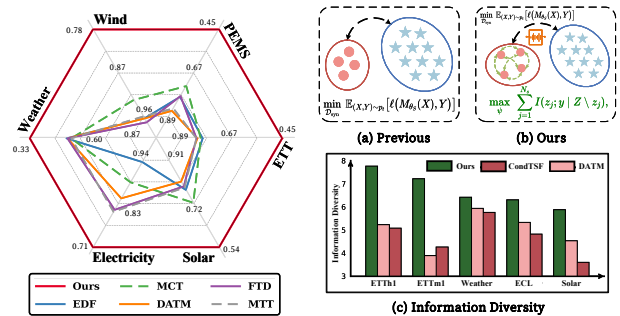


Figure 1. Left: Performance of DDTime. Average results (MSE) are reported following CondTSF [14], see details in Table 2. Right: (a)&(b): Unlike previous distillation frameworks that operate purely in the temporal domain, our method introduces frequency-domain alignment and diversity regularization to enrich synthetic samples. (c) Quantitative comparison of data diversity shows that our method achieves consistently higher diversity scores than CondTSF [14] and DATM [24].

1. Introduction

Recent advances in time-series forecasting (TSF) [1, 2, 13, 17, 23, 33, 47, 48] have been accompanied by a rapid growth in dataset scale, making model training and adaptation increasingly computationally demanding. Dataset distillation (DD) [61] provides an alternative approach by synthesizing compact datasets that preserve the learning behavior of models trained on full data, substantially reducing training time and memory consumption [36]. Although DD has demonstrated success in computer vision [10, 18, 57, 65] and graph [20, 70] domain, extending it to TSF is non-trivial [14, 34, 37] because time series data exhibit autocorrelation across time steps [15, 16, 63], temporal autocorrelation [55], and multi-scale temporal structures [25, 58, 59].

Recent progress in foundation models for TSF further highlights the need for specialized condensation frameworks that account for temporal statistics instead of treating sequences as independent samples.

A principled development in time-series data distillation is the first-order decomposition introduced by CondTSF [14], which reformulates the condensation objective into two complementary components: a parameter term that aligns the student and teacher in parameter space, and a value term that enforces consistency between their predictions. The core challenge, however, lies in the statistical structure of the labels. The temporal domain value term performs pointwise alignment between the student and teacher predictions. Such alignment mixes trend, seasonal, and high-frequency components within a single loss, which over-penalizes dependencies across forecasting horizons and consequently magnifies the bias in teacher–student consistency objectives [55]. In addition, unlike classification tasks where class labels inherently ensure diversity among synthetic examples [12, 21, 30, 60, 67], TSF lacks categorical priors, causing the synthetic trajectories to become redundant and thereby reducing their overall information density.

To address these challenges, we propose *DDTime*, a lightweight and plug-and-play framework for data distillation in TSF. As illustrated in Figure 1, *DDTime* incorporates frequency-domain alignment and diversity regularization to synthesize more informative and diverse trajectories. Building upon the first-order condensation decomposition established in prior work [14], *DDTime* revisits the value term from the perspective of label statistics. Specifically, we adapt frequency-domain alignment, which was originally employed in forecasting models to decorrelate horizon-wise dependencies for teacher–student alignment in data distillation. This design ensures spectral consistency while preserving fine-grained temporal fidelity [55].

Furthermore, motivated by the information bottleneck principle [52], *DDTime* introduces an inter-sample regularization that encourages diversity among synthetic trajectories. This design enhances the information density of the distilled dataset and compensates for the absence of explicit categorical priors in TSF [14, 37]. Because *DDTime* operates directly on the value-term optimization shared across different formulations, it is theoretically compatible with a wide range of dataset distillation paradigms. Within our design, the gradient term is instantiated through trajectory experts, making *DDTime* particularly effective when integrated into trajectory-matching based condensation methods where both terms are jointly optimized. While it can also be incorporated into other distillation paradigms that focus primarily on the value term, the performance gains are less pronounced, reflecting the complementary nature of the two-term formulation in time-series distillation.

Our contributions are as follows:

1. We refine the value term of time-series dataset distillation by introducing frequency-domain alignment, which mitigates horizon dependency bias and improves spectral consistency between teacher and student predictions.
2. We propose an inter-sample regularization strategy inspired by the information bottleneck principle to promote data diversity and increase information density within the synthetic dataset, compensating for the lack of categorical priors in time-series data.
3. We conduct comprehensive experiments across state-of-the-art TSF models on 20 benchmark datasets, demonstrating that our method consistently achieves strong performance and generalization. Although the theoretical decomposition is derived under simplified assumptions, our framework consistently exhibits robust empirical effectiveness and practical applicability across diverse architectures and datasets.

2. Related Work

Time-Series Forecasting (TSF). TSF aims to predict future values from historical temporal observations. Recent advances can be broadly categorized into three families: (1) *Transformer-based models*, which adapt attention mechanisms from NLP to temporal dependencies [2, 8, 15, 39, 63]; (2) *MLP-based models*, such as DLinear [68] and TimeMixer [58], which achieve competitive accuracy with simpler architectures; and (3) *Patch-based models*, which represent sequences as temporal patches for cross-patch interaction learning [16, 27, 33, 49, 51, 62]. Our framework intentionally accounts for the diversity of forecasting architectures and is designed to remain compatible with a wide range of TSF frameworks.

Dataset Distillation (DD). DD aims to synthesize a compact synthetic dataset that preserves the learning behavior of the original data. Existing methods can be grouped into three main classes. (1) *Coreset selection* [4, 9, 45, 54] selects representative subsets directly from real data. (2) *Matching-based approaches* minimize specific metrics between real and synthetic data, including gradient [26, 69, 73], feature or distribution [56, 60, 72, 74], and trajectory matching [5, 11, 18, 19, 24, 75]. (3) *Kernel-based methods* [29, 38] provide closed-form solutions via kernel ridge regression, simplifying the bilevel optimization problem.

Dataset Distillation for Time-Series Forecasting. Most existing DD studies focus on static domains [34, 44]. In contrast, TSF involves continuous-valued outputs and temporal dependencies, making direct extensions of image-based DD non-trivial. *CondTSF* [14] bridges this gap by introducing a one-line plugin that jointly enforces *value-term*

and *gradient-term* alignment between real and synthetic sequences, and can be integrated into parameter-matching-based distillation frameworks [5, 24, 57]. Another recent study [37] further investigates time-series distillation by aligning decomposed temporal patterns and matching long-term training trajectories through an expert buffer. Building on this direction, our work further explores the trajectory-matching paradigm to better capture the temporal optimization dynamics inherent in forecasting models.

3. Method

3.1. Problem Definition.

Let the real training set be $\mathcal{D}_{\text{real}} = \{(X_i, Y_i)\}_{i=1}^{N_r}$, where $X_i \in \mathbb{R}^{L \times d}$ is an input window (with context length L and d variables) and $Y_i \in \mathbb{R}^{T \times d}$ is the corresponding target segment (with prediction horizon T). We seek a compact synthetic set $\mathcal{D}_{\text{syn}} = \{(X_j^{(s)}, Y_j^{(s)})\}_{j=1}^{N_s}$ with $N_s \ll N_r$, and define the condensation ratio $r = N_s/N_r$. We use $\mathbb{E}[\cdot]$ to denote expectation w.r.t. the specified distribution and $\ell(\cdot, \cdot)$ to denote a per-sample forecasting loss.

Given a forecasting model $M_\theta : \mathbb{R}^{L \times d} \rightarrow \mathbb{R}^{T \times d}$, let the *teacher* parameters be obtained by training on $\mathcal{D}_{\text{real}}$:

$$\theta_T = \arg \min_{\theta} \mathbb{E}_{(X, Y) \sim p_r} [\ell(M_\theta(X), Y)], \quad (1)$$

and the *student* parameters by training on \mathcal{D}_{syn} :

$$\theta_S = \arg \min_{\theta} \mathbb{E}_{(X^{(s)}, Y^{(s)}) \sim p_s} [\ell(M_\theta(X^{(s)}), Y^{(s)})], \quad (2)$$

where p_r and p_s denote the distributions of real and synthetic data, respectively. Our ultimate objective is *test performance*: we want the student to perform well on the test distribution p_t ,

$$\min_{\mathcal{D}_{\text{syn}}} \mathbb{E}_{(X, Y) \sim p_t} [\ell(M_{\theta_S}(X), Y)]. \quad (3)$$

However, p_t (and thus Eq. (3)) is not directly optimizable during distillation.

Lemma 1 (First-order condensation decomposition [14])

Under a first-order Taylor approximation of M_θ around θ_T , and assuming Lipschitz continuity of ℓ , the intractable test objective in Eq. (3) can be upper-bounded by two optimizable terms that depend only on quantities available during condensation:

$$\begin{aligned} \mathbb{E}_{(X, Y) \sim p_t} [\ell(M_{\theta_S}(X), Y)] &\lesssim \underbrace{\|\theta_S - \theta_T\|^2}_{\text{Parameter Term}} \\ &+ \underbrace{\mathbb{E}_{X \sim p_s} [\ell(M_{\theta_S}(X^s), M_{\theta_T}(X^s))]}_{\text{Value Term}}. \end{aligned} \quad (4)$$

Where $\|\cdot\|$ is a suitable norm and the hidden constants depend on the local Lipschitz smoothness of M_θ and ℓ .

The distillation objective in Eq. (3) is intractable to optimize directly, since p_t is inaccessible during condensation, **Lemma 1** resolves this intractability via a first-order linearization of M_θ , transforming the implicit test-level goal into two explicit, optimizable terms:

- (1) **Parameter Term**: aligns the student and teacher parameters, encouraging similar optimization end points.
- (2) **Value Term**: enforces prediction consistency on synthetic-data inputs p_s .

Remark. Following [14], the originally introduced *Gradient Term* can be upper-bounded by the parameter discrepancy $|\theta_S - \theta_T|^2$ under a local linearity assumption; thus, our *Parameter Term* serves as its practical surrogate.

Together, these terms replace the unavailable test objective in Eq. (3), enabling optimization within the training process while approximating test-level generalization.

Implementation. We refer to M_{θ_T} trained on $\mathcal{D}_{\text{real}}$ as the *teacher* and M_{θ_S} trained on \mathcal{D}_{syn} as the *student*. In practice, the *Parameter Term* can be optimized by aligning trajectories or final weights against a fixed teacher, while the *Value Term* is optimized by matching teacher–student predictions on inputs drawn from p_r (or minibatches thereof). The *Parameter Term* follows the implementation of CondTSF [14], which adopts a parameter trajectory alignment strategy, formulated as

$$\mathcal{L}_P = \min_{\text{expert}} \frac{\|\theta_S - \theta_T^{(e)}\|_2^2}{\|\theta_T^{(e)} - \theta_T^{(0)}\|_2^2}, \quad (5)$$

where θ_S denotes the student parameters trained on the synthetic dataset \mathcal{D}_{syn} , $\theta_T^{(0)}$ and $\theta_T^{(e)}$ represent the initial and final parameters of a teacher model trained on real data, respectively, and *expert* indicates the selection among multiple stored teacher trajectories. Our method serves as a lightweight plugin that can be plugged into various trajectory matching frameworks [5, 11, 75]. The detailed procedure is provided in Appendix C.

3.2. Revisiting the Value Term from Frequency

The *Value Term* in Lemma 1 enforces output consistency between the student and the teacher on real inputs:

$$\mathcal{L}_{\text{val}}^{\text{tmp}} = \mathbb{E}_{X \sim p_s} [\ell(M_{\theta_S}(X), M_{\theta_T}(X))]. \quad (6)$$

While this formulation aligns predictions in the temporal domain, it overlooks the fact that temporal signals are composed of multiple oscillatory components. As a result, purely time-domain matching may blur periodic structures and amplify the bias of direct forecasting (DF), especially when future steps are autocorrelated.

This phenomenon, termed *label autocorrelation bias* [50, 55], arises when future labels exhibit strong temporal correlation, causing the learning objective of direct

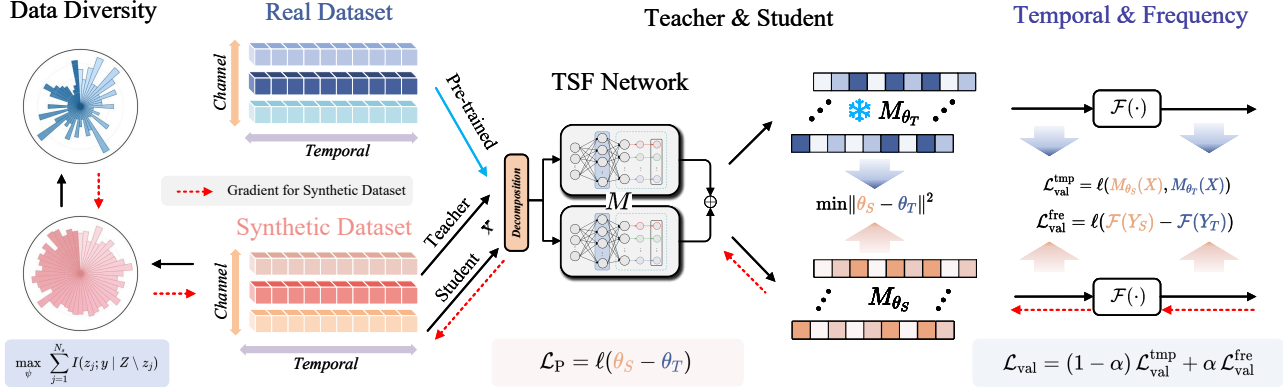


Figure 2. Overall framework of the proposed *DDTime*. The framework consists of three key components: (i) a Data Diversity module that enhances inter-sample diversity by increasing the pairwise KL divergence among synthetic sequences, the rose plots on the left visualize the KL divergence magnitude of each sample as a sector, (ii) a Teacher–Student paradigm that enforces parameter matching between learners trained on real and synthetic data, and (iii) a joint Temporal–Frequency Alignment loss that balances time-domain and spectral-domain supervision via the weighting coefficient α . The TSF network illustrated is the sDLinear architecture [68]. Here, $\mathcal{F}(\cdot)$ denotes the discrete Fourier transform (DFT).

forecasting to be biased toward redundant or low-frequency components. Such bias limits the model’s ability to represent diverse temporal dynamics, motivating our frequency domain reformulation of the value term. Forecasting in the frequency domain has been shown to alleviate such bias by decorrelating future-step dependencies as the frequency representation exposes periodic and trend components that are difficult to model directly in the temporal domain.

Lemma 2 (Decorrelation Property of FFT [55]) *Let Y be a zero-mean wide-sense stationary process and $\mathcal{F}(Y)$ its discrete Fourier transform. As the sequence length $T \rightarrow \infty$, different frequency components become asymptotically uncorrelated:*

$$\mathbb{E}[F_k F_{k'}^*] = \begin{cases} S_Y(f_k), & \text{if } k = k', \\ 0, & \text{if } k \neq k', \end{cases}$$

where $S_Y(f_k)$ denotes the power spectral density of Y . This whitening effect implies that FFT serves as an orthogonal transformation that diagonalizes the label covariance, thereby removing temporal dependencies among future steps.

Leveraging this property, we define the *frequency-domain value term* by aligning teacher and student predictions in the decorrelated spectral space:

$$\mathcal{L}_{\text{val}}^{\text{fre}} = \mathbb{E}_{X \sim p_s} [\|\mathcal{F}(Y_S) - \mathcal{F}(Y_T)\|_1], \quad (7)$$

where $Y_S = M_{\theta_S}(X)$ and $Y_T = M_{\theta_T}(X)$. The FFT acts as a whitening transform that mitigates label autocorrelation bias, yielding a more balanced objective across frequency components.

Since the FFT is differentiable and can be optimized via gradient descent [77], we combine the temporal and frequency domain terms using a trade-off coefficient $\alpha \in [0, 1]$:

$$\mathcal{L}_{\text{val}} = \mathbb{E}_{X \sim p_s} \left[(1 - \alpha) \|Y_S - Y_T\|_2^2 + \alpha \|\mathcal{F}(Y_S) - \mathcal{F}(Y_T)\|_1 \right]. \quad (8)$$

This formulation preserves temporal fidelity while enhancing spectral consistency, thereby mitigating DF bias and stabilizing training.

3.3. Maximizing Information Density via Inter-Sample Information Bottleneck (ISIB)

The existing distillation method [14] for time-series forecasting focuses on aligning the student with the teacher but overlooks the relationships among synthetic samples. This omission leads to redundant trajectories that share similar temporal or spectral patterns, thereby reducing the overall information density, that is, the amount of non-redundant and task-relevant information encoded per synthetic sample. A low-density synthetic dataset covers only limited temporal modes and weakens the student’s generalization.

Motivation. From an information-theoretic view [42, 52], an effective synthetic dataset should contain sufficient information about the real distribution p_r while minimizing internal redundancy. Let $I(X_i^{(s)}; X_j^{(s)})$ denote the mutual information between two synthetic samples. When this value is large, the dataset encodes repetitive content. We therefore seek to maximize the overall task-relevant information while minimizing pairwise redundancy, following the sufficiency–orthogonality principle in [3].

Dataset-level Information Bottleneck. We extend the

Local-Global Information Loss framework [3] from intra-sample features to inter-sample relations within \mathcal{D}_{syn} . Let $z_j = f_\psi(X_j^{(s)}, Y_j^{(s)})$ be the latent representation of each synthetic pair, and $Z = \bigoplus_{j=1}^{N_s} z_j$ the joint synthetic representation. Each z_j should be both sufficient for the forecasting task and complementary to the others. The theoretical objective can be expressed as

$$\max_{\psi} \sum_{j=1}^{N_s} I(z_j; y \mid Z \setminus z_j), \quad (9)$$

where y denotes the target variable from the real distribution. To approximate this objective, we compute a smooth inverse weighting of the symmetric Kullback-Leibler divergence [64] between the normalized probability representations of synthetic samples. For each synthetic sample i , we obtain a temperature-scaled softmax distribution $p_i = \text{softmax}(x_i/\tau)$, and define

$$\mathcal{L}_{\text{IS}} = \frac{1}{S(S-1)} \sum_{i < j} \frac{1}{2} (\text{KL}[p_i \| p_j] + \text{KL}[p_j \| p_i]). \quad (10)$$

This symmetric KL divergence penalizes redundant information and promotes diversity among synthetic samples. Minimizing \mathcal{L}_{IS} encourages each sample to contribute unique information and increases the overall information density of \mathcal{D}_{syn} . Eq. (9) measures the marginal contribution of each synthetic sample to the overall task-relevant information, conditioned on the others. We normalize each synthetic sample via a temperature-scaled softmax, ensuring comparable probability mass functions across samples and avoiding scale sensitivity.

Implementation. For numerical stability and smoother gradients, we use a monotone surrogate that *decreases* with divergence, minimizing $\frac{1}{S(S-1)} \sum_{i < j} \exp(-\lambda_{\text{div}} \cdot \frac{1}{2} (\text{KL}[p_i \| p_j] + \text{KL}[p_j \| p_i]))$ in practice, where $\lambda_{\text{div}} > 0$ is a tunable coefficient. The value of λ_{div} is set to 0.5.

Global Bottleneck. Finally, a global aggregation module $G = g_\phi(Z)$ acts as an information bottleneck, retaining task-relevant content while suppressing redundancy:

$$\mathcal{L}_G = \mathbb{E}_{G \sim E_\phi(G|Z)} [\text{KL}[P_Z \| P_G]]. \quad (11)$$

In practice \mathcal{L}_G is optimized implicitly via shared parameters between f_ψ rather than added as an explicit regularizer.

3.4. Overall Training Objective

The overall optimization pipeline is illustrated in Figure 2. Our distillation framework integrates the previously defined Parameter Term, frequency-aware Value Term, and Inter-Sample Information Bottleneck into a unified objective:

$$\mathcal{L}_{\text{total}} = \mathcal{L}_P + (1 - \alpha) \mathcal{L}_{\text{val}}^{\text{tmp}} + \alpha \mathcal{L}_{\text{val}}^{\text{fre}} + \lambda_{\text{IS}} \mathcal{L}_{\text{IS}} + \mathcal{L}_G. \quad (12)$$

Here, λ_{IS} , and α are global balancing coefficients, while α controls the trade-off between temporal fidelity and frequency consistency as introduced in Sec. 3.2. The \mathcal{L}_{IS} enhance inter-sample diversity.

4. Experiment

4.1. Setup

Datasets. We conduct experiments on twenty benchmark datasets, including ETT (ETTh1, ETTh2, ETTm1, ETTm2) [76], Weather [76], Traffic [41], Electricity [53], Exchange-rate [28], Solar-energy [58], PEMS (03, 04, 07, 08) [41], ILI [6], Wind (L1-L4) [15], Wike2000 [43], and GlobalTemp [48]. The dataset loading, preprocessing, and evaluation benchmarks follow the experimental settings of CondTSF [14].

Baseline. We evaluate DDTime with two groups of baselines. *Dataset distillation frameworks:* We include representative distillation methods originally designed for image classification, including EDF [57], MCT [75], DATM [24], PP [31], IDM [74], FRePo [35], KIP [38], DC [73], DSA [71], MTT [5], TESLA [11], and FTD [18], as well as CondTSF [14], which is specifically developed for time-series forecasting. *Time-series forecasting models:* We conduct experiments across diverse TSF architectures, including SimpleTM [7], xPatch [49], FreTS [66], DLinear [68], PatchTST [39], iTransformer [32], CNN [14], MLP [14] and LSTM [14]. These models collectively cover common TSF paradigms such as decomposition, multi-scale learning, wavelet and frequency-domain analysis, as well as patch-based modeling, encompassing a wide spectrum of architectures including Transformers, CNNs, MLPs, and LSTMs.

Metrics. We use mean squared error (MSE) and mean absolute error (MAE) as evaluation metrics for TSF, following CondTS [14] and iTransformer [32].

Implementation Details. All methods are implemented in PyTorch [40] and trained on a single NVIDIA RTX 5090 GPU. All time-series datasets are standardized and split into training, validation, and test sets with a ratio of 70%, 15%, and 15%, respectively. We follow the unified sliding-window preprocessing adopted in prior work [14], where the input and prediction lengths are set to $T_{\text{in}} = 24$ and $T_{\text{out}} = 24$. Each synthetic sequence \mathbf{X}_{syn} is optimized via differentiable distillation. For a fair comparison with the original [14], we adopt its best-reported hyperparameter settings, where the distillation interval is set to 5 and the conditional update coefficient to 0.01.

The learning rate for student parameters is set to 3×10^{-4} , and the learning rate for synthetic data updates is 0.1. During distillation, expert trajectories are reconstructed from the teacher network’s replay buffers, and random trajectory segments are sampled for imitation. The student

Table 1. Results of DDTime on five datasets. All values are averaged over five runs; lower MSE indicate better performance.

Dataset SynTS Count Ratio (%)	Weather			Electricity			Solar-Energy			ExchangeRate			PEMS03		
	3	5	20	3	5	20	3	5	20	3	5	20	3	5	20
Random	0.1	0.2	0.65	0.2	0.3	1.3	0.1	0.2	0.65	0.68	1.10	4.6	0.2	0.3	1.3
DC	0.75±0.07	0.76±0.10	0.70±0.03	1.11±0.07	1.21±0.15	1.15±0.03	0.95±0.03	0.94±0.04	1.04±0.05	1.31±0.16	1.27±0.13	1.34±0.20	0.99±0.08	0.98±0.05	0.88±0.09
KIP	0.63±0.07	0.61±0.04	0.63±0.02	1.08±0.14	1.07±0.10	1.14±0.06	0.93±0.08	0.85±0.04	0.93±0.02	1.28±0.09	1.20±0.18	1.05±0.20	0.91±0.09	0.83±0.07	0.84±0.05
MTT	0.73±0.06	0.68±0.05	0.68±0.04	1.04±0.05	1.19±0.11	1.11±0.10	0.85±0.06	0.90±0.04	0.87±0.06	0.95±0.06	0.92±0.09	1.45±0.12	0.89±0.07	1.08±0.08	0.81±0.05
FRPo	0.56±0.01	0.55±0.02	0.50±0.01	0.80±0.01	0.82±0.01	0.81±0.02	0.73±0.02	0.79±0.02	0.80±0.01	0.66±0.05	0.60±0.02	0.70±0.09	0.91±0.01	0.91±0.01	0.79±0.03
IDM	0.54±0.02	0.55±0.02	0.53±0.02	1.02±0.06	1.02±0.05	0.92±0.04	0.69±0.03	0.67±0.04	0.78±0.03	1.10±0.24	1.02±0.07	0.90±0.07	0.69±0.02	0.84±0.05	0.64±0.04
TESLA	0.69±0.04	0.63±0.03	0.67±0.07	1.07±0.08	1.04±0.06	1.08±0.13	1.01±0.05	0.94±0.04	0.90±0.05	1.20±0.08	1.28±0.17	1.37±0.05	0.91±0.07	0.95±0.11	0.82±0.04
PP	0.52±0.02	0.56±0.01	0.57±0.02	0.98±0.05	1.07±0.01	1.07±0.02	0.80±0.01	0.74±0.01	0.82±0.06	0.91±0.15	0.89±0.12	0.97±0.06	0.78±0.04	0.74±0.02	0.73±0.03
FTD	0.49±0.01	0.57±0.00	0.52±0.01	0.88±0.02	0.81±0.03	0.84±0.03	0.86±0.01	0.80±0.01	0.80±0.01	0.72±0.03	1.00±0.08	0.70±0.06	0.86±0.01	0.87±0.02	0.82±0.02
DATM	0.53±0.02	0.55±0.01	0.52±0.01	0.81±0.02	0.81±0.02	0.82±0.01	0.74±0.02	0.84±0.01	0.77±0.02	0.98±0.06	0.86±0.05	0.75±0.06	0.78±0.02	0.75±0.02	0.76±0.02
MCT	0.51±0.01	0.48±0.02	0.56±0.01	0.86±0.02	0.81±0.02	0.86±0.02	0.84±0.01	0.81±0.02	0.79±0.01	0.83±0.03	1.04±0.08	0.71±0.05	0.84±0.04	0.86±0.05	0.74±0.05
EDF	0.64±0.05	0.51±0.03	0.48±0.01	0.90±0.03	0.84±0.06	0.90±0.03	0.73±0.02	0.72±0.01	0.74±0.01	1.01±0.11	0.93±0.12	0.99±0.12	0.72±0.05	0.70±0.04	0.80±0.08
DDTime (Ours)	0.50±0.01	0.59±0.01	0.50±0.01	0.86±0.04	0.86±0.04	1.01±0.03	0.77±0.04	0.78±0.01	0.79±0.03	0.90±0.05	0.96±0.03	0.71±0.05	0.72±0.02	0.69±0.03	0.69±0.01
Whole Dataset		0.21±0.00			0.60±0.02			0.45±0.01			0.50±0.07			0.21±0.00	

model is updated for twenty gradient steps on the synthetic data at each iteration. Model performance is evaluated every fifty iterations and averaged over 5 random seeds to ensure stability.

Table 2. Results of DDTime on 15 datasets, including ETTh1, ETTh2, ETTm1, ETTm2, PEMS03, PEMS04, PEMS07, PEMS08, WindL1, WindL2, WindL3, WindL4, Weather, Electricity, Solar dataset. Lower MSE/MAE indicate better performance.

Models	DDTime Ours		EDF [2025]		MCT [2025]		DATM [2024]		FTD [2023]		MTT [2022]	
	MSE	MAE	MSE	MAE	MSE	MAE	MSE	MAE	MSE	MAE	MSE	MAE
ETT (all)	0.448	0.470	0.796	0.686	0.804	0.691	0.819	0.705	0.823	0.702	0.823	0.701
PEMS (all)	0.454	0.531	0.792	0.736	0.738	0.709	0.862	0.773	0.788	0.739	0.850	0.774
Wind (all)	0.776	0.698	0.959	0.800	0.921	0.779	0.959	0.804	0.967	0.808	0.955	0.803
Weather	0.330	0.373	0.525	0.510	0.550	0.518	0.530	0.510	0.530	0.518	0.550	0.528
Electricity	0.715	0.683	0.938	0.775	0.885	0.758	0.843	0.748	0.813	0.730	0.808	0.730
Solar	0.535	0.598	0.780	0.733	0.725	0.698	0.815	0.765	0.795	0.750	0.790	0.745

4.2. Main Results

Although our method is implemented as a plugin rather than an independent distillation framework, it can be flexibly integrated into different trajectory matching paradigms. Specifically, for datasets including ETT (ETTh1, ETTh2, ETTm1, ETTm2) [76], Wind [15], Wike2000 [43], Weather [76], Traffic [41], ILI [6], PEMS03 [41], and PEMS07 [41], we adopt DATM [24] as the base distillation method. For Electricity, Solar, ExchangeRate, and PEMS04, we use FTD, and for GlobalTemp and PEMS08, we employ MTT. All three frameworks, namely DATM, FTD, and MTT, belong to the trajectory matching family, which aligns optimization trajectories between real and synthetic datasets. This flexible configuration allows our plugin to be consistently evaluated under a unified trajectory based condensation paradigm while adapting to the characteristics of each dataset. The comparison results with other models in terms of average performance are shown in Table 1 and Table 2, and more detailed results with additional distillation methods are provided in Appendix Table 16.

Result Analysis. As shown in Table 1 and Table 2, our method consistently achieves superior results compared to existing dataset distillation approaches, using DLinear [68]

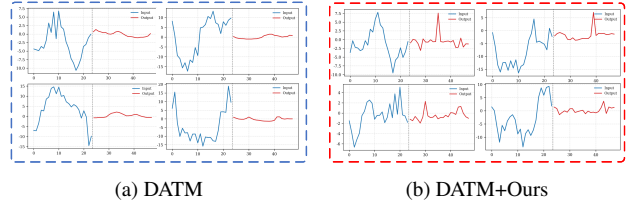


Figure 3. Visualization of synthetic time-series samples generated by DATM and DATM+Ours on the Electricity dataset. The horizontal-axis shows time step, the vertical-axis shows normalized time-series values; blue and red lines indicate inputs and outputs. DATM+Ours produces label segments with richer periodic structures and more natural local oscillations.

as the forecasting backbone. Unlike image classification distillation, where the target is to reach 100% classification accuracy, TSF distillation has no well-defined notion of “optimal” performance, since achieving zero prediction error is practically impossible due to the intrinsic stochasticity and temporal uncertainty of real-world signals.

Interestingly, as reported in Appendix Table 16, several datasets such as ExchangeRate, ILI, ETTh2, PEMS04, and PEMS07 even allow distilled subsets to surpass the models trained on their full datasets when the synthetic samples are carefully optimized. This observation aligns with recent findings [46] that modern time-series benchmarks contain substantial redundancy and noise. Consequently, a compact synthetic set that preserves diverse temporal modes can sometimes outperform the full training set by providing cleaner, more representative supervision signals.

Runtime and Memory Efficiency. We further evaluate the computational overhead of our framework, and detailed results are reported in Appendix I. Overall, our method is on average 2.59% faster than the baseline, with GPU memory usage increasing by only 2.49%. The acceleration mainly stems from faster convergence, as the introduced frequency-domain alignment stabilizes optimization and the diversity regularization provides more informative synthetic samples, enabling efficient learning with minimal additional cost.

Visualization of Samples. Figure 3 visualizes the synthetic time-series samples generated by DATM and

Table 3. Average MSE/MAE performance across four datasets (*Weather*, *Electricity*, *Solar*, and *Exchange*), averaged over four synthetic sample settings (3, 5, 10, and 20). Detailed results are provided in Appendix Table 21.

Models	DATM [2024]		FTD [2023]		PP [2023]		MTT [2022]	
	MSE	MAE	MSE	MAE	MSE	MAE	MSE	MAE
Baseline	0.75	0.70	0.74	0.69	0.75	0.70	0.75	0.69
+TFA	0.63	0.63	0.62	0.63	0.65	0.64	0.64	0.63
+TFA & +ISIB	0.49	0.54	0.50	0.55	0.53	0.57	0.53	0.57

DATM+Ours. The baseline DATM exhibits a strong smoothness bias in the label trajectories, producing sequences with suppressed temporal variance and limited high-frequency components, which leads to a loss of realistic temporal dynamics. In contrast, DATM+Ours generates label segments with richer periodic structures and more natural local oscillations, closely resembling the frequency and amplitude patterns observed in real data. Furthermore, the synthetic samples from DATM+Ours demonstrate higher distributional diversity across sequences, indicating improved fidelity and generalization potential of the distilled dataset. See more details in Appendix Table 9.

4.3. Ablation Experiment

Our method is composed of two modules: the Temporal-Frequency Alignment (TFA) module and the Inter-Sample Information Bottleneck (ISIB) module. As summarized in Table 3, incorporating either TFA or ISIB into different distillation frameworks consistently enhances the forecasting performance compared with the baseline.

Specifically, TFA aligns temporal and frequency representations to stabilize trajectory-level consistency between synthetic and real data, while ISIB encourages inter-sample diversity by suppressing redundant correlations among synthesized sequences. In the reported results, the hyperparameters are fixed as $\alpha = 0.8$ for TFA and $\lambda_{IS} = 0.6$ for ISIB. We deliberately keep α and λ_{IS} constant in the main text to ensure experimental consistency and avoid cherry picking. Even under this conservative setting, the combined use of TFA and ISIB achieves the lowest overall MAE across most frameworks, confirming that the two modules complement each other in enhancing the representational quality and diversity of distilled time-series data.

4.4. Qualitative Analysis

Qualitative Analysis of Frequency Domain Label Loss.

To illustrate the impact of frequency-domain alignment, Figure 5 visualizes the distribution of the Best and Second Best results across different datasets and sample sizes. In all four datasets, the frequency-aligned variant consistently occupies a larger proportion of the Best and Second Best

Table 4. Extended ablation average results across four benchmark datasets (ETTh1, ETTh2, ETTm1, ETTm2) under different synthetic sample sizes. Green rows denote results of each method augmented with *CondTSF*, and the blue rows denote results augmented with our proposed method. All values are averaged over five runs; lower MSE/MAE indicate better performance.

Models	EDF [2025]		MCT [2025]		DATM [2024]		FTD [2023]		MTT [2022]	
	MSE	MAE	MSE	MAE	MSE	MAE	MSE	MAE	MSE	MAE
ETTh1	0.875	0.700	0.973	0.740	0.830	0.700	0.883	0.705	0.885	0.705
CondTSF[14]	0.860	0.693	0.978	0.743	0.835	0.678	0.823	0.673	0.818	0.673
DDTime	0.838	0.678	0.913	0.713	0.688	0.598	0.723	0.615	0.715	0.608
↓ (%)	4.23%	3.14%	6.17%	3.65%	17.11%	14.57%	18.12%	12.77%	19.21%	13.76%
ETTh2	0.665	0.648	0.793	0.705	0.780	0.703	0.750	0.695	0.713	0.673
CondTSF[14]	0.650	0.648	0.763	0.690	0.653	0.645	0.635	0.638	0.573	0.603
DDTime	0.540	0.583	0.633	0.630	0.260	0.385	0.303	0.425	0.275	0.400
↓ (%)	18.80%	10.03%	20.18%	10.64%	66.67%	45.23%	59.60%	38.85%	61.43%	40.56%
ETTh1	0.855	0.688	0.808	0.673	0.870	0.700	0.888	0.708	0.888	0.708
CondTSF[14]	0.780	0.653	0.748	0.630	0.750	0.638	0.777	0.650	0.760	0.643
DDTime	0.735	0.625	0.718	0.593	0.650	0.563	0.683	0.585	0.678	0.588
↓ (%)	14.04%	9.16%	11.14%	11.89%	25.29%	19.57%	23.09%	17.37%	23.65%	16.95%
ETTh2	0.790	0.710	0.643	0.645	0.798	0.718	0.773	0.700	0.805	0.720
CondTSF[14]	0.505	0.573	0.385	0.498	0.493	0.565	0.513	0.575	0.488	0.563
DDTime	0.450	0.538	0.188	0.333	0.193	0.335	0.218	0.365	0.223	0.370
↓ (%)	43.04%	24.23%	70.76%	48.37%	75.81%	53.34%	71.80%	47.86%	72.30%	48.61%

cells than the original method. This pattern holds under various sample scales ($S = 3, 5, 10, 20$), demonstrating that incorporating frequency domain label loss promotes more stable and globally superior performance through improved teacher-student consistency in the spectral space. See more details in Appendix E.

Qualitative Analysis of Data Diversity Loss.

Figure 4 illustrates the sensitivity of different distillation baselines after integrating our ISIB-regularization. The coefficient λ_{IS} controls the strength of the data diversity loss, balancing inter-sample dissimilarity and forecasting performance during distillation. For clarity, the curves are smoothed using the Savitzky-Golay filter [22], while the raw (unsmoothed) results are provided in Appendix Figure 8. As λ_{IS} increases from 0.1 to 1.0, all methods show a clear trade-off: a small value causes redundant synthetic samples, whereas a large value induces excessive dispersion and temporal incoherence. Across datasets, most methods achieve stable performance within $\lambda_{IS} \in [0.4, 0.8]$, indicating that our method functions as a plug-in module that can be directly inserted into existing distillation frameworks without extensive tuning of λ_{IS} . We fix $\lambda_{IS} = 0.6$ in other experiments.

Effect of the number of synthetic samples.

Figure 6 presents the sensitivity of model performance to the number of synthetic samples. Performance steadily improves as the sample number increases from 2 to about 20, since the larger set captures more diverse and representative temporal patterns. Beyond this point, performance declines: our approach explicitly enlarges inter-sample differences, and this objective becomes difficult to satisfy when the synthetic set grows excessively, making the optimization harder to converge. These results suggest that a moderate number of syn-

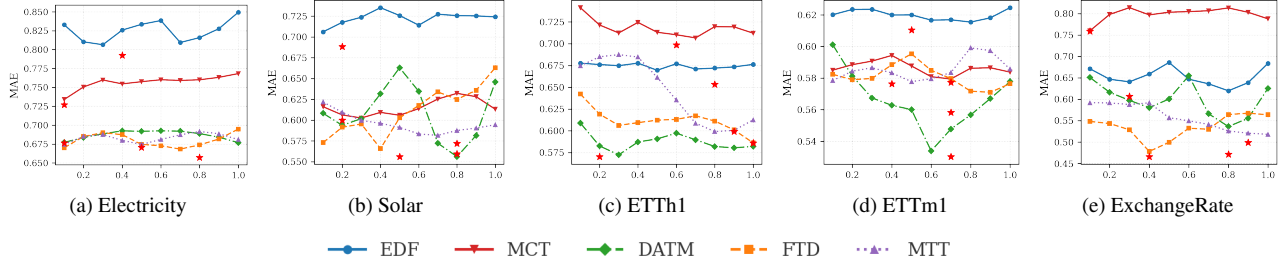


Figure 4. Parameter sensitivity analysis of different distillation baselines integrated with our ISIB-regularization. The coefficient λ_{IS} controls the strength of the data diversity loss in our method. Each curve shows how the forecasting error (MAE) changes with varying λ_{IS} ; curves are smoothed for clarity, and the optimal points are highlighted with red stars.

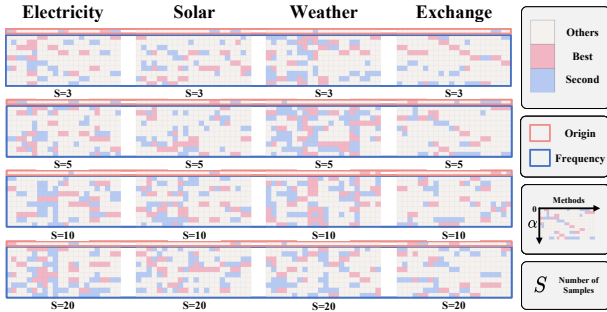


Figure 5. Visualization of Best (pink) and Second Best (blue) results across four representative datasets. Each block represents a specific sample size setting ($S = 3, 5, 10, 20$). Red-bordered regions correspond to the original method, while blue-bordered regions show the results of our frequency domain alignment variant. Gray cells indicate remaining cases.

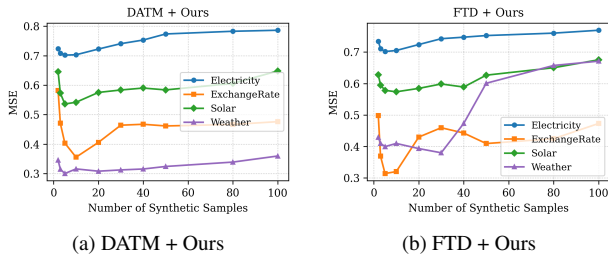


Figure 6. Sensitivity analysis of model performance with respect to the number of synthetic samples. Each curve corresponds to a dataset (Electricity, ExchangeRate, Solar, and Weather), and illustrates how forecasting MSE changes as the sample numbers increases. See detail in Appendix Table 10.

thetic samples is sufficient to capture key temporal dynamics while ensuring stable and efficient training.

Comparison with Plugin-based Methods. As shown in Table 4, both *CondTSF* and our method can serve as generic plugins to existing distillation frameworks. Our plugin consistently achieves better performance across most datasets and baselines, validating its superior compatibil-

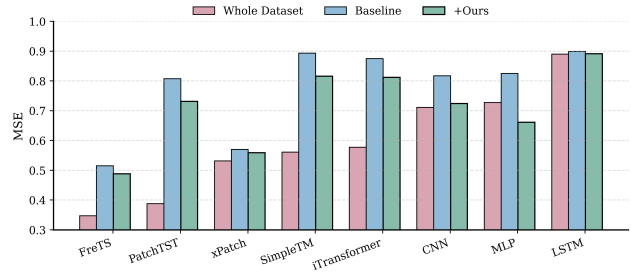


Figure 7. Distillation performance across different forecasting architectures. See more details in Appendix Sec G.

ity and optimization stability. Extended comparisons on broader datasets and methods are reported in Appendix Tables 11, 12, 13, 14 and 15. For ILI and Wike2000, however, both plugins perform relatively poorly due to the low predictability and weak temporal regularities inherent in these datasets.

Different Architectures. The theoretical foundation of our framework is derived under a first-order approximation with a shared model architecture and differentiable forecasting dynamics. When the backbone changes, the equality becomes approximate, but the alignment between the value term and gradient term remains practically effective. As shown in Figure 7, our method consistently outperforms baseline methods across diverse architectures, indicating that the proposed objective remains its effectiveness and generality throughout different forecasting frameworks.

5. Conclusion

We introduced a dataset distillation framework for time-series forecasting (TSF) that jointly aligns value and gradient terms under a first-order optimization scheme. The method effectively condenses temporal dynamics while preserving essential forecasting behavior. Extensive experiments across diverse datasets and architectures demonstrate consistent improvements over baseline methods, confirming the generality and robustness of the proposed objective. The

framework provides a unified perspective for understanding and advancing data condensation in temporal learning, as well as inspires further research into the emerging and impactful area of dataset distillation for TSF.

References

- [1] Taha Aksu, Gerald Woo, Juncheng Liu, Xu Liu, Chenghao Liu, Silvio Savarese, Caiming Xiong, and Doyen Sahoo. Gift-eval: A benchmark for general time series forecasting model evaluation. *arXiv preprint arxiv:2410.10393*, 2024. 1
- [2] Abdul Fatir Ansari, Lorenzo Stella, Caner Turkmen, Xiyuan Zhang, Pedro Mercado, Huibin Shen, Oleksandr Shchur, Syama Syndar Rangapuram, Sebastian Pineda Arango, Shubham Kapoor, Jasper Zschiegner, Danielle C. Maddix, Michael W. Mahoney, Kari Torkkola, Andrew Gordon Wilson, Michael Bohlke-Schneider, and Yuyang Wang. Chronos: Learning the language of time series. *Transactions on Machine Learning Research (TMLR)*, 2024. 1, 2
- [3] Zhongjie Ba, Qingyu Liu, Zhengguang Liu, Shuang Wu, Feng Lin, Li Lu, and Kui Ren. Exposing the deception: Uncovering more forgery clues for deepfake detection. *AAAI*, 2024. 4, 5
- [4] Olivier Bachem, Mario Lucic, and Andreas Krause. Practical coresets constructions for machine learning. *arXiv preprint arXiv:1703.06476*, 2017. 2
- [5] George Cazenavette, Tongzhou Wang, Antonio Torralba, Alexei A Efros, and Jun-Yan Zhu. Dataset distillation by matching training trajectories. In *CVPR*, 2022. 2, 3, 5, 6, 7, 20, 21, 22, 23, 24, 25, 26, 27, 28, 29, 30
- [6] CDC. Illness. <https://gis.cdc.gov/grasp/fluview/fluportal-dashboard.html>. 5, 6
- [7] Hui Chen, Viet Luong, Lopamudra Mukherjee, and Vikas Singh. SimpleTM: A simple baseline for multivariate time series forecasting. In *ICLR*, 2025. 5
- [8] Peng Chen, Yingying Zhang, Yunyao Cheng, Yang Shu, Yihang Wang, Qingsong Wen, Bin Yang, and Chenjuan Guo. Pathformer: Multi-scale transformers with adaptive pathways for time series forecasting. In *International Conference on Learning Representations (ICLR)*, 2024. 2
- [9] Yutian Chen, Max Welling, and Alex Smola. Super-samples from kernel herding. *arXiv preprint arXiv:1203.3472*, 2012. 2
- [10] Justin Cui, Ruochen Wang, Si Si, and Cho-Jui Hsieh. DC-BENCH: Dataset condensation benchmark. In *Proceedings of the Advances in Neural Information Processing Systems (NeurIPS)*, 2022. 1
- [11] Justin Cui, Ruochen Wang, Si Si, and Cho-Jui Hsieh. Scaling up dataset distillation to imagenet-1k with constant memory. In *ICML*, 2023. 2, 3, 5, 20, 21, 22, 23, 24, 25, 26, 27, 28, 29
- [12] Xiao Cui, Yulei Qin, Wengang Zhou, Hongsheng Li, and Houqiang Li. OPTICAL: Leveraging optimal transport for contribution allocation in dataset distillation. In *Proceedings of the IEEE/CVF Conference on Computer Vision and Pattern Recognition (CVPR)*, 2025. 2
- [13] Abhimanyu Das, Weihao Kong, Rajat Sen, and Yichen Zhou. A decoder-only foundation model for time-series forecasting. In *ICML*, 2024. 1
- [14] Jianrong Ding, Zhanyu Liu, Guanjie Zheng, Haiming Jin, and Linghe Kong. Condtfs: One-line plugin of dataset condensation for time series forecasting. In *NeurIPS*, 2024. 1, 2, 3, 4, 5, 7, 13
- [15] Kuiye Ding, Fanda Fan, Chunyi Hou, Zheyu Wang, Lei Wang, Zhengxin Yang, and Jianfeng Zhan. Timemo-saic: Temporal heterogeneity guided time series forecasting via adaptive granularity patch and segment-wise decoding, 2025. 1, 2, 5, 6
- [16] Kuiye Ding, Fanda Fan, Yao Wang, Xiaorui Wang, Luqi Gong, Yishan Jiang, Chunjie Luo, Jianfeng Zhan, et al. Dualsg: A dual-stream explicit semantic-guided multivariate time series forecasting framework. In *arXiv preprint arXiv:2507.21830*, 2025. 1, 2
- [17] Kuiye Ding, Fanda Fan, Zheyu Wang, Hongxiao Li, Yifan Wang, Lei Wang, Chunjie Luo, and Jianfeng Zhan. Kairos: Unified training for universal non-autoregressive time series forecasting, 2025. 1
- [18] Jiawei Du, Yidi Jiang, Vincent YF Tan, Joey Tianyi Zhou, and Haizhou Li. Minimizing the accumulated trajectory error to improve dataset distillation. In *CVPR*, 2023. 1, 2, 5, 6, 7, 19, 20, 21, 22, 23, 24, 25, 26, 27, 28, 29, 30
- [19] Jiawei Du, Qin Shi, and Joey Tianyi Zhou. Sequential subset matching for dataset distillation. *Advances in Neural Information Processing Systems*, 36, 2024. 2
- [20] Xinyi Gao, Junliang Yu, Wei Jiang, Tong Chen, Wentao Zhang, and Hongzhi Yin. Graph condensation: A survey. *IEEE Transactions on Knowledge and Data Engineering*, 2025. 1
- [21] Zongxion Geng, Jiahui andg Chen, Yuandou Wang, Herbert Woisetschlaeger, Sonja Schimmler, Ruben Mayer, Zhiming Zhao, and Chunming Rong. A survey on dataset distillation: Approaches, applications and future directions. In *Proceedings of the International Joint Conference on Artificial Intelligence (IJCAI)*, 2023. 2
- [22] Peter A. Gorry. General least-squares smoothing and differentiation by the convolution (savitzky-golay) method. *Analytical Chemistry*, 1990. 7
- [23] Mononito Goswami, Konrad Szafer, Arjun Choudhry, Yifu Cai, Shuo Li, and Artur Dubrawski. Moment: A family of open time-series foundation models. In *ICML*, 2024. 1
- [24] Ziyao Guo, Kai Wang, George Cazenavette, Hui Li, Kaipeng Zhang, and Yang You. Towards lossless dataset distillation via difficulty-aligned trajectory matching. In *ICLR*, 2024. 1, 2, 3, 5, 6, 7, 19, 20, 21, 22, 23, 24, 25, 26, 27, 28, 29, 30
- [25] Yifan Hu, Peiyuan Liu, Peng Zhu, Dawei Cheng, and Tao Dai. Adaptive multi-scale decomposition framework for time series forecasting. In *AAAI*, 2025. 1
- [26] Jang-Hyun Kim, Jinuk Kim, Seong Joon Oh, Sangdoon Yun, Hwanjun Song, Joonhyun Jeong, Jung-Woo Ha, and Hyun Oh Song. Dataset condensation via efficient synthetic-data parameterization. In *International Conference on Machine Learning*, pages 11102–11118. PMLR, 2022. 2
- [27] Dilfira Kudrat, Zongxia Xie, Yanru Sun, Tianyu Jia, and Qinghua Hu. Patch-wise structural loss for time series forecasting. In *ICML*, 2025. 2
- [28] Guokun Lai, Wei-Cheng Chang, Yiming Yang, and Hanxiao Liu. Modeling long- and short-term temporal patterns with deep neural networks, 2018. 5
- [29] Saehyung Lee, Sanghyuk Chun, Sangwon Jung, Sangdoon Yun, and Sungroh Yoon. Dataset condensation with con-

- trastive signals. In *International Conference on Machine Learning*, pages 12352–12364. PMLR, 2022. 2
- [30] Shiye Lei and Dacheng Tao. A comprehensive survey to dataset distillation. *IEEE Transactions on Pattern Analysis and Machine Intelligence*, 46(1):17–32, 2023. 2
- [31] Guang Li, Ren Togo, Takahiro Ogawa, and Miki Haseyama. Dataset distillation using parameter pruning. *IEICE Transactions on Fundamentals of Electronics, Communications and Computer Sciences*, 2023. 5, 7, 20, 21, 22, 23, 24, 25, 26, 27, 28, 29, 30
- [32] Yong Liu, Tengge Hu, Haoran Zhang, Haixu Wu, Shiyu Wang, Lintao Ma, and Mingsheng Long. itransformer: Inverted transformers are effective for time series forecasting. In *ICLR*, 2024. 5
- [33] Yong Liu, Guo Qin, Zhiyuan Shi, Zhi Chen, Caiyin Yang, Xiangdong Huang, Jianmin Wang, and Mingsheng Long. Sundial: A family of highly capable time series foundation models. In *ICML*, 2025. 1, 2
- [34] Zhanyu Liu, Ke Hao, Guanjie Zheng, and Yanwei Yu. Dataset condensation for time series classification via dual domain matching. In *ACM SIGKDD*, 2024. 1, 2
- [35] Noel Loo, Ramin Hasani, Alexander Amini, and Daniela Rus. Efficient dataset distillation using random feature approximation. In *NeurIPS*, 2022. 5, 20, 21, 22, 23, 24, 25, 26, 27, 28, 29
- [36] Dougal Maclaurin, David Duvenaud, and Ryan Adams. Gradient-based hyperparameter optimization through reversible learning. In *Proceedings of the International Conference on Machine Learning (ICML)*, pages 2113–2122, 2015. 1
- [37] Hao Miao, Ziqiao Liu, Yan Zhao, Chenjuan Guo, Bin Yang, Kai Zheng, and Christian S. Jensen. Less is More: Efficient time series dataset condensation via two-fold modal matching—extended version. In *Proceedings of the International Conference on Very Large Data Bases (VLDB)*, 2025. 1, 2, 3
- [38] Timothy Nguyen, Zhoung Chen, and Jaehoon Lee. Dataset meta-learning from kernel ridge-regression. In *ICLR*, 2021. 2, 5, 20, 21, 22, 23, 24, 25, 26, 27, 28, 29
- [39] Yuqi Nie, Nam H Nguyen, Phanwadee Sinthong, and Jayant Kalagnanam. A time series is worth 64 words: Long-term forecasting with transformers. In *International Conference on Learning Representations (ICLR)*, 2023. 2, 5
- [40] Adam Paszke, Sam Gross, Francisco Massa, Adam Lerer, James Bradbury, Gregory Chanan, Trevor Killeen, Zeming Lin, Natalia Gimelshein, Luca Antiga, Alban Desmaison, Andreas Köpf, Edward Yang, Zach DeVito, Martin Raison, Alykhan Tejani, Sasank Chilamkurthy, Benoit Steiner, Lu Fang, Junjie Bai, and Soumith Chintala. Pytorch: An imperative style, high-performance deep learning library. 2019. 5
- [41] PEMS. Traffic. <http://pems.dot.ca.gov/>. 5, 6
- [42] Ben Poole, Sherjil Ozair, Aaron Van Den Oord, Alex Alemi, and George Tucker. On variational bounds of mutual information. In *Proceedings of the 36th International Conference on Machine Learning*, pages 5171–5180. PMLR, 2019. 4
- [43] Xiangfei Qiu, Jilin Hu, Lekui Zhou, Xingjian Wu, Junyang Du, Buang Zhang, Chenjuan Guo, Aoying Zhou, Christian S. Jensen, Zhenli Sheng, and Bin Yang. Tfb: Towards comprehensive and fair benchmarking of time series forecasting methods. *Proc. VLDB Endow.*, 17(9):2363–2377, 2024. 5, 6
- [44] Naveen Sachdeva and Julian McAuley. Data distillation: A survey, 2023. 2
- [45] Ozan Sener and Silvio Savarese. Active learning for convolutional neural networks: A core-set approach. *arXiv preprint arXiv:1708.00489*, 2017. 2
- [46] Zezhi Shao, Yujie Li, Fei Wang, Chengqing Yu, Yisong Fu, Tangwen Qian, Bin Xu, Boyu Diao, Yongjun Xu, and Xueqi Cheng. Blast: Balanced sampling time series corpus for universal forecasting models. In *Proceedings of the 31st ACM SIGKDD Conference on Knowledge Discovery and Data Mining V.2*, 2025. 6
- [47] Lefei Shen, Mouxiang Chen, Xu Liu, Han Fu, Xiaoxue Ren, Jianling Sun, Zhuo Li, and Chenghao Liu. Visionts++: Cross-modal time series foundation model with continual pre-trained visual backbones, 2025. 1
- [48] Xiaoming Shi, Shiyu Wang, Yuqi Nie, Dianqi Li, Zhou Ye, Qingsong Wen, and Ming Jin. Time-moe: Billion-scale time series foundation models with mixture of experts. In *ICLR*, 2025. 1, 5
- [49] Artyom Stitsyuk and Jaesik Choi. xpatch: Dual-stream time series forecasting with exponential seasonal-trend decomposition. In *AAAI*, 2025. 2, 5
- [50] Jialong Sun, Xinpeng Ling, Jiaxuan Zou, Jiawen Kang, and Kejia Zhang. Freie: Low-frequency spectral bias in neural networks for time-series tasks, 2025. 3
- [51] Peiwang Tang and Weitai Zhang. Unlocking the power of patch: Patch-based mlp for long-term time series forecasting. In *AAAI*, 2025. 2
- [52] Naftali Tishby, Fernando C. Pereira, and William Bialek. The information bottleneck method, 2000. 2, 4
- [53] Artur Trindade. ElectricityLoadDiagrams20112014. UCI Machine Learning Repository, 2015. DOI: <https://doi.org/10.24432/C58C86>. 5
- [54] Ivor W Tsang, James T Kwok, Pak-Ming Cheung, and Nello Cristianini. Core vector machines: Fast svm training on very large data sets. *Journal of Machine Learning Research*, 6(4), 2005. 2
- [55] Hao Wang, Licheng Pan, Zhichao Chen, Degui Yang, Sen Zhang, Yifei Yang, Xinggao Liu, Haoxuan Li, and Dacheng Tao. Fredf: Learning to forecast in the frequency domain. In *ICLR*, 2025. 1, 2, 3, 4
- [56] Kai Wang, Bo Zhao, Xiangyu Peng, Zheng Zhu, Shuo Yang, Shuo Wang, Guan Huang, Hakan Bilen, Xinchao Wang, and Yang You. Cafe: Learning to condense dataset by aligning features. In *CVPR*, 2022. 2
- [57] Kai Wang, Zekai Li, Zhi-Qi Cheng, Samir Khaki, Ahmad Sajedi, Ramakrishna Vedantam, Konstantinos N Plataniotis, Alexander Hauptmann, and Yang You. Emphasizing discriminative features for dataset distillation in complex scenarios. In *CVPR*, 2025. 1, 3, 5, 6, 7, 20, 21, 22, 23, 24, 25, 26, 27, 28, 29, 30
- [58] Shiyu Wang, Haixu Wu, Xiaoming Shi, Tengge Hu, Huakun Luo, Lintao Ma, James Y Zhang, and JUN ZHOU. Timemixer: Decomposable multiscale mixing for time series forecasting. In *ICLR*, 2024. 1, 2, 5

- [59] Shiyu Wang, Jiawei Li, Xiaoming Shi, Zhou Ye, Baichuan Mo, Wenze Lin, Shengtong Ju, Zhixuan Chu, and Ming Jin. Timemixer++: A general time series pattern machine for universal predictive analysis. In *ICLR*, 2025. 1
- [60] Shaobo Wang, Yicun Yang, Zhiyuan Liu, Chenghao Sun, Xuming Hu, Conghui He, and Linfeng Zhang. Dataset distillation with neural characteristic function: A minmax perspective. In *CVPR*, 2025. 2
- [61] Tongzhou Wang, Jun-Yan Zhu, Antonio Torralba, and Alexei A. Efros. Dataset distillation, 2020. 1
- [62] Gerald Woo, Chenghao Liu, Akshat Kumar, Caiming Xiong, Silvio Savarese, and Doyen Sahoo. Unified training of universal time series forecasting transformers. In *ICML*, 2024. 2
- [63] Haixu Wu, Jiehui Xu, Jianmin Wang, and Mingsheng Long. Autoformer: Decomposition transformers with auto-correlation for long-term series forecasting. In *NeurIPS*, 2021. 1, 2
- [64] Taiqiang Wu, Chaofan Tao, Jiahao Wang, Runming Yang, Zhe Zhao, and Ngai Wong. Rethinking Kullback-Leibler divergence in knowledge distillation for large language models. In *Proceedings of the 31st International Conference on Computational Linguistics*, 2025. 5
- [65] Yifan Wu, Jiawei Du, Ping Liu, Yuewei Lin, Wenqing Cheng, and Wei Xu. DD-RobustBench: An adversarial robustness benchmark for dataset distillation. *IEEE Transactions on Image Processing*, 2025. 1
- [66] Kun Yi, Qi Zhang, Wei Fan, Shoujin Wang, Pengyang Wang, Hui He, Ning An, Defu Lian, Longbing Cao, and Zhendong Niu. Frequency-domain MLPs are more effective learners in time series forecasting. In *NeurIPS*, 2023. 5
- [67] Ruonan Yu, Songhua Liu, and Xinchao Wang. A comprehensive survey to dataset distillation. *IEEE Transactions on Pattern Analysis and Machine Intelligence*, 46(1):150–170, 2023. 2
- [68] Ailing Zeng, Muxi Chen, Lei Zhang, and Qiang Xu. Are transformers effective for time series forecasting? In *AAAI*, 2023. 2, 4, 5, 6
- [69] Lei Zhang, Jie Zhang, Bowen Lei, Subhabrata Mukherjee, Xiang Pan, Bo Zhao, Caiwen Ding, Yao Li, and Dongkuan Xu. Accelerating dataset distillation via model augmentation. In *Proceedings of the IEEE/CVF Conference on Computer Vision and Pattern Recognition*, pages 11950–11959, 2023. 2
- [70] Yuchen Zhang, Tianle Zhang, Kai Wang, Ziyao Guo, Yuxuan Liang, Xavier Bresson, Wei Jin, and Yang You. Navigating complexity: Toward lossless graph condensation via expanding window matching. In *ICML*, 2024. 1
- [71] Bo Zhao and Hakan Bilen. Dataset condensation with differentiable siamese augmentation. In *ICML*, 2021. 5
- [72] Bo Zhao and Hakan Bilen. Dataset condensation with distribution matching. In *Proceedings of the IEEE/CVF Winter Conference on Applications of Computer Vision*, pages 6514–6523, 2023. 2
- [73] Bo Zhao, Konda Reddy Mopuri, and Hakan Bilen. Dataset condensation with gradient matching. In *ICLR*, 2021. 2, 5, 20, 21, 22, 23, 24, 25, 26, 27, 28, 29
- [74] Ganlong Zhao, Guanbin Li, Yipeng Qin, and Yizhou Yu. Improved distribution matching for dataset condensation. In *CVPR*, 2023. 2, 5, 20, 21, 22, 23, 24, 25, 26, 27, 28, 29
- [75] Wenliang Zhong, Haoyu Tang, Qinghai Zheng, Mingzhu Xu, Yupeng Hu, and Liqiang Nie. Towards stable and storage-efficient dataset distillation: Matching convexified trajectory. In *CVPR*, 2025. 2, 3, 5, 6, 7, 20, 21, 22, 23, 24, 25, 26, 27, 28, 29, 30
- [76] Haoyi Zhou, Shanghang Zhang, Jieqi Peng, Shuai Zhang, Jianxin Li, Hui Xiong, and Wancai Zhang. Informer: Beyond efficient transformer for long sequence time-series forecasting. In *AAAI*, 2021. 5, 6
- [77] Tian Zhou, Ziqing Ma, Qingsong Wen, Xue Wang, Liang Sun, and Rong Jin. FEDformer: Frequency enhanced decomposed transformer for long-term series forecasting. In *ICML*, 2022. 4

A. Detailed Dataset Descriptions

To comprehensively evaluate forecasting performance across diverse temporal dynamics and application domains, we employ a collection of widely adopted benchmark datasets summarized in Table 5. Following CondTFSF [14], both the input and prediction horizons are set to $T_{\text{in}} = T_{\text{out}} = 24$ for all datasets. Each multivariate time series $\mathbf{X} \in \mathbb{R}^{N \times L}$ is first standardized and segmented into input–output pairs using a fixed-stride sliding window. For each window position, the input sequence $\mathbf{X}^{(i)} \in \mathbb{R}^{N \times T_{\text{in}}}$ and its forecasting target $\mathbf{Y}^{(i)} \in \mathbb{R}^{N \times T_{\text{out}}}$ are defined as

$$\mathbf{X}^{(i)} = \mathbf{X}_{[:, i:i+T_{\text{in}}]}, \quad \mathbf{Y}^{(i)} = \mathbf{X}_{[:, i+T_{\text{in}}:i+T_{\text{in}}+T_{\text{out}}]}, \quad (13)$$

where the window index i advances by a constant stride s along the temporal axis. This overlapping-window formulation preserves temporal continuity while producing sufficient training instances for stable optimization across datasets with different lengths and frequencies.

A.1. Environmental Domain Datasets

Weather Dataset: Provides comprehensive meteorological observations including dry and wet bulb temperatures in both Fahrenheit and Celsius, dew point measurements, relative humidity, wind speed and direction, atmospheric pressure readings, and visibility conditions.

Global Temp Dataset: Hourly global temperature dataset comprising 1,000 variables across multiple regions, used to evaluate long-term forecasting performance and model generalization in climate and environmental domains.

A.2. Energy Domain Datasets

Wind Power Dataset: High-frequency wind power output records enabling detailed studies on renewable integration dynamics, system stability, and near-term generation forecasting.

Solar Power Dataset: Minute-resolution photovoltaic power generation data supporting fine-grained analysis of solar output dynamics, cloud-induced intermittency, and renewable energy variability.

ETT (Electricity Transformer Temperature) Datasets: Four complementary datasets (ETTh1, ETTh2, ETTm1, ETTm2) recording transformer load and temperature variations at hourly and 15-minute intervals, serving as standard benchmarks for power grid condition monitoring and predictive maintenance research.

Electricity Dataset: Electricity consumption records from 321 individual consumers, providing a detailed representation of distributed usage behavior suitable for demand response evaluation and consumer load modeling.

Table 5. Statistics of the benchmark datasets used in our study. Each dataset is characterized by its variable dimensionality (Dim), the number of samples in training/validation/testing splits, and the original sampling frequency. All datasets are processed under a unified normalization and fixed-stride $S = 12$ windowing protocol to ensure consistent temporal segmentation across experiments, follow the CondTFSF [14].

Dataset	Dim	Dataset Size	Frequency
ETTh1, ETTh2	7	(837,357,357)	Hourly
ETTm1, ETTm2	7	(3357,1437,1437)	15 min
Weather	21	(3070,1314,1314)	10 min
Traffic	862	(1020,435,435)	Hourly
Electricity	321	(1531,654,654)	Hourly
Exchange-rate	8	(439,186,186)	Daily
Solar-energy	137	(3063,1311,1311)	10 min
Wind (L1–L4)	9	(2551,1092,1092)	Hourly
PEMS03	358	(1525,652,652)	5 min
PEMS04	307	(988,421,421)	5 min
PEMS07	883	(1643,702,702)	5 min
PEMS08	170	(1038,443,443)	5 min
Wike2000	2000	(43,16,16)	Daily
ILI	7	(53,21,21)	Weekly
Global Temp	1000	(201,84,84)	Hourly

A.3. Web Domain Datasets

Wike2000 Dataset: The Wike2000 dataset belongs to the web domain and consists of daily multivariate time series comprising 2,000 variables with a total sequence length of 792. It captures large-scale web traffic dynamics and is widely used to evaluate forecasting models under high-dimensional, short-horizon, and nonstationary conditions.

A.4. Transportation Domain Datasets

Traffic Dataset: Comprehensive traffic monitoring data collected from 862 highway sensor stations, recording vehicle occupancy and flow dynamics to support research in intelligent transportation systems and congestion management.

PEMS Dataset: The PEMS datasets (PEMS03, PEMS04, PEMS07, PEMS08) originate from the California Department of Transportation Performance Measurement System (Caltrans PeMS) and are widely used benchmarks in traffic flow forecasting research.

A.5. Financial Domain Datasets

Exchange Rate Dataset: Daily records of foreign exchange rate dynamics across multiple international currency pairs, supporting quantitative analyses of financial markets, currency volatility, and macroeconomic forecasting.

A.6. Healthcare Domain Datasets

National Illness Dataset: Weekly surveillance records capturing influenza-like illness (ILI) prevalence across multiple age groups and healthcare provider networks, serving as a critical resource for epidemiological modeling and public health surveillance.

B. Implementation Details

Training Configuration. The training process consists of two stages: collecting teacher trajectories and optimizing synthetic sequences with the Synthetic Dataset module. All experiments are implemented in PyTorch and conducted on a single NVIDIA RTX 5090 GPU.

Metrics. We use mean squared error (MSE) and mean absolute error (MAE) as evaluation metrics for time-series forecasting. These metrics are calculated as follows:

$$\text{MSE} = \frac{1}{H} \sum_{i=1}^H (x_i - \hat{x}_i)^2, \quad \text{MAE} = \frac{1}{H} \sum_{i=1}^H |x_i - \hat{x}_i|, \quad (14)$$

where $x_i, \hat{x}_i \in \mathbb{R}$ denote the ground truth and the predicted values of the i -th forecasting step, and H is the forecasting horizon.

Teacher trajectory collection. For each dataset, forty teacher trajectories are generated. Each teacher model is trained using stochastic gradient descent with a learning rate of 5×10^{-4} , momentum of 0.9, and no weight decay. Training is performed for 80 epochs with a batch size of 32. At every epoch, model parameters are stored as checkpoints to form a complete parameter trajectory. Every five trajectories are saved together in replay buffer files which are later used for parameter-matching during distillation. During training, both training and testing mean squared error (MSE) and mean absolute error (MAE) are recorded after each epoch. For all datasets, 40 teacher trajectories are collected (5 per replay buffer, yielding 8 buffers). Each teacher is trained for 80 epochs using SGD, while synthetic samples are optimized with Adam. Distillation alternates between student update and data refinement following CondTSF’s default protocol.

Synthetic sequence optimization. The GCOND module maintains a set of learnable synthetic time-series samples, each represented as a tensor of shape $[S, N, T]$, where S is the number of synthetic samples, N is the number of variables in the dataset, and T equals the sum of the input and prediction lengths ($T_{\text{in}} = 24$ and $T_{\text{out}} = 24$). Synthetic samples are initialized by randomly extracting contiguous windows from the normalized real data to ensure realistic temporal patterns. The synthetic parameters are optimized directly by the Adam optimizer with a learning rate of 0.1. In each distillation iteration, the student model is trained on

the synthetic data for twenty gradient steps, and then the synthetic sequences are refined based on the resulting parameter trajectories.

distillation protocol. The distillation procedure alternates between parameter imitation and data refinement. To ensure fair comparison with the original CondTSF framework, we adopt the same hyperparameter configuration: the distillation interval is set to five iterations, and the conditional update coefficient, which controls how much model predictions are blended back into the synthetic data, is set to 0.01. All random seeds are fixed to ensure reproducibility, and deterministic CuDNN settings are enabled.

Evaluation. After distillation, the distilled datasets are evaluated using multiple independently initialized student networks for each forecasting architecture. The results are reported as the mean and standard deviation of MSE and MAE over five runs and across twenty benchmark datasets. All experiments use fixed preprocessing and consistent train-validation-test splits for comparability across methods.

C. Parameter Term

The Parameter Term \mathcal{L}_P is optimized via a *parameter trajectory alignment* strategy, which aligns the student parameters with those of multiple pre-trained teachers.

(1) Expert trajectories. Several teacher models are trained on real data, and their parameter snapshots are saved as $\Theta_T = \{\theta_T^{(0)}, \theta_T^{(1)}, \dots, \theta_T^{(E)}\}$, recording the optimization paths at different epochs.

(2) Student training. The student model M_{θ_S} is trained on the synthetic dataset \mathcal{D}_{syn} , with parameters $\theta_S^{(k)}$ recorded after each iteration.

(3) Trajectory matching. During distillation, the student is aligned with the most similar teacher trajectory by minimizing the normalized parameter distance:

$$\mathcal{L}_P = \min_{\text{expert}} \frac{\|\theta_S - \theta_T^{(E)}\|_2^2}{\|\theta_T^{(E)} - \theta_T^{(0)}\|_2^2}. \quad (15)$$

This distance is computed using the L2 norm without back-propagation through teacher models, while gradients are propagated only through the student network.

We follow prior trajectory matching using them as backbones for optimization. Our method is implemented as a *plug-in objective* that replaces the standard gradient-matching loss with this parameter-alignment formulation.

D. Information Diversity Measurement via KL Divergence

To quantify the diversity and information content of the distilled synthetic datasets, we compute the *average symmetric Kullback-Leibler (KL) divergence* among all synthetic samples. Given a set of S synthetic time series

$\{\mathbf{X}_i \in \mathbb{R}^{N \times T}\}_{i=1}^S$, each sample is first normalized and converted into a probability distribution over the temporal dimension via the temperature-controlled softmax:

$$p_i = \text{Softmax}\left(\frac{\mathbf{X}_i - \mu_i}{\sigma_i + \epsilon} / \tau\right), \quad (16)$$

where μ_i and σ_i denote the mean and standard deviation across time steps, and τ is the softmax temperature.

The symmetric KL divergence between two samples p_i and p_j is defined as

$$D_{\text{sym}}(p_i, p_j) = \frac{1}{2} \left(\text{KL}(p_i \| p_j) + \text{KL}(p_j \| p_i) \right), \quad (17)$$

and the overall average divergence within the synthetic set is

$$\bar{D}_{\text{KL}} = \frac{2}{S(S-1)} \sum_{i < j} D_{\text{sym}}(p_i, p_j). \quad (18)$$

Intuitively, a larger \bar{D}_{KL} indicates greater dissimilarity among synthetic samples, suggesting that the distilled dataset captures richer temporal patterns and covers a broader portion of the underlying data manifold. Therefore, we use \bar{D}_{KL} as a quantitative proxy for the *Information diversity* of synthetic time-series data.

Table 6 reports the computed average symmetric KL divergences across multiple datasets and sample sizes. As shown, our method consistently achieves higher Information diversity than both the DATM and CondTSF baselines, demonstrating its ability to generate more diverse and informative synthetic sequences.

E. Ablation Study on Frequency Domain Label Loss Alignment

To further examine the effectiveness of incorporating frequency domain information into the distillation objective, we conduct an ablation study across four representative datasets: Weather, Electricity, Solar, and ExchangeRate (see Tables 17–20). Each table reports the forecasting results under different values of the alignment coefficient $\alpha \in \{0.1, 0.2, 0.3, 0.4, 0.5, 0.6, 0.7, 0.8, 0.9, 1.0\}$, which controls the relative strength of the frequency domain label loss in the overall training objective.

When $\alpha = 0$, the distillation process does not include frequency domain alignment, and the student model tends to overfit to local temporal fluctuations, leading to less stable generalization. Introducing the frequency domain label loss term ($\alpha > 0$) consistently improves model stability and reduces forecasting error across all datasets, demonstrating that aligning teacher and student representations in the spectral space effectively complements time-domain supervision.

However, the performance does not monotonically increase with larger α values. Excessive spectral alignment

Table 6. Average symmetric KL divergence under different numbers of synthetic samples (S). The average KL divergence between synthetic samples is used as a proxy to measure their *Information diversity*. All results are obtained under our method with $\alpha = 0.1$ and $\lambda_{\text{IS}} = 0.2$.

Method	Electricity (321)	Solar (137)	Weather (21)	ETTm1 (7)	ETTh1 (7)
<i>Ours</i>					
$S=3$	7.9562	6.0624	6.1783	7.5984	7.5065
$S=5$	5.9573	7.1132	5.8814	7.1882	7.8194
$S=10$	5.6014	4.6531	6.7383	6.9596	7.9601
$S=20$	5.7005	5.6690	6.8403	7.1020	7.7295
Mean	6.3038	5.8744	6.4096	7.2121	7.7539
<i>CondTSF</i>					
$S=3$	4.7510	3.2314	7.6868	3.8616	5.2092
$S=5$	5.9471	6.4680	5.0484	3.7866	5.8175
$S=10$	5.3922	5.0312	4.9754	3.9649	4.7749
$S=20$	5.2139	3.3957	6.0091	3.9374	5.1213
Mean	5.3261	4.5316	5.9299	3.8876	5.2307
<i>DATM</i>					
$S=3$	2.9747	3.0964	6.6312	5.5428	5.1283
$S=5$	5.0359	3.3059	5.9489	3.8608	4.1114
$S=10$	5.8011	3.8497	5.6042	3.6268	5.8774
$S=20$	5.4619	4.1256	4.8433	4.0031	5.1918
Mean	4.8184	3.5944	5.7569	4.2584	5.0772

Table 7. Compact comparison of **Best** and **Second Best** marks across datasets and sample sizes (S). Each block compares the baseline and our frequency-domain label-loss alignment method. Higher shares indicate stronger consistency across datasets.

Dataset	S	Original			Ours			Ours Share (%)		
		Best	Second	Sum	Best	Second	Sum	Best	Second	Sum
Exchange	3	0	2	2	24	24	48	100.0	92.3	96.0
	5	2	5	7	24	24	48	92.3	82.8	87.3
	10	2	1	3	27	28	55	93.1	96.6	94.8
	20	4	3	7	25	36	61	86.2	92.3	89.7
	Sum	8	11	19	100	112	212	92.9	91.0	91.9
ECL	3	4	4	8	29	30	59	87.9	88.2	88.1
	5	2	6	8	36	35	71	94.7	85.4	89.9
	10	0	1	1	32	51	83	100.0	98.1	98.8
	20	2	2	4	39	54	93	95.1	96.4	95.9
	Sum	8	13	21	136	170	306	94.4	92.0	93.2
Solar	3	0	4	4	29	27	56	100.0	87.1	93.3
	5	2	2	4	29	31	60	93.5	93.9	93.8
	10	1	1	2	36	46	82	97.3	97.9	97.6
	20	1	1	2	34	42	76	97.1	97.7	97.4
	Sum	4	8	12	128	146	274	97.0	94.1	95.6
Weather	3	0	1	1	38	48	86	100.0	98.0	98.9
	5	0	1	1	50	68	118	100.0	98.6	99.2
	10	3	0	3	50	52	102	94.3	100.0	97.1
	20	0	1	1	31	49	80	100.0	98.0	98.8
	Sum	3	3	6	169	217	386	98.6	98.7	98.6
Total	23	35	58	533	645	1178	95.9	94.0	94.9	

may overemphasize global frequency matching and dampen short-term temporal adaptation. Empirically, values of α between 0.3 and 0.8 achieve a good balance between temporal fitting and spectral regularization, providing robust im-

improvements over the baseline without frequency alignment.

Table 7 summarizes the aggregated statistics of Best and Second Best results derived from the four dataset-specific tables (17, 18, 19, 20). The aggregated data confirm that introducing frequency domain label loss yields clear overall gains in both forecasting accuracy and consistency across datasets and sample sizes. This supports our core hypothesis that frequency domain alignment serves as an effective inductive bias for preserving multi-scale temporal-spectral structure during time-series distillation.

F. Detailed Ablation Results

Table 21 presents the full ablation results of our method across multiple datasets and distillation baselines. Each block corresponds to a specific dataset (*Weather*, *Electricity*, *Solar*, and *Exchange*), with four synthetic sample settings (3, 5, 10, and 20). For each distillation baseline, results are reported in terms of MSE and MAE, averaged over 5 independent runs.

Our method consists of two plugin modules: the Temporal-Frequency Alignment (TFA) module and the Inter-Sample Information Bottleneck (ISIB) module. TFA enhances the temporal-frequency consistency between synthetic and real trajectories, while ISIB promotes inter-sample diversity by constraining redundancy in the condensed set. The results under “+TFA” and “+ISIB” indicate the effect of each module independently. Unless otherwise specified, the hyperparameters are fixed as $\alpha = 0.8$ for TFA and $\lambda_{IS} = 0.6$ for ISIB to ensure consistency across all experiments.

The corresponding summarized averages in the main text (Table 3) are obtained by averaging the MAE values across the four datasets and four sample settings. As discussed in Section 4.3, while EDF and MCT under $\alpha = 0.8$ on *Electricity* and *Solar* are slightly higher than the baseline, adjusting α (see Appendix Tables 18 and 19) yields superior results beyond the baseline. Overall, the full results in Table 21 confirm that both TFA and ISIB consistently improve data efficiency across different trajectory-matching distillation frameworks.

G. Ablation under Different Architectures.

We evaluate the DATM-based distillation on the ETTh1 dataset across diverse forecasting architectures. As shown in Table 8, our method consistently improves performance over the baseline for both Transformer-based and conventional models. Although the formulation in Eq. 4 strictly holds under linear forecasting settings, the experimental results indicate that this distillation paradigm can be directly transferred to other forecasting architectures without modification.

Table 8. Distillation performance (MSE) across different forecasting architectures.

Model	Whole Dataset	Baseline	+Ours
FreTS	0.347	0.515	0.488
PatchTST	0.388	0.807	0.731
xPatch	0.531	0.570	0.559
SimpleTM	0.561	0.893	0.816
iTransformer	0.577	0.875	0.812
CNN	0.711	0.817	0.724
MLP	0.727	0.825	0.661
LSTM	0.890	0.899	0.891

H. Model Size and Storage Analysis

Table 9 summarizes the model buffer sizes (in MB) trained on the full original datasets across various forecasting architectures. These values reflect the actual storage footprint of each model after being trained on its corresponding real dataset, providing a reference for comparing the relative parameter and representation capacity among different architectures. As shown, lightweight models such as *DLinear* and *MLP* occupy minimal space, whereas more complex architectures like *FreTS* and large-scale CNN-based models exhibit substantially larger storage sizes, indicating higher model complexity and memory demand. It is worth noting that models with identical architectures show consistent file sizes across datasets (e.g., the ETT family), since the storage size is primarily determined by the number and precision of learnable parameters rather than dataset-specific characteristics.

I. Runtime and Memory Overhead Analysis

To evaluate the computational efficiency of the proposed framework, we measure the wall-clock runtime and GPU memory consumption of each distillation framework under both the baseline and the enhanced (*ours*) settings across all datasets. Table 22 reports the results in detail.

Overall, the proposed improvements incur only marginal computational overhead. When aggregated over all datasets and frameworks, the total runtime of the *ours* version is **2.59% faster** than the baseline on average, while the overall GPU memory usage increases by only **2.49%**. This demonstrates that our method introduces negligible additional cost in training and inference, yet provides consistent performance gains reported in the main experiments. The acceleration mainly stems from faster convergence, as the introduced frequency-domain alignment stabilizes optimization and the diversity regularization provides more informative synthetic samples, enabling efficient learning with minimal additional cost.

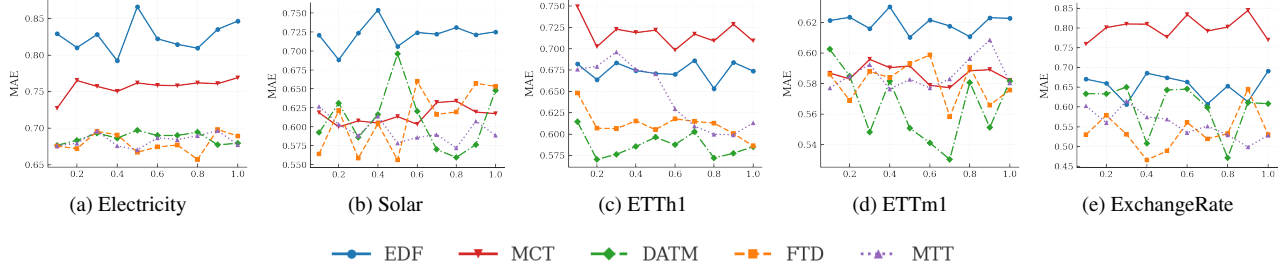


Figure 8. Parameter sensitivity comparison of five dataset condensation methods across datasets. Each curve shows MAE under different parameter values (0.1–1.0), and the legend below applies to all subplots.

Table 9. Model buffer size (MB) across datasets.

Dataset	CNN	DLinear	FreTS	LSTM	MLP	PatchTST	SimpleTM	iTransformer	xPatch
ETTh1	3.05	0.45	265.71	3.65	1.06	5.90	5.01	4.90	3.71
ETTh2	3.05	0.45	265.71	3.65	1.06	5.90	5.01	4.90	3.71
ETTh1	3.05	0.45	265.71	3.65	1.06	5.90	5.01	4.90	3.71
ETTh2	3.05	0.45	265.71	3.65	1.06	5.90	5.01	4.90	3.71
Electricity	4077.25	0.45	265.71	3.65	1.06	5.90	5.78	4.90	3.91
ExchangeRate	3.65	0.45	265.71	3.65	1.06	5.90	5.01	4.90	3.71
Global_Temp	39554.36	0.45	265.71	3.65	1.06	29.49	7.46	4.90	21.64
ILI	3.05	0.45	265.71	3.65	1.06	5.90	5.01	4.90	3.71
PEMS03	5070.97	0.45	265.71	3.65	1.06	5.90	5.86	4.90	3.93
PEMS04	3729.48	0.45	265.71	3.65	1.06	5.90	5.74	4.90	3.90
PEMS07	30840.60	0.45	265.71	3.65	1.06	5.90	7.16	4.90	4.26
PEMS08	1144.54	0.45	265.71	3.65	1.06	5.90	5.40	4.90	3.81
Solar	743.77	0.45	265.71	3.65	1.06	5.90	5.32	4.90	3.79
Traffic	29391.21	2.25	265.71	3.65	5.30	29.49	35.52	24.50	21.24
Weather	18.59	2.25	1328.53	18.24	5.30	29.49	25.14	4.90	3.72
Wike2000	277.50	2.25	1328.53	18.24	5.30	29.49	49.66	4.90	4.95
WindL1	4.32	0.45	265.71	3.65	1.06	5.90	5.01	4.90	3.71
WindL2	4.32	0.45	265.71	3.65	1.06	5.90	5.01	4.90	3.71
WindL3	4.32	0.45	265.71	3.65	1.06	5.90	5.01	4.90	3.71
WindL4	4.32	0.45	265.71	3.65	1.06	5.90	5.01	4.90	3.71

J. Discussion: Image Distillation vs. Time-Series Distillation

Most existing dataset distillation methods are developed for image classification, where inputs are static, approximately i.i.d. samples and labels are discrete class indices. In this regime, the distilled dataset is mainly required to preserve decision boundaries in a high-dimensional feature space, and the evaluation metric is usually top-1 accuracy with a clear upper bound given by training on the full dataset. In contrast, time-series forecasting involves continuous-valued outputs, long-range temporal dependencies, and multi-scale patterns, which fundamentally change both the learning objective and the role of the distilled data.

A first key difference lies in the label space and diversity priors. In image classification, categorical labels naturally

partition the data into classes, and most distillation objectives operate under an explicit per-class structure, which implicitly regularizes diversity within and across classes. For time-series forecasting, however, the targets are multi-step real-valued trajectories without explicit categorical priors. As discussed in our main text, synthetic sequences can easily collapse to a few redundant temporal patterns, leading to low information density even when the condensation ratio is fixed. This motivates the inter-sample regularization in our framework, which explicitly penalizes redundancy among synthetic trajectories instead of relying on class labels.

A second difference concerns temporal structure and label autocorrelation. Image distillation methods typically assume weak correlations across samples and do not model ordered dependencies within a sample. Time-series data, by contrast, exhibit strong autocorrelation and multi-scale

Figure 9. Comprehensive visualization of synthetic time-series samples generated by four representative dataset distillation frameworks (DATM, EDF, MCT, and MTT) and their plug-in enhanced variants (+Ours) across eight benchmark datasets: ETTh1, ETTh2, ETTm1, ETTm2, Electricity, ExchangeRate, Solar, Traffic, PEMS03, PEMS04, PEMS07, PEMS08, Wike2000 and Weather. Each dataset row compares the baseline and our plug-in variants across all frameworks. The plug-in method consistently produces more realistic temporal fluctuations and richer label dynamics, highlighting improved fidelity and inter-sample diversity of synthetic sequences, without introducing any additional trainable parameters.

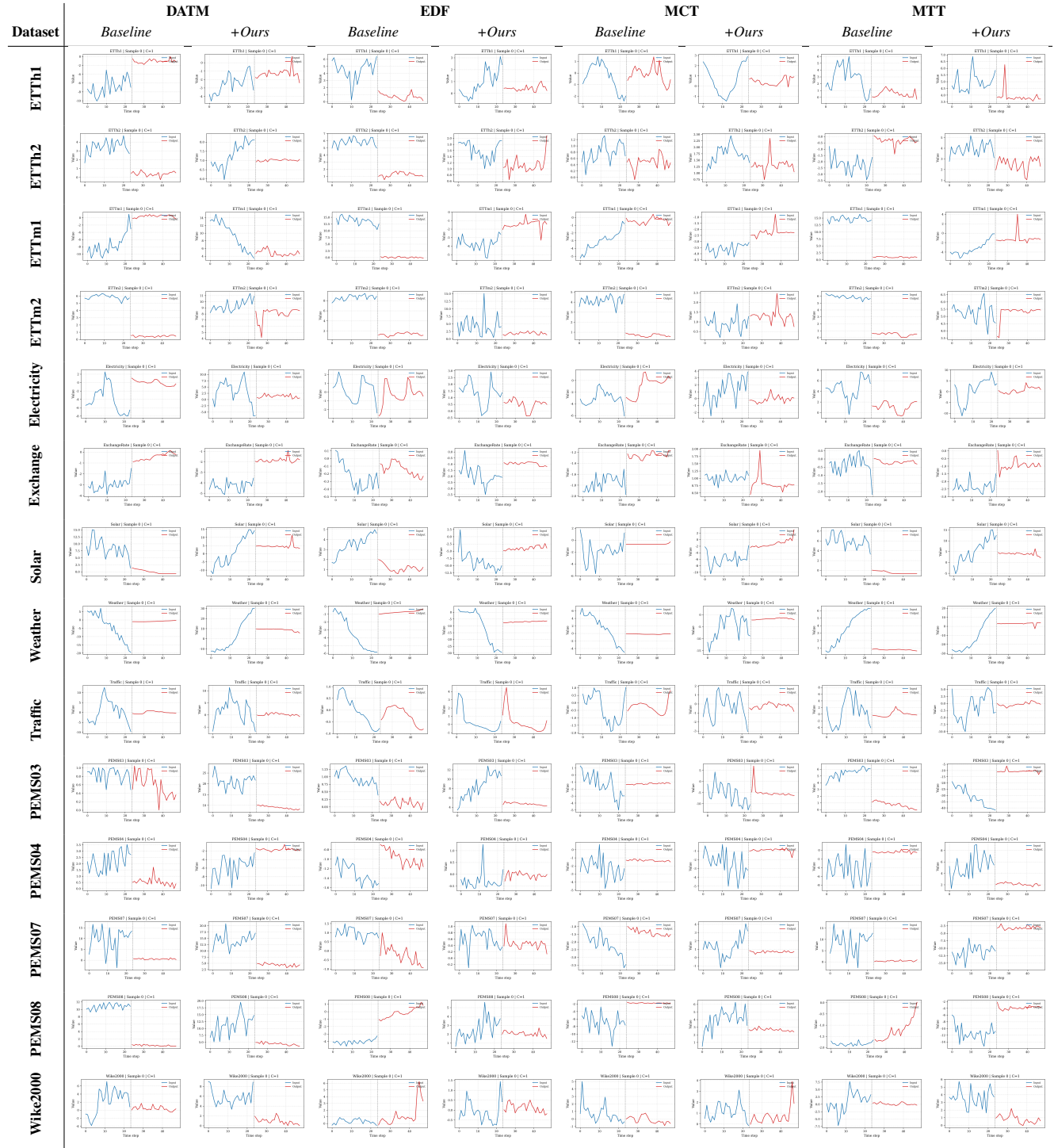


Table 10. Sensitivity analysis of model performance to the number of synthetic samples. The observation that 3–5 synthetic sequences suffice to drive meaningful performance suggests that existing TSF architectures may not fully exploit the whole information present in real data.

Models	DATM+Ours [2024]		FTD+Ours [2023]		
	MSE	MAE	MSE	MAE	
Electricity	2	0.72±0.01	0.69±0.01	0.73±0.01	0.69±0.01
	3	0.72±0.02	0.69±0.01	0.72±0.02	0.68±0.01
	5	0.69±0.02	0.68±0.01	0.70±0.02	0.68±0.01
	10	0.71±0.01	0.69±0.01	0.70±0.03	0.68±0.02
	20	0.72±0.02	0.69±0.01	0.73±0.02	0.69±0.01
	30	0.74±0.03	0.70±0.01	0.74±0.04	0.70±0.02
	40	0.76±0.03	0.71±0.02	0.75±0.03	0.70±0.02
	50	0.76±0.03	0.71±0.01	0.75±0.02	0.70±0.01
	80	0.80±0.03	0.72±0.01	0.76±0.02	0.70±0.01
	100	0.78±0.02	0.72±0.01	0.77±0.06	0.71±0.03
ExchangeRate	2	0.55±0.02	0.62±0.01	0.47±0.03	0.57±0.02
	3	0.54±0.05	0.61±0.03	0.44±0.06	0.54±0.04
	5	0.39±0.03	0.52±0.02	0.27±0.03	0.42±0.02
	10	0.33±0.03	0.47±0.02	0.32±0.01	0.47±0.01
	20	0.43±0.04	0.55±0.02	0.44±0.03	0.55±0.02
	30	0.46±0.03	0.56±0.02	0.48±0.03	0.57±0.02
	40	0.47±0.02	0.57±0.02	0.41±0.05	0.53±0.03
	50	0.46±0.03	0.56±0.02	0.44±0.02	0.55±0.01
	80	0.46±0.04	0.56±0.03	0.40±0.03	0.53±0.02
	100	0.48±0.04	0.58±0.02	0.48±0.03	0.58±0.02
Solar	2	0.65±0.01	0.66±0.01	0.62±0.01	0.65±0.01
	3	0.57±0.01	0.61±0.01	0.61±0.00	0.64±0.01
	5	0.52±0.01	0.58±0.01	0.58±0.01	0.62±0.02
	10	0.56±0.01	0.61±0.02	0.56±0.01	0.60±0.02
	20	0.56±0.01	0.60±0.01	0.60±0.01	0.63±0.02
	30	0.60±0.01	0.62±0.02	0.59±0.01	0.62±0.02
	40	0.58±0.01	0.63±0.01	0.60±0.01	0.63±0.01
	50	0.59±0.01	0.62±0.01	0.60±0.01	0.63±0.01
	80	0.60±0.01	0.63±0.01	0.69±0.02	0.67±0.01
	100	0.65±0.01	0.66±0.01	0.66±0.01	0.67±0.01
Weather	2	0.36±0.01	0.41±0.01	0.44±0.01	0.47±0.01
	3	0.28±0.01	0.31±0.01	0.38±0.01	0.43±0.01
	5	0.32±0.01	0.37±0.01	0.42±0.01	0.45±0.01
	10	0.31±0.00	0.36±0.01	0.40±0.01	0.44±0.01
	20	0.31±0.01	0.36±0.02	0.40±0.01	0.44±0.01
	30	0.31±0.01	0.37±0.01	0.39±0.01	0.43±0.01
	40	0.32±0.01	0.36±0.01	0.42±0.01	0.45±0.01
	50	0.32±0.01	0.37±0.01	0.66±0.06	0.56±0.03
	80	0.34±0.02	0.38±0.02	0.66±0.06	0.56±0.03
	100	0.36±0.00	0.40±0.01	0.66±0.05	0.56±0.02

temporal structures, so directly matching teacher–student predictions in the temporal domain can mix trend, seasonal, and high-frequency components in a single loss and amplify the bias of direct forecasting. Our frequency-domain reformulation of the value term is precisely designed to alleviate this label autocorrelation bias by aligning predictions in a decorrelated spectral space while preserving temporal fidelity.

Finally, the notion of “optimal” performance is less clear in time-series distillation than in image classification. In classification, distilled datasets are often judged by how closely they recover full-data accuracy, and in many cases aiming for 100% accuracy is a reasonable conceptual target. For forecasting, achieving zero prediction error is unrealistic due to intrinsic stochasticity and noise in real-world sig-

nals. Our experiments show that carefully optimized synthetic datasets can sometimes even surpass models trained on the full data, reflecting the presence of redundancy and noise in modern time-series benchmarks. This observation suggests that, beyond simply mimicking full-data training, time-series distillation should be viewed as a tool for constructing compact, diverse, and denoised supervision signals tailored to temporal dynamics, rather than a direct extension of image-based distillation objectives.

K. Practical Guidelines for Applying DDTIME

This section summarizes practical recommendations derived from the experiments and ablations already reported in the paper, without introducing new empirical claims.

Synthetic Sample Size. Across all benchmarks, using only 3–5 synthetic sequences per dataset already provides strong performance at condensation ratios below 1%. As shown in Table 1, increasing the number of synthetic samples brings diminishing returns. We therefore suggest starting with 3 or 5 sequences and increasing the budget only when necessary.

Temporal–Frequency Trade-off α . The coefficient α controls the strength of frequency-domain alignment. Our reported results indicate that activating the frequency term ($\alpha > 0$) consistently stabilizes learning and improves forecasting, while overly large values may overly bias spectral matching. Values in $[0.3, 0.8]$ work robustly, and we adopt $\alpha = 0.8$ as a universal default.

Diversity Regularization λ_{IS} . ISIB encourages diverse synthetic trajectories by penalizing redundant patterns. We use a fixed $\lambda_{\text{IS}} = 0.6$ in all experiments, which provides stable improvements without requiring dataset-specific tuning. Adjustments are only necessary if synthetic sequences visibly collapse to similar shapes.

When DDTIME Helps Most. DDTIME is compatible with many distillation frameworks, but the improvements are most pronounced when combined with trajectory-matching methods, where Parameter and Value terms are jointly optimized. For value-only distillation, DDTIME still offers benefits, though typically smaller, reflecting the complementary role of multi-term optimization in TSF.

Recommended Default Setup. For new forecasting tasks, a practical configuration is: 3–5 synthetic sequences per dataset, $\alpha = 0.8$ for balanced temporal–frequency alignment, $\lambda_{\text{IS}} = 0.6$ for stable diversity, and integration with a trajectory-matching framework when possible. This setup matches all reported experiments and requires no additional tuning.

Table 11. Extended ablation results across four benchmark datasets (PEMS03, PEMS04, PEMS07, PEMS08) under different synthetic sample sizes. **Green rows** denote results of each method augmented with *CondTSP*, and the **blue rows** denote results augmented with our proposed method. All values are averaged over three runs; lower MSE/MAE indicate better performance.

Models	Metric	EDF [2025]		MCT [2025]		DATM [2024]		FTD [2023]		PP [2023]		TESLA [2023]		IDM [2023]		FRePo [2022]		MTT [2022]		KIP [2021]		DC [2021]	
		MSE	MAE	MSE	MAE	MSE	MAE	MSE	MAE	MSE	MAE	MSE	MAE	MSE	MAE	MSE	MAE	MSE	MAE	MSE	MAE	MSE	MAE
PEMS03	3	0.72±0.02	0.71±0.01	0.72±0.05	0.70±0.03	0.84±0.04	0.75±0.01	0.78±0.02	0.75±0.01	0.86±0.01	0.79±0.01	0.78±0.04	0.73±0.02	0.91±0.07	0.78±0.04	0.69±0.02	0.69±0.01	0.91±0.01	0.81±0.01	0.89±0.07	0.77±0.04	0.91±0.09	0.78±0.04
	5	0.69±0.03	0.69±0.01	0.70±0.04	0.69±0.02	0.86±0.05	0.76±0.02	0.75±0.02	0.73±0.01	0.87±0.02	0.80±0.01	0.74±0.02	0.72±0.01	0.95±0.11	0.79±0.05	0.84±0.05	0.76±0.02	0.91±0.01	0.81±0.00	1.08±0.08	0.86±0.03	0.83±0.07	0.75±0.03
	10	0.71±0.03	0.70±0.02	0.83±0.08	0.75±0.04	0.91±0.06	0.79±0.03	0.80±0.05	0.73±0.02	0.93±0.02	0.82±0.01	0.68±0.02	0.69±0.01	0.83±0.03	0.74±0.01	0.84±0.06	0.76±0.03	0.85±0.02	0.78±0.01	0.82±0.06	0.75±0.03	0.88±0.07	0.78±0.03
	20	0.69±0.01	0.69±0.01	0.80±0.08	0.74±0.04	0.74±0.05	0.71±0.02	0.76±0.02	0.74±0.01	0.82±0.02	0.77±0.01	0.73±0.03	0.71±0.02	0.82±0.04	0.74±0.02	0.64±0.04	0.66±0.02	0.79±0.03	0.76±0.01	0.81±0.05	0.74±0.03	0.84±0.05	0.75±0.02
	3	0.62±0.01	0.66±0.01	0.54±0.03	0.59±0.02	0.57±0.04	0.62±0.03	0.59±0.01	0.65±0.00	0.60±0.01	0.65±0.00	0.59±0.01	0.64±0.01	1.07±0.18	0.85±0.07	0.59±0.05	0.62±0.03	0.62±0.01	0.66±0.00	0.72±0.03	0.69±0.01	0.82±0.12	0.74±0.06
	5	0.64±0.01	0.67±0.00	0.52±0.03	0.59±0.02	0.45±0.01	0.54±0.01	0.63±0.01	0.67±0.00	0.59±0.00	0.65±0.00	0.55±0.01	0.61±0.00	1.01±0.07	0.82±0.02	0.64±0.06	0.66±0.04	0.62±0.01	0.66±0.00	0.83±0.06	0.75±0.03	0.85±0.05	0.76±0.03
	10	0.66±0.01	0.68±0.01	0.53±0.04	0.59±0.02	0.46±0.01	0.54±0.01	0.64±0.01	0.68±0.00	0.60±0.01	0.65±0.01	0.61±0.02	0.64±0.01	0.90±0.10	0.77±0.04	0.59±0.04	0.63±0.03	0.61±0.01	0.66±0.00	0.80±0.07	0.72±0.03	0.88±0.15	0.77±0.07
	20	0.61±0.01	0.64±0.01	0.62±0.05	0.64±0.03	0.47±0.02	0.55±0.01	0.65±0.00	0.68±0.00	0.63±0.01	0.67±0.00	0.68±0.01	0.69±0.00	0.89±0.07	0.78±0.03	0.57±0.02	0.62±0.02	0.64±0.01	0.67±0.00	0.78±0.08	0.72±0.04	0.83±0.08	0.75±0.04
	3	0.59±0.01	0.64±0.01	0.57±0.04	0.61±0.02	0.28±0.01	0.40±0.00	0.45±0.01	0.55±0.00	0.40±0.01	0.51±0.01	0.54±0.01	0.59±0.00	0.98±0.06	0.82±0.03	0.69±0.05	0.68±0.03	0.39±0.01	0.51±0.01	0.83±0.07	0.75±0.04	0.69±0.03	0.68±0.01
	5	0.62±0.02	0.66±0.01	0.52±0.03	0.59±0.02	0.34±0.01	0.45±0.01	0.47±0.01	0.57±0.01	0.47±0.01	0.56±0.01	0.51±0.01	0.58±0.01	1.05±0.05	0.84±0.02	0.52±0.03	0.59±0.02	0.50±0.01	0.59±0.00	0.82±0.05	0.74±0.03	0.82±0.08	0.74±0.04
	10	0.65±0.01	0.67±0.01	0.50±0.01	0.57±0.00	0.33±0.01	0.44±0.01	0.45±0.00	0.55±0.00	0.47±0.01	0.57±0.00	0.55±0.02	0.60±0.01	0.87±0.07	0.76±0.04	0.58±0.04	0.61±0.02	0.44±0.01	0.54±0.00	0.80±0.02	0.73±0.01	0.83±0.04	0.74±0.02
	20	0.61±0.02	0.65±0.01	0.54±0.03	0.60±0.02	0.37±0.00	0.48±0.00	0.55±0.01	0.62±0.00	0.53±0.01	0.61±0.00	0.61±0.01	0.64±0.00	0.85±0.08	0.76±0.04	0.58±0.02	0.63±0.01	0.53±0.01	0.61±0.00	0.79±0.05	0.73±0.02	0.82±0.03	0.74±0.01
PEMS04	3	0.80±0.03	0.75±0.01	0.73±0.03	0.71±0.01	0.78±0.03	0.73±0.01	0.72±0.02	0.71±0.01	0.83±0.02	0.77±0.01	0.73±0.02	0.69±0.01	0.97±0.09	0.81±0.05	0.78±0.03	0.73±0.02	0.87±0.01	0.79±0.00	0.87±0.05	0.76±0.02	0.95±0.10	0.80±0.04
	5	0.75±0.03	0.72±0.01	0.82±0.03	0.75±0.01	0.85±0.02	0.78±0.01	0.82±0.01	0.76±0.00	0.78±0.02	0.74±0.01	0.90±0.05	0.78±0.02	0.90±0.04	0.72±0.02	0.80±0.06	0.74±0.02	0.78±0.02	0.75±0.01	0.81±0.04	0.74±0.02	0.97±0.09	0.81±0.05
	10	0.86±0.04	0.77±0.02	0.73±0.05	0.70±0.03	0.76±0.02	0.73±0.01	0.77±0.01	0.74±0.00	0.77±0.02	0.74±0.01	0.79±0.05	0.72±0.03	0.90±0.06	0.78±0.02	0.89±0.08	0.78±0.04	0.72±0.02	0.71±0.01	0.91±0.03	0.79±0.02	0.79±0.05	0.72±0.03
	20	0.78±0.03	0.71±0.02	0.72±0.04	0.70±0.02	0.79±0.03	0.74±0.01	0.81±0.01	0.76±0.01	0.82±0.01	0.76±0.01	0.92±0.06	0.78±0.02	0.86±0.06	0.76±0.03	0.75±0.04	0.72±0.02	0.80±0.04	0.75±0.02	0.89±0.04	0.77±0.02	0.97±0.09	0.80±0.04
	3	0.73±0.02	0.71±0.01	0.76±0.04	0.72±0.02	0.72±0.02	0.71±0.01	0.68±0.03	0.68±0.01	0.73±0.02	0.71±0.01	0.83±0.07	0.74±0.04	0.83±0.04	0.73±0.02	0.80±0.06	0.74±0.03	0.63±0.02	0.65±0.01	0.98±0.09	0.81±0.04	0.98±0.08	0.82±0.04
	5	0.76±0.03	0.72±0.01	0.75±0.05	0.71±0.02	0.72±0.01	0.71±0.01	0.66±0.02	0.67±0.01	0.68±0.01	0.68±0.00	0.93±0.07	0.80±0.04	0.93±0.07	0.79±0.03	0.88±0.06	0.78±0.03	0.61±0.03	0.64±0.01	0.88±0.08	0.77±0.04	0.93±0.03	0.79±0.01
	10	0.88±0.03	0.77±0.01	0.74±0.02	0.71±0.01	0.72±0.01	0.71±0.00	0.69±0.02	0.68±0.01	0.70±0.01	0.69±0.01	0.89±0.10	0.77±0.05	0.99±0.06	0.81±0.03	0.84±0.06	0.76±0.03	0.68±0.02	0.68±0.01	0.88±0.06	0.77±0.03	0.95±0.10	0.79±0.05
	20	0.87±0.01	0.77±0.05	0.73±0.02	0.70±0.01	0.70±0.01	0.70±0.01	0.69±0.02	0.69±0.01	0.70±0.02	0.69±0.01	0.99±0.03	0.82±0.01	0.98±0.13	0.81±0.07	0.75±0.04	0.71±0.02	0.67±0.03	0.68±0.01	0.92±0.07	0.79±0.03	0.88±0.05	0.77±0.02
	3	0.84±0.06	0.76±0.03	0.76±0.01	0.72±0.01	0.66±0.01	0.68±0.01	0.50±0.01	0.55±0.00	0.64±0.01	0.66±0.01	0.96±0.08	0.81±0.03	1.10±0.11	0.86±0.04	0.95±0.05	0.80±0.02	0.65±0.02	0.66±0.01	0.72±0.05	0.68±0.02	0.85±0.06	0.75±0.03
	5	0.82±0.04	0.75±0.02	0.74±0.02	0.71±0.01	0.48±0.01	0.55±0.01	0.66±0.00	0.67±0.00	0.63±0.03	0.65±0.02	0.89±0.06	0.77±0.03	0.86±0.02	0.75±0.01	0.94±0.07	0.80±0.03	0.60±0.02	0.63±0.01	0.92±0.07	0.78±0.04	0.82±0.03	0.73±0.01
	10	0.79±0.03	0.73±0.01	0.75±0.02	0.71±0.01	0.50±0.01	0.56±0.00	0.52±0.01	0.57±0.01	0.55±0.03	0.58±0.02	0.92±0.04	0.79±0.02	0.97±0.10	0.81±0.04	0.80±0.03	0.74±0.02	0.54±0.02	0.58±0.01	0.92±0.06	0.79±0.01	0.91±0.07	0.79±0.04
	20	0.96±0.04	0.80±0.02	0.76±0.03	0.72±0.01	0.58±0.01	0.62±0.00	0.55±0.01	0.59±0.00	0.61±0.02	0.63±0.01	0.96±0.03	0.81±0.01	0.95±0.07	0.80±0.03	0.72±0.02	0.71±0.01	0.58±0.01	0.62±0.01	0.84±0.07	0.75±0.03	0.92±0.05	0.78±0.03
PEMS07	3	0.86±0.04	0.77±0.01	0.61±0.01	0.63±0.00	0.89±0.02	0.80±0.01	0.88±0.02	0.79±0.01	0.81±0.01	0.75±0.01	0.91±0.05	0.78±0.02	0.90±0.07	0.77±0.03	0.92±0.06	0.78±0.03	0.84±0.03	0.77±0.01	1.00±0.07	0.80±0.04	0.94±0.07	0.79±0.03
	5	0.79±0.01	0.73±0.01	0.63±0.01	0.64±0.00	0.89±0.01	0.80±0.00	0.81±0.01	0.76±0.01	0.85±0.02	0.78±0.01	0.79±0.04	0.72±0.02	0.89±0.08	0.76±0.03	0.90±0.11	0.78±0.05	0.74±0.01	0.72±0.01	0.92±0.08	0.78±0.04	0.93±0.05	0.79±0.03
	10	0.82±0.04	0.74±0.01	0.64±0.01	0.66±0.01	0.82±0.02	0.76±0.01	0.85±0.01	0.78±0.00	0.80±0.02	0.75±0.01	0.93±0.08	0.78±0.03	0.99±0.07	0.81±0.03	0.90±0.11	0.77±0.05	0.81±0.02	0.75±0.01	0.81±0.05	0.74±0.02	0.86±0.02	0.76±0.01
	20	0.86±0.04	0.75±0.02	0.71±0.01	0.69±0.01	0.84±0.02	0.76±0.01	0.83±0.02	0.77±0.01	0.83±0.02	0.76±0.01	0.85±0.08	0.75±0.04	0.84±0.06	0.74±0.02	0.75±0.03	0.71±0.02	0.80±0.02	0.75±0.01	0.94±0.09	0.78±0.04	0.89±0.09	0.76±0.04
	3	0.74±0.05	0.71±0.02	0.61±0.02	0.63±0.01	0.65±0.02	0.66±0.01	0.66±0.01	0.67±0.01	0.66±0.03	0.67±0.02	0.93±0.05	0.79±0.02	1.08±0.13	0.85±0.05	0.82±0.05	0.74±0.02	0.62±0.01	0.64±0.01	0.90±0.07	0.77±0.03	0.75±0.09	0.69±0.04
	5	0.72±0.02	0.68±0.01	0.61±0.02	0.63±0.01	0.66±0.02	0.67±0.01	0.63±0.02	0.65±0.01	0.62±0.02	0.64±0.01	0.76±0.06	0.71±0.03	0.97±0.09	0.80±0.04	0.84±0.04	0.75±0.02	0.61±0.01	0.64±0.01	1.03±0.09	0.83±0.04	0.80±0.03	0.72±0.01
	10	0.93±0.03	0.79±0.02	0.65±0.03	0.66±0.02	0.66±0.01	0.67±0.01	0.67±0.03	0.67±0.01	0.63±0.01	0.66±0.00	0.89±0.02	0.76±0.01	1.04±0.10	0.82±0.04	0.83±0.05	0.74±0.03	0.66±0.01	0.67±0.00	0.88±0.06	0.76±0.03	0.74±0.02	0.70±0.01
	20	0.86±0.03	0.75±0.01	0.62±0.02	0.64±0.01	0.67±0.01	0.68±0.00	0.66±0.03	0.67±0.02	0.66±0.02	0.67±0.01	0.90±0.06	0.77±0.03	0.94±0.04	0.79±0.02	0.68±0.03	0.67±0.02	0.66±0.01	0.67±0.01	0.84±0.07	0.74±0.03	0.91±0.04	0.77±0.01
	3	0.72±0.02	0.69±0.01	0.54±0.01	0.58±0.01	0.43±0.00	0.52±0.00	0.58±0.01	0.61±0.00	0.62±0.01	0.65±0.00	0.87±0.05	0.76±0.02	0.91±0.08	0.77±0.03	0.95±0.09	0.79±0.04	0.46±0.01	0.53±0.00	0.78±0.05	0.71±0.03	0.83±0.06	0.74±0.03
	5	0.67±0.03	0.67±0.01	0.59±0.02	0.62±0.01	0.45±0.01	0.53±0.00	0.51±0.01	0.56±0.00	0.52±0.01	0.57±0.01	0.86±0.10	0.75±0.05	1.17±0.10	0.88±0.04	0.85±0.06	0.75±0.02	0.50±0.00	0.56±0.00	0.94±0.10	0.79±0.05	0.86±0.04	0.75±0.02
	10	0.86±0.08	0.75±0.04	0.55±0.02	0.59±0.01	0.5																	

Table 12. Extended ablation results across four benchmark datasets(ETTh1, ETTh2, ETTm1, ETTm2) under different synthetic sample sizes. **Green rows** denote results of each method augmented with *CondTSP*, and the **blue rows** denote results augmented with our proposed method. All values are averaged over three runs; lower MSE/MAE indicate better performance.

Models	EDF [2025]		MCT [2025]		DATM [2024]		FTD [2023]		PP [2023]		TESLA [2023]		IDM [2023]		FRPo [2022]		MTT [2022]		KIP [2021]		DC [2021]		
	Metric	MSE	MAE	MSE	MAE	MSE	MAE	MSE	MAE	MSE	MAE	MSE	MAE	MSE	MAE	MSE	MAE	MSE	MAE	MSE	MAE	MSE	MAE
ETTh1	3	0.87±0.02	0.70±0.01	0.98±0.07	0.74±0.02	0.70±0.01	0.71±0.01	0.90±0.03	0.71±0.01	0.89±0.02	0.71±0.01	0.93±0.05	0.72±0.02	1.17±0.06	0.81±0.01	0.97±0.05	0.74±0.02	0.92±0.04	0.72±0.02	0.96±0.02	0.73±0.01	1.07±0.04	0.77±0.01
	5	0.90±0.04	0.71±0.02	0.95±0.03	0.73±0.01	0.87±0.05	0.70±0.02	0.90±0.05	0.71±0.02	0.86±0.02	0.70±0.01	0.94±0.02	0.73±0.01	1.10±0.06	0.78±0.02	0.98±0.06	0.75±0.02	0.88±0.03	0.70±0.01	1.05±0.04	0.77±0.02	1.05±0.04	0.77±0.02
	10	0.86±0.04	0.69±0.01	0.98±0.03	0.74±0.01	0.86±0.04	0.69±0.02	0.86±0.01	0.70±0.01	0.83±0.01	0.68±0.00	0.91±0.05	0.71±0.02	1.10±0.11	0.79±0.04	0.88±0.04	0.70±0.02	0.87±0.05	0.70±0.02	1.13±0.07	0.80±0.03	1.06±0.04	0.77±0.01
	20	0.87±0.04	0.70±0.02	0.98±0.07	0.75±0.02	0.89±0.03	0.70±0.01	0.87±0.03	0.70±0.01	0.86±0.04	0.69±0.02	0.97±0.06	0.73±0.02	1.17±0.05	0.81±0.02	0.84±0.03	0.68±0.01	0.87±0.03	0.70±0.01	1.15±0.07	0.81±0.03	1.07±0.10	0.77±0.04
ETTh2	3	0.82±0.03	0.67±0.01	0.99±0.07	0.75±0.03	0.83±0.03	0.68±0.01	0.77±0.03	0.65±0.01	0.85±0.03	0.68±0.01	0.93±0.02	0.72±0.01	1.09±0.04	0.79±0.02	1.05±0.03	0.77±0.02	0.78±0.03	0.65±0.02	1.15±0.03	0.81±0.01	1.05±0.02	0.77±0.01
	5	0.87±0.02	0.70±0.01	0.93±0.05	0.72±0.02	0.84±0.03	0.68±0.01	0.84±0.02	0.68±0.01	0.78±0.05	0.65±0.02	0.96±0.03	0.72±0.01	1.12±0.07	0.79±0.03	0.87±0.02	0.70±0.01	0.86±0.05	0.69±0.01	1.11±0.09	0.80±0.03	1.08±0.07	0.77±0.02
	10	0.88±0.02	0.70±0.01	1.00±0.07	0.75±0.02	0.82±0.03	0.67±0.01	0.84±0.01	0.68±0.01	0.80±0.04	0.66±0.02	0.94±0.03	0.72±0.01	1.09±0.08	0.78±0.03	0.90±0.03	0.71±0.02	0.81±0.03	0.67±0.01	1.01±0.04	0.75±0.02	1.06±0.03	0.77±0.01
	20	0.87±0.04	0.70±0.02	0.99±0.08	0.75±0.03	0.85±0.04	0.68±0.01	0.84±0.02	0.68±0.01	0.84±0.05	0.68±0.02	0.95±0.08	0.73±0.03	1.17±0.08	0.81±0.03	0.80±0.02	0.67±0.01	0.82±0.03	0.68±0.01	1.17±0.06	0.81±0.02	1.04±0.08	0.77±0.03
ETTh1	3	0.81±0.03	0.67±0.01	0.89±0.03	0.70±0.01	0.68±0.03	0.59±0.01	0.74±0.02	0.63±0.01	0.76±0.03	0.63±0.01	0.97±0.07	0.73±0.02	1.06±0.07	0.78±0.03	0.87±0.03	0.69±0.01	0.73±0.03	0.62±0.01	1.13±0.08	0.80±0.03	1.10±0.11	0.79±0.04
	5	0.84±0.04	0.68±0.02	0.92±0.04	0.72±0.02	0.68±0.04	0.59±0.01	0.72±0.04	0.61±0.02	0.72±0.02	0.62±0.01	0.99±0.06	0.74±0.03	1.13±0.11	0.80±0.04	0.81±0.01	0.66±0.00	0.69±0.03	0.59±0.01	0.87±0.07	0.70±0.03	1.02±0.09	0.76±0.04
	10	0.85±0.02	0.68±0.01	0.93±0.03	0.72±0.02	0.66±0.02	0.59±0.01	0.70±0.03	0.60±0.01	0.74±0.02	0.62±0.01	0.98±0.04	0.74±0.01	1.07±0.06	0.78±0.02	0.76±0.02	0.64±0.01	0.70±0.02	0.60±0.01	1.14±0.08	0.80±0.03	1.04±0.07	0.77±0.03
	20	0.85±0.06	0.68±0.02	0.91±0.06	0.71±0.02	0.73±0.02	0.62±0.01	0.73±0.03	0.62±0.01	0.73±0.04	0.63±0.02	0.98±0.04	0.74±0.02	1.13±0.07	0.80±0.03	0.74±0.02	0.63±0.01	0.74±0.03	0.62±0.01	1.17±0.11	0.82±0.04	1.10±0.08	0.79±0.03
ETTh2	3	0.69±0.05	0.66±0.02	0.86±0.07	0.73±0.03	0.84±0.05	0.73±0.02	0.75±0.03	0.70±0.02	0.86±0.07	0.74±0.03	0.75±0.02	0.69±0.01	0.98±0.08	0.78±0.03	0.69±0.07	0.66±0.04	0.75±0.02	0.69±0.01	0.75±0.06	0.67±0.03	0.92±0.08	0.76±0.03
	5	0.63±0.05	0.63±0.03	0.84±0.03	0.73±0.02	0.81±0.04	0.72±0.02	0.66±0.03	0.65±0.01	0.77±0.06	0.70±0.03	0.83±0.09	0.72±0.05	0.88±0.14	0.74±0.07	0.86±0.08	0.74±0.04	0.61±0.03	0.62±0.01	0.74±0.08	0.69±0.04	0.94±0.03	0.76±0.01
	10	0.69±0.02	0.66±0.01	0.82±0.10	0.72±0.03	0.73±0.04	0.68±0.02	0.77±0.05	0.70±0.02	0.64±0.01	0.64±0.02	0.59±0.02	0.60±0.01	1.09±0.05	0.74±0.01	0.70±0.05	0.67±0.03	0.77±0.04	0.70±0.02	0.83±0.02	0.78±0.04	0.85±0.08	0.73±0.04
	20	0.65±0.06	0.64±0.03	0.65±0.05	0.64±0.03	0.74±0.03	0.68±0.01	0.82±0.06	0.73±0.03	0.76±0.03	0.70±0.01	0.61±0.07	0.61±0.03	0.79±0.08	0.70±0.04	0.77±0.06	0.70±0.03	0.72±0.05	0.68±0.03	0.95±0.04	0.77±0.02	0.91±0.13	0.75±0.06
ETTh1	3	0.67±0.03	0.66±0.02	0.76±0.06	0.69±0.03	0.66±0.03	0.65±0.01	0.67±0.05	0.65±0.03	0.67±0.03	0.65±0.02	0.70±0.05	0.67±0.02	0.97±0.15	0.77±0.05	0.88±0.07	0.75±0.03	0.54±0.02	0.59±0.02	1.14±0.11	0.84±0.06	0.87±0.07	0.73±0.03
	5	0.65±0.02	0.65±0.01	0.82±0.08	0.72±0.04	0.63±0.02	0.63±0.01	0.64±0.04	0.64±0.02	0.64±0.02	0.64±0.01	0.69±0.04	0.66±0.02	0.85±0.07	0.72±0.03	0.85±0.09	0.73±0.04	0.59±0.03	0.61±0.02	1.07±0.15	0.81±0.06	0.94±0.12	0.76±0.06
	10	0.63±0.04	0.64±0.02	0.75±0.09	0.68±0.04	0.68±0.05	0.66±0.03	0.61±0.02	0.63±0.01	0.57±0.03	0.61±0.02	0.71±0.06	0.67±0.03	0.86±0.05	0.74±0.02	0.82±0.09	0.72±0.04	0.59±0.05	0.61±0.03	1.08±0.12	0.83±0.05	0.79±0.10	0.70±0.05
	20	0.65±0.07	0.64±0.04	0.72±0.02	0.67±0.01	0.64±0.02	0.64±0.01	0.62±0.02	0.63±0.01	0.58±0.01	0.61±0.00	0.75±0.03	0.68±0.02	1.01±0.05	0.80±0.02	0.67±0.04	0.65±0.02	0.57±0.02	0.60±0.01	1.04±0.10	0.80±0.04	0.75±0.11	0.68±0.05
ETTh2	3	0.62±0.02	0.63±0.01	0.71±0.05	0.67±0.03	0.26±0.02	0.38±0.02	0.34±0.03	0.46±0.02	0.35±0.01	0.46±0.01	0.72±0.05	0.67±0.02	1.02±0.08	0.80±0.03	0.42±0.04	0.51±0.03	0.31±0.03	0.43±0.02	0.65±0.09	0.64±0.04	0.85±0.06	0.73±0.02
	5	0.45±0.04	0.53±0.03	0.62±0.06	0.62±0.03	0.24±0.01	0.37±0.01	0.31±0.02	0.43±0.02	0.27±0.02	0.40±0.02	0.71±0.07	0.66±0.04	0.98±0.07	0.78±0.03	0.53±0.02	0.57±0.01	0.26±0.02	0.39±0.02	0.80±0.13	0.71±0.07	0.95±0.09	0.77±0.04
	10	0.56±0.04	0.59±0.03	0.61±0.07	0.62±0.03	0.26±0.01	0.38±0.01	0.26±0.01	0.39±0.01	0.28±0.02	0.41±0.02	0.73±0.07	0.67±0.03	1.03±0.07	0.80±0.03	0.39±0.04	0.49±0.02	0.24±0.01	0.37±0.01	0.84±0.11	0.72±0.07	0.91±0.13	0.75±0.06
	20	0.53±0.02	0.58±0.01	0.59±0.07	0.61±0.04	0.28±0.02	0.41±0.02	0.30±0.02	0.42±0.02	0.35±0.03	0.46±0.02	0.80±0.04	0.70±0.03	1.08±0.16	0.83±0.06	0.54±0.04	0.58±0.02	0.29±0.01	0.41±0.01	0.82±0.05	0.71±0.03	0.88±0.12	0.74±0.06
ETTh1	3	0.86±0.02	0.69±0.01	0.82±0.02	0.68±0.01	0.83±0.02	0.68±0.01	0.88±0.01	0.70±0.00	0.88±0.03	0.70±0.00	0.81±0.01	0.67±0.01	1.07±0.05	0.77±0.02	0.89±0.04	0.70±0.02	0.88±0.01	0.71±0.00	1.04±0.07	0.76±0.03	0.99±0.06	0.74±0.02
	5	0.87±0.01	0.69±0.01	0.80±0.03	0.67±0.01	0.90±0.02	0.71±0.01	0.89±0.02	0.71±0.01	0.89±0.01	0.71±0.00	0.80±0.02	0.67±0.01	1.06±0.04	0.77±0.01	0.90±0.02	0.71±0.01	0.91±0.01	0.71±0.01	1.11±0.07	0.78±0.03	0.97±0.04	0.74±0.02
	10	0.85±0.02	0.69±0.01	0.79±0.03	0.66±0.01	0.88±0.02	0.71±0.01	0.89±0.03	0.71±0.01	0.85±0.02	0.69±0.01	0.83±0.02	0.67±0.01	1.10±0.08	0.78±0.02	0.90±0.04	0.71±0.02	0.86±0.01	0.70±0.00	1.06±0.03	0.77±0.02	1.03±0.09	0.76±0.04
	20	0.84±0.04	0.68±0.01	0.82±0.02	0.68±0.01	0.87±0.01	0.70±0.00	0.89±0.02	0.71±0.01	0.89±0.02	0.71±0.01	0.82±0.01	0.67±0.01	1.03±0.04	0.76±0.02	0.85±0.01	0.68±0.00	0.90±0.03	0.71±0.01	1.06±0.05	0.77±0.02	0.99±0.06	0.74±0.02
ETTh2	3	0.79±0.01	0.65±0.01	0.76±0.03	0.63±0.01	0.74±0.01	0.63±0.00	0.80±0.02	0.66±0.01	0.75±0.02	0.64±0.01	0.71±0.02	0.60±0.01	0.87±0.04	0.69±0.02	0.89±0.03	0.70±0.01	0.75±0.02	0.64±0.01	0.94±0.02	0.72±0.01	1.05±0.06	0.76±0.03
	5	0.77±0.03	0.65±0.01	0.74±0.02	0.63±0.01	0.73±0.01	0.63±0.00	0.76±0.02	0.64±0.01	0.73±0.01	0.63±0.00	0.75±0.02	0.63±0.01	1.06±0.02	0.77±0.00	0.90±0.01	0.70±0.01	0.76±0.02	0.64±0.01	1.09±0.08	0.78±0.03	1.01±0.03	0.75±0.01
	10	0.75±0.01	0.64±0.00	0.74±0.02	0.63±0.01	0.74±0.01	0.63±0.00	0.78±0.01	0.65±0.01	0.74±0.02	0.64±0.01	0.73±0.01	0.62±0.01	1.05±0.05	0.77±0.02	0.85±0.03	0.68±0.02	0.75±0.01	0.64±0.00	1.04±0.07	0.76±0.03	1.01±0.07	0.75±0.03
	20	0.81±0.02	0.67±0.01	0.75±0.02	0.63±0.01	0.79±0.02	0.66±0.01	0.77±0.01	0.65±0.00	0.75±0.02	0.64±0.01	0.75±0.02	0.63±0.01	1.01±0.03	0.75±0.01	0.81±0.02	0.66±0.01	0.78±0.02	0.65±0.01	1.01±0.06	0.75±0.02	1.01±0.03	0.75±0.02
ETTh1	3	0.70±0.01	0.61±0.01	0.73±0.02	0.59±0.01	0.67±0.02	0.58±0.01	0.69±0.01	0.59±0.01	0.71±0.02	0.61±0.01	0.82±0.02	0.67±0.01	1.17±0.07	0.82±0.03	1.13±0.05	0.80±0.02	0.70±0.01	0.60±0.01	1.13±0.08	0.81±0.03	1.05±0.07	0.77±0.03
	5	0.75±0.02	0.63±0.01	0.71±0.01	0.54±0.01	0.63±0.01	0.54±0.01	0.68±0.02	0.58±0.01	0.66±0.01	0.58±0.00	0.73±0.01	0.62±0.01	1.03±0.07	0.76±0.03	0.76±0.02	0.62±0.01	0.68±0.02	0.59±0.01	1.07±0.05	0.77±0.02	1.02±0.04	0.75±0.02
	10	0.7																					

Table 13. Extended ablation results across four benchmark datasets(WindL1, WindL2, WindL3, WindL4) under different synthetic sample sizes. **Green rows** denote results of each method augmented with *CondTSP*, and the **blue rows** denote results augmented with our proposed method. All values are averaged over three runs; lower MSE/MAE indicate better performance.

Models	EDF [2025]		MCT [2025]		DATM [2024]		FTD [2023]		PP [2023]		TESLA [2023]		IDM [2023]		FRPo [2022]		MTT [2022]		KIP [2021]		DC [2021]		
	MSE	MAE	MSE	MAE	MSE	MAE	MSE	MAE	MSE	MAE	MSE	MAE	MSE	MAE	MSE	MAE	MSE	MAE	MSE	MAE	MSE	MAE	
WindL1	3	0.93±0.01	0.79±0.00	0.93±0.02	0.78±0.01	0.97±0.02	0.81±0.01	0.99±0.01	0.82±0.00	0.96±0.01	0.80±0.00	0.94±0.02	0.79±0.01	1.19±0.04	0.88±0.01	1.09±0.07	0.85±0.03	0.96±0.01	0.80±0.01	1.21±0.06	0.89±0.02	1.19±0.07	0.88±0.03
	5	0.95±0.01	0.80±0.00	0.94±0.02	0.79±0.01	0.95±0.01	0.80±0.00	0.94±0.01	0.80±0.01	0.93±0.01	0.79±0.00	0.93±0.02	0.78±0.01	1.16±0.04	0.87±0.02	1.02±0.01	0.82±0.01	0.95±0.01	0.80±0.00	1.18±0.09	0.87±0.03	1.17±0.07	0.87±0.03
	10	0.94±0.00	0.79±0.00	0.92±0.01	0.78±0.01	0.95±0.01	0.80±0.01	0.95±0.01	0.80±0.00	0.96±0.01	0.81±0.00	0.92±0.01	0.78±0.00	1.17±0.02	0.87±0.02	1.00±0.03	0.81±0.01	0.94±0.01	0.80±0.01	1.22±0.06	0.89±0.02	1.17±0.07	0.87±0.03
	20	0.98±0.01	0.81±0.00	0.92±0.01	0.78±0.00	0.94±0.01	0.80±0.00	0.96±0.01	0.81±0.00	0.95±0.01	0.80±0.00	0.92±0.03	0.78±0.01	1.20±0.09	0.88±0.03	0.99±0.03	0.81±0.01	0.94±0.02	0.80±0.01	1.18±0.05	0.88±0.02	1.14±0.02	0.86±0.01
	CondTSP	3	0.89±0.01	0.77±0.00	0.93±0.01	0.78±0.00	0.90±0.01	0.77±0.01	0.89±0.02	0.77±0.01	0.89±0.01	0.77±0.01	0.91±0.01	0.77±0.00	1.18±0.07	0.87±0.03	1.04±0.01	0.83±0.01	0.91±0.01	0.78±0.00	1.22±0.06	0.89±0.02	1.16±0.07
WindL2	3	0.86±0.01	0.75±0.00	0.86±0.02	0.74±0.01	0.82±0.01	0.73±0.00	0.82±0.01	0.73±0.00	0.81±0.01	0.71±0.00	0.93±0.03	0.78±0.01	1.23±0.05	0.89±0.02	0.93±0.02	0.77±0.01	0.84±0.00	0.74±0.00	1.11±0.03	0.84±0.01	1.18±0.03	0.87±0.01
	5	0.89±0.01	0.76±0.00	0.82±0.02	0.72±0.01	0.78±0.00	0.71±0.00	0.78±0.01	0.69±0.01	0.79±0.01	0.70±0.00	0.89±0.01	0.76±0.00	1.17±0.06	0.86±0.02	0.94±0.01	0.77±0.01	0.79±0.01	0.70±0.01	1.21±0.06	0.88±0.02	1.16±0.07	0.87±0.03
	10	0.88±0.00	0.76±0.00	0.83±0.02	0.72±0.01	0.80±0.01	0.71±0.00	0.79±0.00	0.70±0.00	0.79±0.00	0.70±0.00	0.92±0.02	0.77±0.01	1.22±0.06	0.89±0.02	0.91±0.01	0.77±0.00	0.76±0.01	0.68±0.00	1.24±0.05	0.89±0.02	1.18±0.04	0.87±0.02
	20	0.90±0.01	0.77±0.00	0.85±0.01	0.73±0.01	0.80±0.01	0.71±0.01	0.81±0.01	0.72±0.01	0.83±0.01	0.73±0.00	0.97±0.02	0.79±0.01	1.25±0.07	0.90±0.03	0.92±0.01	0.78±0.01	0.83±0.01	0.73±0.00	1.27±0.09	0.90±0.03	1.17±0.05	0.87±0.02
	CondTSP	3	0.95±0.02	0.77±0.00	0.90±0.01	0.77±0.00	0.95±0.01	0.80±0.01	0.97±0.00	0.80±0.00	0.94±0.01	0.79±0.00	0.82±0.01	0.72±0.00	1.21±0.02	0.88±0.00	0.95±0.02	0.78±0.01	0.97±0.01	0.81±0.00	1.06±0.02	0.82±0.01	1.16±0.06
WindL3	3	0.84±0.00	0.74±0.00	0.80±0.01	0.70±0.00	0.80±0.01	0.72±0.00	0.78±0.01	0.70±0.00	0.79±0.01	0.71±0.00	0.87±0.02	0.74±0.01	1.15±0.03	0.86±0.01	0.86±0.02	0.71±0.01	0.79±0.01	0.71±0.00	1.19±0.07	0.87±0.03	1.11±0.04	0.84±0.01
	5	0.83±0.01	0.74±0.00	0.79±0.02	0.70±0.01	0.77±0.01	0.70±0.00	0.78±0.01	0.70±0.00	0.78±0.01	0.71±0.00	0.85±0.02	0.74±0.01	1.15±0.04	0.86±0.02	0.85±0.01	0.73±0.00	0.76±0.01	0.69±0.00	1.16±0.04	0.85±0.02	1.10±0.05	0.84±0.02
	10	0.84±0.01	0.74±0.01	0.78±0.01	0.69±0.01	0.71±0.01	0.66±0.00	0.77±0.01	0.70±0.00	0.77±0.00	0.70±0.00	0.86±0.01	0.74±0.00	1.19±0.03	0.87±0.01	0.89±0.02	0.76±0.01	0.73±0.01	0.67±0.00	1.23±0.05	0.89±0.02	1.12±0.07	0.85±0.03
	20	0.84±0.01	0.74±0.00	0.80±0.02	0.71±0.01	0.76±0.01	0.69±0.00	0.76±0.01	0.69±0.01	0.78±0.01	0.70±0.00	0.90±0.02	0.76±0.01	1.13±0.07	0.85±0.03	0.87±0.02	0.75±0.01	0.77±0.02	0.70±0.01	1.22±0.03	0.88±0.01	1.10±0.04	0.84±0.01
	CondTSP	3	0.98±0.01	0.81±0.00	0.94±0.01	0.79±0.01	0.99±0.02	0.82±0.01	1.00±0.02	0.82±0.01	0.96±0.01	0.80±0.00	0.90±0.02	0.77±0.01	1.17±0.07	0.87±0.03	1.06±0.03	0.83±0.01	0.97±0.01	0.81±0.00	1.13±0.04	0.86±0.01	1.16±0.08
WindL4	3	0.97±0.01	0.81±0.00	0.91±0.01	0.77±0.00	0.99±0.01	0.81±0.01	0.99±0.01	0.81±0.00	1.01±0.01	0.82±0.00	0.94±0.02	0.78±0.01	1.24±0.04	0.89±0.02	1.06±0.03	0.83±0.01	0.98±0.01	0.81±0.00	1.16±0.07	0.86±0.03	1.21±0.07	0.88±0.02
	5	0.97±0.02	0.81±0.01	0.93±0.01	0.78±0.00	0.97±0.01	0.80±0.01	0.99±0.01	0.82±0.00	0.98±0.01	0.81±0.00	0.95±0.01	0.79±0.00	1.23±0.07	0.89±0.03	1.01±0.02	0.81±0.01	0.97±0.01	0.80±0.00	1.16±0.04	0.86±0.02	1.19±0.05	0.88±0.02
	10	0.98±0.00	0.81±0.00	0.93±0.01	0.78±0.00	0.98±0.02	0.81±0.01	0.96±0.01	0.80±0.00	0.98±0.02	0.81±0.01	0.96±0.01	0.80±0.00	1.21±0.06	0.88±0.02	1.02±0.04	0.81±0.02	0.97±0.01	0.81±0.00	1.25±0.10	0.89±0.04	1.20±0.03	0.88±0.01
	20	0.98±0.02	0.81±0.01	0.95±0.01	0.79±0.00	0.97±0.01	0.80±0.01	1.00±0.02	0.82±0.01	0.98±0.01	0.81±0.00	0.98±0.02	0.80±0.01	1.17±0.02	0.86±0.01	0.98±0.01	0.80±0.00	0.97±0.01	0.81±0.01	1.17±0.05	0.86±0.02	1.19±0.03	0.87±0.01
	CondTSP	3	0.95±0.02	0.79±0.01	0.89±0.01	0.75±0.00	0.91±0.01	0.77±0.00	0.90±0.01	0.76±0.01	0.91±0.02	0.77±0.01	0.94±0.02	0.78±0.01	1.16±0.05	0.86±0.02	1.13±0.05	0.85±0.02	0.90±0.01	0.77±0.01	1.15±0.05	0.86±0.02	1.20±0.02

Table 14. Extended ablation results across four benchmark datasets(Wike2000, Weather, Electricity, Traffic) under different synthetic sample sizes. **Green rows** denote results of each method augmented with *CondTSP*, and the **blue rows** denote results augmented with our proposed method. All values are averaged over three runs; lower MSE/MAE indicate better performance.

Models	Metric	EDF [2025]		MCT [2025]		DATM [2024]		FTD [2023]		PP [2023]		TESLA [2023]		IDM [2023]		FRPo [2022]		MTT [2022]		KIP [2021]		DC [2021]			
		MSE	MAE	MSE	MAE	MSE	MAE	MSE	MAE	MSE	MAE	MSE	MAE	MSE	MAE	MSE	MAE	MSE	MAE	MSE	MAE	MSE	MAE		
Wike2000	3	1.19±0.02	0.73±0.01	1.14±0.07	0.71±0.04	0.97±0.03	0.64±0.02	1.00±0.01	0.66±0.01	1.06±0.02	0.68±0.01	1.17±0.04	0.72±0.02	1.17±0.04	0.72±0.02	1.18±0.03	0.73±0.02	1.05±0.04	0.68±0.03	1.27±0.06	0.77±0.03	1.16±0.01	0.71±0.01	1.19±0.09	0.72±0.04
	5	1.18±0.06	0.73±0.03	1.15±0.04	0.72±0.02	0.99±0.02	0.65±0.01	0.99±0.02	0.64±0.02	1.03±0.02	0.66±0.01	1.19±0.07	0.72±0.03	1.20±0.03	0.74±0.01	1.18±0.07	0.72±0.03	1.05±0.03	0.68±0.02	1.14±0.03	0.71±0.02	1.19±0.09	0.72±0.04	1.18±0.05	0.72±0.03
	10	1.17±0.03	0.73±0.02	1.17±0.04	0.72±0.03	0.99±0.05	0.66±0.03	0.98±0.02	0.64±0.01	1.07±0.05	0.69±0.03	1.21±0.05	0.73±0.03	1.17±0.05	0.72±0.03	1.18±0.04	0.72±0.02	1.03±0.04	0.66±0.03	1.21±0.09	0.73±0.04	1.18±0.05	0.73±0.02	1.18±0.05	0.72±0.03
	20	1.18±0.05	0.72±0.03	1.16±0.04	0.72±0.03	1.00±0.02	0.66±0.02	1.00±0.04	0.65±0.03	1.05±0.03	0.68±0.02	1.17±0.04	0.73±0.02	1.21±0.05	0.74±0.02	1.22±0.06	0.74±0.02	1.04±0.05	0.68±0.03	1.21±0.06	0.74±0.02	1.15±0.05	0.71±0.03	1.18±0.05	0.72±0.03
	3	1.16±0.04	0.72±0.03	1.17±0.03	0.72±0.01	1.02±0.03	0.67±0.02	1.05±0.03	0.68±0.02	1.09±0.03	0.70±0.03	1.20±0.06	0.74±0.03	1.19±0.06	0.74±0.03	1.16±0.04	0.72±0.02	1.06±0.04	0.68±0.03	1.22±0.03	0.75±0.02	1.18±0.04	0.72±0.02	1.18±0.04	0.72±0.02
	5	1.20±0.06	0.73±0.02	1.17±0.04	0.72±0.01	1.01±0.02	0.67±0.02	1.05±0.02	0.67±0.01	1.05±0.01	0.67±0.00	1.16±0.04	0.71±0.03	1.17±0.02	0.72±0.01	1.23±0.05	0.75±0.03	1.04±0.04	0.67±0.03	1.19±0.02	0.72±0.01	1.21±0.07	0.74±0.04	1.19±0.02	0.74±0.04
	10	1.20±0.04	0.74±0.02	1.17±0.04	0.72±0.02	1.02±0.03	0.67±0.02	1.06±0.03	0.68±0.01	1.07±0.03	0.69±0.02	1.19±0.05	0.73±0.03	1.21±0.04	0.74±0.02	1.22±0.01	0.73±0.03	1.05±0.02	0.68±0.02	1.25±0.03	0.77±0.03	1.17±0.02	0.72±0.02	1.17±0.02	0.72±0.02
	20	1.16±0.07	0.70±0.03	1.17±0.02	0.73±0.02	1.02±0.03	0.66±0.02	1.06±0.04	0.69±0.02	1.09±0.04	0.70±0.02	1.21±0.04	0.73±0.02	1.20±0.03	0.73±0.02	1.14±0.03	0.70±0.02	1.08±0.05	0.69±0.03	1.20±0.06	0.73±0.03	1.19±0.04	0.73±0.02	1.17±0.04	0.73±0.02
	3	1.17±0.06	0.72±0.02	1.17±0.05	0.72±0.03	1.01±0.01	0.67±0.01	1.08±0.04	0.69±0.03	1.07±0.06	0.69±0.04	1.18±0.06	0.73±0.03	1.21±0.05	0.73±0.03	1.22±0.07	0.75±0.04	1.07±0.05	0.69±0.03	1.25±0.06	0.76±0.04	1.18±0.03	0.73±0.01	1.18±0.03	0.73±0.01
	5	1.16±0.03	0.71±0.02	1.15±0.03	0.71±0.01	1.02±0.04	0.67±0.03	1.05±0.03	0.67±0.02	1.09±0.05	0.70±0.03	1.18±0.08	0.72±0.04	1.17±0.04	0.72±0.01	1.27±0.02	0.76±0.02	1.05±0.04	0.67±0.03	1.26±0.08	0.76±0.04	1.17±0.06	0.72±0.02	1.17±0.06	0.72±0.02
	10	1.19±0.07	0.73±0.03	1.14±0.02	0.70±0.01	1.01±0.03	0.66±0.02	1.03±0.05	0.67±0.03	1.09±0.05	0.70±0.04	1.20±0.04	0.73±0.02	1.19±0.03	0.73±0.01	1.19±0.07	0.73±0.03	1.06±0.02	0.68±0.02	1.21±0.08	0.73±0.03	1.18±0.07	0.73±0.04	1.18±0.07	0.73±0.04
	20	1.17±0.05	0.73±0.03	1.18±0.08	0.73±0.04	0.99±0.03	0.66±0.02	1.07±0.06	0.69±0.03	1.07±0.05	0.69±0.03	1.17±0.07	0.73±0.03	1.22±0.04	0.74±0.02	1.26±0.06	0.77±0.04	1.05±0.03	0.67±0.02	1.25±0.06	0.75±0.04	1.20±0.07	0.73±0.04	1.20±0.07	0.73±0.04
Weather	3	0.50±0.01	0.50±0.01	0.64±0.05	0.57±0.03	0.51±0.01	0.50±0.01	0.53±0.02	0.52±0.02	0.49±0.01	0.49±0.01	0.52±0.02	0.51±0.01	0.69±0.04	0.56±0.02	0.54±0.02	0.51±0.01	0.56±0.01	0.54±0.01	0.73±0.06	0.59±0.03	0.63±0.07	0.54±0.03	0.63±0.07	0.54±0.03
	5	0.59±0.01	0.55±0.01	0.51±0.03	0.49±0.01	0.48±0.02	0.47±0.01	0.55±0.01	0.53±0.01	0.57±0.00	0.54±0.00	0.56±0.01	0.53±0.01	0.63±0.03	0.55±0.02	0.55±0.02	0.51±0.01	0.56±0.01	0.53±0.01	0.68±0.05	0.57±0.02	0.61±0.04	0.54±0.02	0.61±0.04	0.54±0.02
	10	0.51±0.00	0.50±0.00	0.57±0.04	0.53±0.02	0.57±0.01	0.54±0.01	0.52±0.01	0.51±0.01	0.56±0.01	0.53±0.01	0.61±0.02	0.56±0.01	0.66±0.07	0.55±0.04	0.55±0.03	0.52±0.02	0.58±0.01	0.54±0.01	0.61±0.04	0.53±0.03	0.61±0.06	0.53±0.04	0.61±0.06	0.53±0.04
	20	0.50±0.01	0.49±0.01	0.48±0.01	0.48±0.01	0.56±0.01	0.53±0.01	0.52±0.01	0.51±0.01	0.52±0.01	0.51±0.01	0.57±0.02	0.53±0.01	0.67±0.07	0.56±0.04	0.53±0.02	0.51±0.01	0.50±0.01	0.50±0.01	0.68±0.04	0.57±0.02	0.63±0.02	0.54±0.01	0.63±0.02	0.54±0.01
	3	0.48±0.01	0.49±0.01	0.53±0.01	0.52±0.01	0.39±0.01	0.42±0.01	0.49±0.01	0.49±0.01	0.47±0.01	0.49±0.01	0.37±0.00	0.41±0.01	0.64±0.04	0.55±0.02	0.53±0.02	0.49±0.02	0.47±0.01	0.48±0.01	0.69±0.08	0.57±0.04	0.65±0.09	0.55±0.04	0.65±0.09	0.55±0.04
	5	0.46±0.01	0.48±0.01	0.46±0.01	0.48±0.01	0.38±0.02	0.42±0.02	0.48±0.01	0.49±0.01	0.47±0.01	0.48±0.01	0.39±0.01	0.43±0.01	0.61±0.07	0.53±0.04	0.46±0.02	0.46±0.01	0.48±0.01	0.49±0.00	0.63±0.04	0.55±0.02	0.61±0.06	0.54±0.03	0.61±0.06	0.54±0.03
	10	0.46±0.01	0.48±0.01	0.48±0.01	0.49±0.01	0.39±0.00	0.42±0.01	0.47±0.01	0.48±0.01	0.48±0.01	0.49±0.01	0.40±0.01	0.43±0.01	0.62±0.05	0.54±0.03	0.48±0.03	0.48±0.02	0.47±0.01	0.49±0.01	0.64±0.08	0.55±0.03	0.62±0.06	0.54±0.03	0.62±0.06	0.54±0.03
	20	0.44±0.01	0.47±0.01	0.47±0.01	0.48±0.01	0.36±0.01	0.40±0.01	0.48±0.01	0.48±0.01	0.48±0.01	0.48±0.01	0.42±0.00	0.44±0.00	0.66±0.03	0.56±0.02	0.47±0.03	0.48±0.02	0.49±0.01	0.50±0.01	0.59±0.03	0.53±0.02	0.62±0.04	0.53±0.02	0.62±0.04	0.53±0.02
	3	0.43±0.01	0.46±0.01	0.38±0.01	0.42±0.01	0.33±0.01	0.36±0.01	0.41±0.01	0.45±0.01	0.41±0.01	0.44±0.01	0.33±0.01	0.38±0.01	0.81±0.09	0.62±0.04	0.42±0.02	0.44±0.01	0.43±0.01	0.46±0.01	0.71±0.08	0.58±0.03	0.62±0.05	0.54±0.02	0.62±0.05	0.54±0.02
	5	0.45±0.01	0.47±0.01	0.37±0.01	0.41±0.01	0.33±0.01	0.38±0.01	0.37±0.01	0.41±0.01	0.34±0.01	0.39±0.01	0.39±0.01	0.43±0.01	0.62±0.05	0.54±0.02	0.40±0.02	0.42±0.02	0.38±0.01	0.42±0.01	0.70±0.07	0.57±0.03	0.62±0.05	0.54±0.02	0.62±0.05	0.54±0.02
	10	0.45±0.01	0.47±0.01	0.40±0.02	0.44±0.01	0.33±0.01	0.37±0.01	0.39±0.00	0.43±0.01	0.37±0.00	0.41±0.01	0.37±0.01	0.41±0.01	0.67±0.05	0.56±0.03	0.43±0.02	0.45±0.02	0.39±0.01	0.43±0.01	0.71±0.05	0.57±0.03	0.63±0.04	0.54±0.02	0.63±0.04	0.54±0.02
	20	0.46±0.01	0.48±0.01	0.40±0.01	0.43±0.01	0.33±0.01	0.38±0.01	0.37±0.00	0.42±0.00	0.39±0.01	0.43±0.01	0.36±0.01	0.40±0.01	0.60±0.04	0.52±0.02	0.43±0.01	0.45±0.01	0.40±0.00	0.44±0.00	0.60±0.05	0.53±0.02	0.62±0.04	0.54±0.02	0.62±0.04	0.54±0.02
Electricity	3	0.86±0.04	0.74±0.02	0.90±0.03	0.76±0.01	0.86±0.02	0.75±0.01	0.81±0.02	0.73±0.01	0.88±0.02	0.77±0.01	0.98±0.05	0.79±0.03	1.07±0.08	0.83±0.03	1.02±0.06	0.81±0.03	0.80±0.01	0.72±0.01	1.04±0.05	0.81±0.02	1.08±0.14	0.83±0.06	1.08±0.14	0.83±0.06
	5	0.86±0.04	0.74±0.02	0.84±0.06	0.74±0.03	0.81±0.02	0.74±0.03	0.81±0.02	0.73±0.01	0.81±0.03	0.73±0.01	1.07±0.01	0.83±0.00	1.04±0.06	0.82±0.02	1.02±0.05	0.82±0.02	0.82±0.01	0.74±0.00	1.19±0.11	0.88±0.04	1.07±0.10	0.83±0.05	1.07±0.10	0.83±0.05
	10	1.02±0.05	0.81±0.02	0.90±0.03	0.77±0.01	0.84±0.01	0.75±0.01	0.81±0.02	0.73±0.01	0.86±0.02	0.75±0.01	1.07±0.04	0.83±0.02	1.03±0.02	0.82±0.01	0.90±0.03	0.77±0.01	0.80±0.02	0.73±0.01	1.08±0.03	0.84±0.01	1.08±0.05	0.84±0.02	1.08±0.05	0.84±0.02
	20	1.01±0.03	0.81±0.01	0.90±0.03	0.76±0.01	0.86±0.02	0.75±0.01	0.82±0.01	0.73±0.01	0.84±0.03	0.75±0.01	1.07±0.02	0.83±0.01	1.08±0.13	0.83±0.05	0.92±0.04	0.78±0.02	0.81±0.02	0.73±0.01	1.11±0.10	0.85±0.04	1.14±0.06	0.85±0.03	1.14±0.06	0.85±0.03
	3	0.90±0.02	0.76±0.01	0.89±0.03	0.76±0.01	0.73±0.02	0.69±0.01	0.73±0.02	0.69±0.01	0.77±0.02	0.70±0.01	0.95±0.04	0.78±0.02	1.10±0.15	0.84±0.06	1.02±0.06	0.80±0.03	0.73±0.02	0.69±0.01	1.09±0.08	0.84±0.02	1.06±0.06	0.83±0.03	1.06±0.06	0.83±0.03
	5	1.02±0.07	0.80±0.03	0.86±0.04	0.75±0.02	0.72±0.01	0.69±0.01	0.74±0.01	0.69±0.01	0.75±0.02	0.69±0.01	1.09±0.09	0.83±0.04	1.12±0.04	0.85±0.02	0.97±0.08	0.80±0.04	0.73±0.02	0.69±0.01	1.03±0.07	0.81±0.03	1.15±0.08	0.86±0.02	1.15±0.08	0.86±0.02
	10	1.00±0.08	0.80±0.04	0.85±0.03	0.74±0.02	0.72±0.02	0.69±0.01	0.73±0.02	0.69±0.01	0.74±0.02	0.69±0.01	1.12±0.07	0.85±0.03	1.10±0.06	0.84±0.03	0.90±0.02	0.77±0.01	0.71±0.02	0.68±0.01	1.08±0.12	0.83±0.05	1.14±0.11	0.86±0.04	1.14±0.11	0.86±0.04
	20	1.06±0.08	0.82±0.03	0.85±0.01	0.74±0.01	0.77±0.02	0.71±0.01	0.72±0.03	0.68±0.02	0.75±0.02	0.69±0.01	1.05±0.08	0.82±0.03												

Table 15. Extended ablation results across four benchmark datasets(Solar, Global Temp, ExchangeRate, ILI) under different synthetic sample sizes. **Green rows** denote results of each method augmented with *CondTSF*, and the **blue rows** denote results augmented with our proposed method. All values are averaged over three runs; lower MSE/MAE indicate better performance.

Models	Metric	EDF [2025]		MCT [2025]		DATM [2024]		FTD [2023]		PP [2023]		TESLA [2023]		IDM [2023]		FRPo [2022]		MTT [2022]		KIP [2021]		DC [2021]	
		MSE	MAE	MSE	MAE	MSE	MAE	MSE	MAE	MSE	MAE	MSE	MAE	MSE	MAE	MSE	MAE	MSE	MAE	MSE	MAE	MSE	MAE
Solar	3	0.77±0.04	0.71±0.02	0.73±0.02	0.69±0.01	0.84±0.01	0.77±0.02	0.74±0.02	0.74±0.02	0.86±0.01	0.78±0.01	0.80±0.01	0.75±0.01	1.01±0.05	0.83±0.03	0.69±0.03	0.69±0.02	0.73±0.02	0.71±0.02	0.85±0.06	0.74±0.04	0.93±0.08	0.77±0.03
	5	0.78±0.01	0.75±0.02	0.72±0.01	0.69±0.01	0.81±0.02	0.76±0.01	0.84±0.01	0.76±0.01	0.80±0.01	0.76±0.02	0.74±0.01	0.73±0.01	0.94±0.04	0.78±0.02	0.67±0.04	0.66±0.03	0.79±0.02	0.75±0.01	0.90±0.04	0.76±0.03	0.85±0.04	0.76±0.01
	10	0.78±0.02	0.73±0.02	0.71±0.01	0.70±0.02	0.82±0.01	0.78±0.01	0.83±0.02	0.77±0.01	0.84±0.02	0.77±0.01	0.73±0.02	0.71±0.01	1.03±0.08	0.83±0.04	0.77±0.04	0.70±0.02	0.84±0.04	0.77±0.02	1.01±0.05	0.82±0.03	0.89±0.05	0.77±0.03
	20	0.79±0.03	0.74±0.02	0.74±0.01	0.71±0.01	0.79±0.01	0.75±0.01	0.77±0.02	0.73±0.01	0.80±0.01	0.75±0.01	0.82±0.06	0.76±0.02	0.90±0.05	0.76±0.02	0.78±0.03	0.72±0.02	0.80±0.01	0.75±0.01	0.87±0.06	0.76±0.03	0.93±0.02	0.79±0.01
	3	0.66±0.01	0.68±0.01	0.66±0.01	0.66±0.01	0.69±0.01	0.67±0.01	0.62±0.01	0.65±0.01	0.69±0.01	0.68±0.02	0.67±0.02	0.67±0.02	0.99±0.03	0.79±0.03	0.84±0.05	0.75±0.02	0.69±0.01	0.69±0.01	0.90±0.06	0.74±0.03	0.93±0.03	0.77±0.03
	5	0.63±0.01	0.66±0.02	0.62±0.00	0.64±0.02	0.65±0.01	0.67±0.01	0.67±0.01	0.68±0.01	0.67±0.01	0.68±0.01	0.71±0.02	0.68±0.01	0.83±0.03	0.71±0.01	0.76±0.03	0.72±0.01	0.65±0.01	0.66±0.01	1.04±0.08	0.82±0.03	0.91±0.05	0.78±0.02
	10	0.79±0.02	0.74±0.02	0.62±0.01	0.63±0.01	0.66±0.01	0.68±0.01	0.67±0.01	0.68±0.02	0.64±0.01	0.65±0.01	0.71±0.03	0.68±0.01	0.88±0.06	0.77±0.04	0.72±0.01	0.71±0.01	0.63±0.01	0.65±0.01	0.91±0.06	0.78±0.02	0.89±0.06	0.78±0.02
	20	0.82±0.02	0.68±0.02	0.66±0.01	0.66±0.01	0.69±0.01	0.70±0.01	0.68±0.01	0.70±0.00	0.65±0.01	0.66±0.01	0.77±0.04	0.72±0.02	0.97±0.06	0.80±0.03	0.79±0.03	0.73±0.02	0.67±0.01	0.67±0.01	0.88±0.02	0.75±0.03	0.94±0.03	0.77±0.03
	3	0.82±0.03	0.75±0.01	0.64±0.01	0.64±0.01	0.56±0.01	0.61±0.01	0.50±0.01	0.58±0.02	0.60±0.01	0.63±0.02	1.00±0.03	0.79±0.02	0.87±0.05	0.68±0.03	0.68±0.01	0.67±0.01	0.65±0.00	0.66±0.01	0.89±0.03	0.70±0.03	0.94±0.04	0.78±0.02
	5	0.81±0.02	0.73±0.01	0.60±0.01	0.61±0.01	0.52±0.01	0.58±0.01	0.49±0.01	0.57±0.01	0.53±0.01	0.59±0.01	0.80±0.04	0.74±0.02	0.89±0.07	0.76±0.03	0.76±0.05	0.72±0.03	0.57±0.01	0.62±0.01	0.87±0.04	0.74±0.02	0.89±0.03	0.77±0.02
	10	0.77±0.04	0.71±0.02	0.58±0.00	0.60±0.01	0.57±0.01	0.62±0.02	0.48±0.01	0.55±0.02	0.48±0.01	0.55±0.02	0.58±0.00	0.61±0.02	0.86±0.03	0.74±0.02	0.92±0.07	0.76±0.03	0.53±0.01	0.59±0.01	0.93±0.06	0.78±0.04	0.88±0.09	0.76±0.04
	20	0.82±0.05	0.72±0.01	0.64±0.01	0.63±0.01	0.56±0.01	0.60±0.01	0.58±0.00	0.62±0.01	0.56±0.01	0.61±0.01	0.87±0.03	0.75±0.02	0.90±0.04	0.76±0.01	0.77±0.04	0.72±0.03	0.59±0.01	0.62±0.01	0.93±0.03	0.78±0.02	0.87±0.06	0.73±0.03
Global_T	3	1.05±0.05	0.87±0.03	0.87±0.04	0.79±0.02	0.97±0.08	0.80±0.05	1.18±0.10	0.95±0.05	1.17±0.11	0.94±0.05	0.68±0.04	0.68±0.02	1.09±0.29	0.86±0.14	0.70±0.04	0.68±0.02	1.14±0.05	0.93±0.03	0.86±0.14	0.76±0.07	1.02±0.07	0.83±0.03
	5	0.96±0.08	0.82±0.04	1.01±0.05	0.86±0.03	1.19±0.06	0.95±0.03	1.13±0.05	0.92±0.02	1.01±0.14	0.82±0.06	0.73±0.05	0.70±0.03	1.45±0.19	1.00±0.08	0.87±0.05	0.78±0.03	0.95±0.07	0.80±0.03	1.26±0.15	0.92±0.07	1.04±0.09	0.83±0.04
	10	0.81±0.05	0.75±0.02	0.86±0.05	0.79±0.03	0.81±0.07	0.73±0.04	1.13±0.13	0.92±0.06	1.08±0.05	0.90±0.03	0.73±0.11	0.70±0.06	1.25±0.16	0.93±0.08	0.79±0.09	0.72±0.05	1.03±0.05	0.83±0.02	0.89±0.08	0.77±0.03	1.10±0.08	0.86±0.04
	20	0.81±0.12	0.75±0.07	0.78±0.11	0.74±0.06	0.99±0.09	0.81±0.04	1.07±0.08	0.90±0.04	1.08±0.06	0.90±0.03	0.82±0.14	0.74±0.07	1.18±0.06	0.90±0.02	0.76±0.05	0.73±0.03	1.13±0.03	0.93±0.02	0.91±0.13	0.78±0.06	1.03±0.14	0.83±0.07
	3	0.79±0.04	0.74±0.03	0.52±0.02	0.59±0.01	0.64±0.07	0.67±0.04	0.63±0.04	0.66±0.02	0.64±0.03	0.67±0.02	0.73±0.03	0.71±0.02	1.16±0.19	0.88±0.08	1.07±0.19	0.85±0.09	0.56±0.03	0.62±0.01	1.31±0.10	0.94±0.04	1.14±0.09	0.88±0.05
	5	0.62±0.05	0.64±0.04	0.55±0.06	0.61±0.04	0.62±0.03	0.66±0.02	0.62±0.04	0.66±0.03	0.60±0.05	0.65±0.02	0.84±0.05	0.76±0.03	1.24±0.26	0.91±0.10	0.88±0.06	0.78±0.03	0.56±0.04	0.62±0.03	0.92±0.07	0.78±0.04	1.06±0.17	0.83±0.07
	10	0.68±0.05	0.68±0.03	0.52±0.02	0.58±0.02	0.60±0.01	0.65±0.01	0.61±0.05	0.65±0.03	0.60±0.05	0.64±0.03	0.77±0.09	0.72±0.04	1.13±0.09	0.86±0.05	0.92±0.12	0.79±0.05	0.62±0.04	0.65±0.02	1.03±0.15	0.83±0.07	1.00±0.13	0.82±0.06
	20	0.76±0.09	0.72±0.05	0.51±0.04	0.58±0.02	0.64±0.03	0.67±0.02	0.67±0.02	0.68±0.01	0.60±0.03	0.64±0.02	1.01±0.08	0.83±0.04	0.97±0.03	0.79±0.02	0.70±0.08	0.69±0.03	0.65±0.04	0.67±0.02	1.19±0.12	0.90±0.06	1.12±0.16	0.89±0.07
	3	0.72±0.05	0.70±0.03	0.52±0.02	0.60±0.01	0.39±0.02	0.50±0.02	0.39±0.01	0.50±0.01	0.36±0.01	0.48±0.01	0.84±0.07	0.76±0.03	1.23±0.19	0.91±0.08	0.77±0.05	0.72±0.03	0.39±0.02	0.50±0.01	1.19±0.23	0.89±0.10	1.15±0.15	0.88±0.06
	5	0.72±0.02	0.71±0.01	0.38±0.02	0.49±0.01	0.50±0.02	0.58±0.01	0.42±0.04	0.52±0.03	0.44±0.01	0.54±0.01	0.71±0.03	0.69±0.01	0.99±0.18	0.81±0.08	0.88±0.07	0.77±0.04	0.41±0.02	0.51±0.02	1.15±0.17	0.88±0.08	0.83±0.09	0.73±0.05
	10	0.82±0.04	0.75±0.02	0.40±0.03	0.50±0.02	0.47±0.03	0.56±0.02	0.48±0.03	0.57±0.02	0.52±0.02	0.59±0.01	0.78±0.08	0.72±0.04	1.40±0.33	0.97±0.15	0.76±0.11	0.71±0.05	0.42±0.03	0.52±0.02	1.03±0.12	0.82±0.04	1.06±0.18	0.85±0.08
	20	0.79±0.06	0.72±0.04	0.49±0.03	0.57±0.02	0.53±0.04	0.60±0.03	0.55±0.03	0.61±0.02	0.50±0.04	0.58±0.03	1.05±0.08	0.84±0.03	1.12±0.15	0.87±0.03	0.72±0.05	0.71±0.03	0.52±0.02	0.59±0.01	1.17±0.05	0.89±0.03	1.00±0.13	0.82±0.06
Exchange	3	0.90±0.05	0.79±0.03	1.01±0.11	0.81±0.05	0.83±0.03	0.77±0.02	0.98±0.06	0.83±0.03	0.72±0.03	0.71±0.01	0.91±0.15	0.77±0.06	1.20±0.08	0.88±0.03	1.10±0.24	0.85±0.09	0.66±0.05	0.68±0.03	0.95±0.06	0.78±0.03	1.28±0.09	0.93±0.04
	5	0.96±0.03	0.83±0.01	0.93±0.12	0.77±0.06	1.04±0.08	0.86±0.03	0.86±0.05	0.78±0.02	1.00±0.08	0.84±0.03	0.89±0.12	0.75±0.05	1.28±0.17	0.91±0.06	1.02±0.07	0.82±0.03	0.60±0.02	0.64±0.01	0.92±0.09	0.76±0.04	1.20±0.18	0.88±0.06
	10	0.74±0.03	0.72±0.01	1.10±0.12	0.85±0.05	0.71±0.03	0.71±0.01	0.72±0.06	0.71±0.03	0.66±0.04	0.68±0.03	1.01±0.07	0.82±0.03	1.32±0.09	0.91±0.03	1.00±0.12	0.82±0.05	0.72±0.04	0.71±0.02	0.90±0.09	0.75±0.04	1.16±0.13	0.87±0.04
	20	0.71±0.05	0.70±0.02	0.99±0.12	0.81±0.06	0.71±0.05	0.71±0.03	0.75±0.06	0.73±0.03	0.70±0.06	0.69±0.03	0.97±0.06	0.80±0.03	1.37±0.05	0.93±0.03	0.90±0.07	0.79±0.03	0.70±0.09	0.70±0.05	1.45±0.12	0.96±0.03	1.05±0.20	0.81±0.08
	3	0.68±0.06	0.69±0.03	1.11±0.20	0.85±0.09	0.77±0.03	0.74±0.01	0.65±0.02	0.68±0.01	0.75±0.06	0.73±0.03	1.16±0.09	0.88±0.03	1.13±0.10	0.86±0.04	0.90±0.06	0.78±0.03	0.75±0.06	0.73±0.03	1.42±0.20	0.95±0.05	1.22±0.16	0.90±0.06
	5	0.72±0.05	0.71±0.03	1.14±0.11	0.86±0.04	0.70±0.04	0.71±0.02	0.70±0.02	0.71±0.01	0.80±0.09	0.75±0.05	1.02±0.06	0.83±0.03	1.01±0.21	0.81±0.08	1.07±0.12	0.85±0.04	0.67±0.04	0.69±0.02	1.14±0.17	0.85±0.07	1.17±0.13	0.86±0.06
	10	0.66±0.05	0.68±0.03	1.07±0.07	0.84±0.05	0.71±0.04	0.71±0.02	0.61±0.03	0.65±0.02	0.69±0.04	0.69±0.02	1.03±0.08	0.83±0.03	1.03±0.10	0.81±0.05	1.12±0.25	0.87±0.10	0.66±0.03	0.68±0.02	1.35±0.11	0.92±0.06	1.15±0.11	0.86±0.03
	20	0.66±0.05	0.68±0.03	1.01±0.17	0.80±0.08	0.73±0.04	0.72±0.02	0.60±0.02	0.64±0.02	0.68±0.04	0.68±0.02	1.02±0.18	0.81±0.08	1.21±0.21	0.87±0.07	0.77±0.10	0.73±0.05	0.75±0.07	0.72±0.04	1.44±0.15	0.96±0.05	1.21±0.04	0.88±0.02
	3	0.60±0.06	0.64±0.04	0.93±0.11	0.78±0.05	0.40±0.05	0.52±0.04	0.39±0.04	0.51±0.03	0.30±0.02	0.45±0.01	1.40±0.21	0.95±0.09	1.21±0.12	0.89±0.05	0.48±0.05	0.54±0.03	0.37±0.02	0.51±0.02	0.68±0.16	0.59±0.08	1.19±0.20	0.88±0.08
	5	0.62±0.03	0.66±0.02	1.09±0.18	0.84±0.08	0.49±0.02	0.58±0.02	0.56±0.04	0.62±0.02	0.61±0.04	0.64±0.02	1.32±0.16	0.93±0.06	1.52±0.18	0.99±0.07	0.39±0.06	0.49±0.04	0.54±0.03	0.60±0.02	1.25±0.16	0.89±0.07	1.11±0.09	0.85±0.04
	10	0.79±0.06	0.73±0.03	0.95±0.09	0.80±0.04	0.18±0.01	0.35±0																

Table 16. Comparison of trajectory-matching dataset distillation frameworks on 20 datasets and synthetic-set sizes {3, 5, 10, 20}, evaluated by MSE and MAE. The best and second best outcomes are highlighted in **best** and **second**, respectively. The notation ”1st Count” denotes the frequency of each method achieving the top results.

Models	DDTime		EDF		MCT		DATM		FTD		PP		TESLA		IDM		FrePo		MTT		KIP		DC		
	Ours		[2025]		[2025]																				
Metric	MSE	MAE	MSE	MAE	MSE	MAE	MSE	MAE	MSE	MAE	MSE	MAE	MSE	MAE	MSE	MAE	MSE	MAE	MSE	MAE	MSE	MAE	MSE	MAE	
ETM	3	0.68±0.03	0.59±0.01	0.87±0.02	0.70±0.01	0.98±0.07	0.74±0.02	0.70±0.01	0.71±0.01	0.90±0.03	0.71±0.01	0.89±0.02	0.71±0.01	0.93±0.05	0.72±0.02	1.17±0.06	0.81±0.01	0.97±0.05	0.74±0.02	0.92±0.04	0.72±0.02	0.96±0.02	0.73±0.01	1.07±0.04	0.77±0.01
	5	0.68±0.03	0.59±0.01	0.90±0.04	0.71±0.01	0.95±0.03	0.73±0.01	0.87±0.05	0.70±0.02	0.90±0.05	0.70±0.02	0.86±0.02	0.70±0.02	0.94±0.02	0.73±0.01	1.10±0.06	0.78±0.02	0.98±0.06	0.75±0.02	0.88±0.03	0.70±0.02	1.05±0.04	0.77±0.02	1.05±0.04	0.77±0.02
	10	0.66±0.03	0.59±0.01	0.86±0.04	0.69±0.01	0.98±0.03	0.74±0.01	0.86±0.06	0.69±0.02	0.86±0.01	0.70±0.01	0.83±0.01	0.68±0.01	0.91±0.05	0.71±0.02	1.10±0.11	0.79±0.04	0.88±0.04	0.70±0.02	0.88±0.03	0.70±0.02	1.13±0.07	0.80±0.03	1.06±0.04	0.77±0.01
20	0.75±0.02	0.62±0.01	0.87±0.04	0.70±0.02	0.98±0.07	0.75±0.02	0.89±0.03	0.70±0.01	0.87±0.03	0.70±0.01	0.86±0.01	0.69±0.02	0.97±0.06	0.73±0.02	1.17±0.05	0.81±0.02	0.84±0.01	0.68±0.01	0.87±0.05	0.70±0.02	1.15±0.07	0.81±0.03	1.07±0.10	0.77±0.04	
ETM2	3	0.26±0.02	0.38±0.02	0.69±0.05	0.66±0.02	0.86±0.07	0.73±0.03	0.84±0.05	0.73±0.02	0.75±0.03	0.70±0.02	0.86±0.07	0.74±0.03	0.75±0.02	0.69±0.01	0.98±0.08	0.78±0.03	0.69±0.07	0.66±0.01	0.75±0.02	0.69±0.01	0.75±0.06	0.67±0.03	0.92±0.08	0.76±0.03
	5	0.24±0.01	0.37±0.01	0.63±0.05	0.63±0.03	0.84±0.03	0.73±0.02	0.81±0.04	0.72±0.02	0.66±0.05	0.65±0.01	0.77±0.06	0.70±0.03	0.83±0.09	0.72±0.05	0.88±0.14	0.74±0.07	0.86±0.08	0.74±0.03	0.61±0.03	0.62±0.01	0.74±0.06	0.69±0.04	0.84±0.03	0.76±0.01
	10	0.26±0.03	0.38±0.01	0.69±0.02	0.66±0.01	0.82±0.10	0.72±0.05	0.73±0.04	0.68±0.02	0.77±0.05	0.70±0.02	0.64±0.03	0.64±0.02	0.59±0.02	0.60±0.01	1.09±0.05	0.74±0.01	0.70±0.05	0.67±0.01	0.77±0.04	0.70±0.02	0.83±0.02	0.78±0.02	0.84±0.05	0.73±0.04
20	0.28±0.01	0.41±0.02	0.65±0.06	0.64±0.03	0.85±0.05	0.64±0.03	0.74±0.06	0.68±0.01	0.82±0.06	0.73±0.03	0.76±0.03	0.70±0.01	0.61±0.07	0.61±0.01	0.79±0.03	0.70±0.01	0.77±0.06	0.70±0.01	0.77±0.04	0.68±0.03	0.95±0.04	0.77±0.02	0.91±0.13	0.75±0.06	
ETM1	3	0.67±0.02	0.58±0.01	0.86±0.02	0.69±0.01	0.82±0.02	0.68±0.01	0.83±0.02	0.68±0.01	0.88±0.01	0.70±0.01	0.88±0.01	0.70±0.01	0.81±0.01	0.67±0.01	1.07±0.05	0.77±0.02	0.89±0.04	0.70±0.02	0.88±0.01	0.71±0.01	1.04±0.07	0.76±0.01	0.99±0.06	0.74±0.02
	5	0.63±0.01	0.54±0.01	0.87±0.01	0.69±0.01	0.89±0.02	0.67±0.01	0.89±0.02	0.71±0.01	0.89±0.01	0.71±0.01	0.89±0.01	0.71±0.01	0.80±0.02	0.67±0.01	1.06±0.04	0.77±0.01	0.90±0.02	0.71±0.01	0.91±0.01	0.71±0.01	1.11±0.07	0.78±0.01	0.97±0.04	0.74±0.02
	10	0.65±0.01	0.56±0.01	0.85±0.02	0.69±0.01	0.79±0.02	0.66±0.01	0.88±0.02	0.71±0.01	0.89±0.03	0.71±0.01	0.85±0.02	0.69±0.01	0.83±0.02	0.67±0.01	1.10±0.06	0.78±0.02	0.90±0.04	0.71±0.02	0.86±0.01	0.70±0.01	1.06±0.05	0.77±0.02	1.03±0.09	0.76±0.04
20	0.65±0.02	0.57±0.01	0.84±0.03	0.68±0.01	0.82±0.02	0.68±0.01	0.87±0.01	0.70±0.01	0.89±0.02	0.71±0.01	0.89±0.02	0.71±0.01	0.82±0.01	0.67±0.01	1.03±0.04	0.76±0.02	0.85±0.01	0.68±0.01	0.90±0.03	0.71±0.01	1.06±0.05	0.77±0.02	0.99±0.06	0.74±0.02	
ETM2	3	0.19±0.03	0.34±0.01	0.93±0.01	0.77±0.01	0.63±0.02	0.64±0.01	0.86±0.06	0.74±0.02	0.76±0.04	0.70±0.02	0.93±0.05	0.77±0.02	0.77±0.02	0.70±0.01	0.87±0.05	0.73±0.02	0.96±0.10	0.78±0.02	0.83±0.01	0.73±0.01	0.74±0.11	0.68±0.05	0.92±0.04	0.76±0.02
	5	0.18±0.03	0.32±0.01	0.78±0.04	0.71±0.01	0.63±0.04	0.64±0.02	0.78±0.01	0.71±0.02	0.75±0.03	0.70±0.01	0.69±0.02	0.65±0.01	0.72±0.02	0.68±0.01	1.17±0.08	0.85±0.06	0.87±0.05	0.73±0.02	0.81±0.03	0.72±0.01	1.10±0.11	0.83±0.06	0.88±0.04	0.74±0.01
	10	0.17±0.03	0.31±0.01	0.72±0.06	0.67±0.01	0.65±0.04	0.65±0.02	0.82±0.06	0.73±0.02	0.79±0.08	0.69±0.04	0.81±0.02	0.72±0.01	0.73±0.03	0.68±0.01	0.73±0.06	0.67±0.03	0.72±0.10	0.67±0.05	0.82±0.04	0.73±0.02	0.90±0.04	0.76±0.02	0.86±0.10	0.72±0.02
20	0.23±0.01	0.37±0.01	0.74±0.02	0.69±0.01	0.66±0.04	0.65±0.02	0.73±0.02	0.69±0.01	0.79±0.03	0.71±0.02	0.85±0.04	0.74±0.02	0.66±0.06	0.65±0.01	1.02±0.11	0.79±0.05	0.54±0.07	0.58±0.01	0.76±0.03	0.70±0.01	0.95±0.10	0.76±0.04	0.92±0.08	0.76±0.02	
PEMS03	3	0.28±0.01	0.40±0.01	0.72±0.02	0.71±0.01	0.72±0.05	0.70±0.03	0.84±0.04	0.75±0.01	0.78±0.02	0.75±0.01	0.86±0.01	0.79±0.01	0.78±0.04	0.73±0.02	0.91±0.07	0.78±0.04	0.69±0.02	0.69±0.01	0.91±0.01	0.81±0.01	0.89±0.07	0.77±0.01	0.91±0.09	0.78±0.04
	5	0.34±0.01	0.45±0.01	0.69±0.01	0.69±0.01	0.70±0.04	0.69±0.02	0.86±0.05	0.76±0.02	0.75±0.02	0.73±0.01	0.87±0.02	0.80±0.01	0.74±0.02	0.72±0.01	0.95±0.11	0.79±0.05	0.84±0.05	0.76±0.02	0.91±0.01	0.81±0.01	1.08±0.06	0.86±0.03	0.83±0.07	0.75±0.02
	10	0.33±0.01	0.44±0.01	0.71±0.01	0.70±0.01	0.80±0.05	0.75±0.04	0.91±0.06	0.79±0.03	0.80±0.05	0.73±0.02	0.93±0.02	0.82±0.01	0.68±0.02	0.69±0.01	0.83±0.03	0.74±0.01	0.84±0.06	0.76±0.02	0.85±0.03	0.74±0.01	0.82±0.06	0.75±0.03	0.85±0.07	0.78±0.03
20	0.37±0.01	0.48±0.01	0.69±0.01	0.69±0.01	0.80±0.03	0.70±0.01	0.74±0.05	0.71±0.01	0.76±0.02	0.74±0.01	0.82±0.02	0.77±0.01	0.73±0.01	0.71±0.01	0.82±0.04	0.74±0.02	0.64±0.04	0.66±0.01	0.79±0.03	0.76±0.01	0.81±0.05	0.74±0.01	0.84±0.05	0.75±0.02	
PEMS04	3	0.50±0.01	0.55±0.01	0.80±0.03	0.75±0.01	0.73±0.03	0.71±0.01	0.78±0.03	0.73±0.01	0.72±0.02	0.71±0.01	0.83±0.03	0.77±0.01	0.73±0.02	0.69±0.01	0.97±0.09	0.81±0.05	0.78±0.03	0.73±0.02	0.87±0.01	0.79±0.01	0.87±0.03	0.76±0.02	0.95±0.10	0.80±0.04
	5	0.66±0.01	0.67±0.01	0.75±0.01	0.72±0.01	0.82±0.03	0.75±0.01	0.85±0.02	0.78±0.01	0.82±0.03	0.76±0.01	0.78±0.02	0.74±0.01	0.82±0.03	0.75±0.01	0.79±0.04	0.72±0.02	0.80±0.06	0.74±0.02	0.78±0.02	0.75±0.01	0.81±0.04	0.97±0.05	0.78±0.02	
	10	0.52±0.01	0.57±0.01	0.86±0.04	0.77±0.01	0.86±0.04	0.77±0.01	0.76±0.02	0.73±0.01	0.73±0.01	0.70±0.01	0.77±0.02	0.74±0.01	0.77±0.02	0.71±0.01	0.90±0.06	0.78±0.02	0.89±0.08	0.78±0.02	0.81±0.02	0.71±0.01	0.77±0.04	0.74±0.01	0.93±0.08	0.78±0.03
20	0.55±0.01	0.59±0.01	0.78±0.01	0.71±0.02	0.72±0.04	0.70±0.02	0.79±0.03	0.74±0.01	0.72±0.02	0.70±0.01	0.82±0.01	0.76±0.01	0.80±0.04	0.70±0.02	0.87±0.06	0.76±0.03	0.75±0.04	0.72±0.02	0.80±0.04	0.73±0.02	0.89±0.07	0.77±0.02	0.92±0.06	0.78±0.02	
PEMS07	3	0.43±0.01	0.52±0.01	0.86±0.04	0.77±0.01	0.61±0.01	0.63±0.01	0.89±0.02	0.80±0.01	0.88±0.02	0.79±0.01	0.81±0.01	0.75±0.01	0.91±0.05	0.78±0.02	0.90±0.07	0.77±0.02	0.92±0.06	0.78±0.03	0.84±0.03	0.77±0.01	1.00±0.07	0.80±0.04	0.91±0.05	0.78±0.02
	5	0.45±0.01	0.53±0.01	0.79±0.01	0.73±0.01	0.63±0.04	0.64±0.01	0.89±0.02	0.80±0.01	0.81±0.01	0.78±0.01	0.85±0.02	0.78±0.01	0.79±0.04	0.72±0.02	0.90±0.08	0.76±0.03	0.90±0.11	0.78±0.05	0.74±0.01	0.72±0.01	0.92±0.05	0.78±0.04	0.79±0.04	0.72±0.02
	10	0.57±0.01	0.62±0.01	0.82±0.04	0.74±0.01	0.64±0.01	0.66±0.01	0.82±0.02	0.76±0.01	0.85±0.01	0.78±0.01	0.80±0.02	0.75±0.01	0.99±0.07	0.81±0.01	0.83±0.02	0.76±0.01	0.90±0.11	0.77±0.05	0.81±0.02	0.75±0.01	0.81±0.05	0.74±0.02	0.93±0.08	0.78±0.03
20	0.60±0.01	0.63±0.01	0.86±0.04	0.75±0.01	0.71±0.01	0.69±0.01	0.84±0.02	0.76±0.01	0.83±0.02	0.77±0.01	0.83±0.02	0.76±0.01	0.84±0.06	0.74±0.02	0.84±0.06	0.74±0.02	0.80±0.03	0.71±0.02	0.80±0.02	0.75±0.01	0.94±0.09	0.78±0.04	0.85±0.05	0.75±0.01	
PEMS08	3	0.36±0.01	0.46±0.01	0.92±0.02	0.81±0.01	0.78±0.02	0.74±0.01	1.06±0.02	0.87±0.01	0.87±0.06	0.76±0.01	0.93±0.03	0.83±0.01	0.74±0.02	0.70±0.01	1.07±0.13	0.84±0.06	1.00±0.10	0.82±0.05	0.93±0.08	0.79±0.01	0.78±0.04	0.74±0.01	0.74±0.02	0.70±0.01
	5	0.36±0.01	0.48±0.01	0.84±0.02	0.77±0.01	0.78±0.01	0.74±0.01	0.94±0.01	0.81±0.01	0.82±0.04	0.75±0.02	0.99±0.02	0.84±0.01	0.78±0.01	0.74±0.01	1.07±0.10	0.84±0.06	0.81±0.08	0.73±0.01	0.94±0.02	0.82±0.01	0.78±0.04	0.74±0.01	0.89±0.03	0.80±0.02
	10	0.44±0.01	0.53±0.01	0.78±0.02	0.73±0.01	0.79±0.04	0.74±0.02	0.92±0.08	0.78±0.03	0.74±0.01	0.70±0.01														

Table 17. Comparison of synthetic data distillation methods on the Weather dataset. MSE and MAE results are shown for $S \in \{3, 5, 10, 20\}$. Our frequency domain label loss alignment approach yields consistent improvements in predictive accuracy and robustness against noise across meteorological variables.

Models	EDF [2025]		MCT [2025]		DATM [2024]		FTD [2023]		PP [2023]		TESLA [2023]		IDM [2023]		FRePo [2022]		MTT [2022]		KIP [2021]		DC [2021]		
	MSE	MAE	MSE	MAE	MSE	MAE	MSE	MAE	MSE	MAE	MSE	MAE	MSE	MAE	MSE	MAE	MSE	MAE	MSE	MAE	MSE	MAE	
Weather	3	0.50±0.01	0.50±0.01	0.64±0.05	0.57±0.03	0.51±0.01	0.50±0.01	0.53±0.02	0.52±0.02	0.49±0.01	0.49±0.01	0.52±0.02	0.51±0.01	0.69±0.04	0.56±0.02	0.54±0.02	0.51±0.01	0.56±0.01	0.54±0.01	0.73±0.06	0.59±0.03	0.63±0.07	0.54±0.03
	5	0.59±0.01	0.55±0.01	0.51±0.03	0.49±0.01	0.48±0.02	0.47±0.01	0.55±0.01	0.53±0.01	0.57±0.00	0.54±0.00	0.56±0.01	0.53±0.01	0.63±0.03	0.55±0.02	0.55±0.02	0.51±0.01	0.56±0.01	0.53±0.01	0.68±0.05	0.57±0.02	0.61±0.04	0.54±0.02
	10	0.51±0.00	0.50±0.00	0.57±0.04	0.53±0.02	0.57±0.01	0.54±0.01	0.52±0.01	0.51±0.01	0.56±0.01	0.53±0.01	0.61±0.02	0.56±0.01	0.66±0.07	0.55±0.04	0.55±0.03	0.52±0.02	0.58±0.01	0.54±0.01	0.61±0.04	0.53±0.03	0.61±0.06	0.53±0.04
	20	0.50±0.01	0.49±0.01	0.48±0.01	0.48±0.01	0.56±0.01	0.53±0.01	0.52±0.01	0.51±0.01	0.52±0.01	0.51±0.01	0.57±0.02	0.53±0.01	0.67±0.07	0.56±0.04	0.53±0.02	0.51±0.01	0.50±0.01	0.50±0.01	0.68±0.04	0.57±0.02	0.63±0.02	0.54±0.01
C=0.1	3	0.46±0.01	0.48±0.01	0.41±0.02	0.44±0.02	0.41±0.01	0.44±0.01	0.48±0.00	0.48±0.01	0.46±0.01	0.48±0.01	0.44±0.01	0.46±0.00	0.78±0.06	0.62±0.03	0.53±0.03	0.50±0.02	0.50±0.01	0.51±0.01	0.68±0.05	0.57±0.02	0.50±0.03	0.48±0.03
	5	0.46±0.01	0.48±0.01	0.48±0.02	0.49±0.02	0.39±0.01	0.43±0.01	0.47±0.01	0.48±0.01	0.47±0.01	0.48±0.01	0.41±0.01	0.44±0.01	0.62±0.06	0.54±0.03	0.51±0.02	0.49±0.01	0.47±0.01	0.48±0.01	0.75±0.04	0.60±0.02	0.61±0.06	0.53±0.03
	10	0.47±0.01	0.49±0.01	0.51±0.01	0.51±0.01	0.39±0.01	0.43±0.01	0.48±0.01	0.49±0.01	0.47±0.01	0.48±0.01	0.40±0.01	0.44±0.01	0.52±0.04	0.49±0.02	0.50±0.02	0.49±0.01	0.47±0.01	0.48±0.01	0.70±0.06	0.58±0.03	0.62±0.06	0.54±0.03
	20	0.46±0.01	0.48±0.01	0.50±0.03	0.50±0.02	0.38±0.01	0.42±0.01	0.48±0.00	0.48±0.00	0.48±0.01	0.49±0.01	0.41±0.01	0.44±0.01	0.64±0.03	0.55±0.02	0.48±0.01	0.48±0.01	0.48±0.01	0.48±0.01	0.60±0.05	0.52±0.03	0.63±0.05	0.54±0.03
C=0.2	3	0.47±0.01	0.48±0.01	0.48±0.01	0.49±0.01	0.39±0.01	0.42±0.01	0.47±0.01	0.48±0.01	0.47±0.01	0.48±0.01	0.40±0.01	0.43±0.01	0.48±0.01	0.47±0.01	0.56±0.01	0.51±0.00	0.47±0.01	0.48±0.01	0.67±0.06	0.57±0.02	0.59±0.06	0.53±0.03
	5	0.44±0.01	0.46±0.01	0.48±0.02	0.49±0.02	0.39±0.01	0.42±0.01	0.48±0.01	0.49±0.01	0.47±0.01	0.48±0.01	0.39±0.00	0.43±0.00	0.55±0.03	0.50±0.02	0.50±0.02	0.48±0.01	0.47±0.01	0.49±0.01	0.56±0.03	0.51±0.02	0.63±0.04	0.55±0.02
	10	0.45±0.01	0.47±0.00	0.46±0.02	0.48±0.01	0.39±0.01	0.43±0.01	0.47±0.01	0.48±0.01	0.47±0.01	0.48±0.01	0.41±0.00	0.44±0.01	0.61±0.02	0.54±0.02	0.47±0.01	0.47±0.01	0.47±0.01	0.48±0.01	0.66±0.04	0.56±0.02	0.62±0.02	0.54±0.01
	20	0.46±0.01	0.48±0.01	0.48±0.01	0.48±0.01	0.37±0.00	0.41±0.01	0.48±0.00	0.48±0.01	0.46±0.01	0.47±0.01	0.42±0.01	0.45±0.01	0.68±0.06	0.57±0.03	0.45±0.02	0.46±0.01	0.46±0.01	0.47±0.01	0.62±0.03	0.54±0.01	0.64±0.05	0.55±0.02
C=0.3	3	0.47±0.01	0.49±0.01	0.55±0.02	0.53±0.01	0.40±0.01	0.43±0.01	0.48±0.00	0.48±0.01	0.49±0.01	0.50±0.01	0.39±0.00	0.42±0.00	0.56±0.04	0.50±0.03	0.54±0.04	0.51±0.03	0.46±0.00	0.47±0.00	0.68±0.03	0.56±0.01	0.59±0.03	0.53±0.02
	5	0.45±0.01	0.47±0.00	0.49±0.01	0.50±0.01	0.37±0.00	0.41±0.00	0.47±0.01	0.48±0.01	0.48±0.01	0.49±0.01	0.41±0.01	0.44±0.01	0.58±0.03	0.52±0.02	0.49±0.03	0.48±0.02	0.48±0.00	0.49±0.00	0.73±0.06	0.59±0.04	0.58±0.01	0.52±0.01
	10	0.46±0.01	0.48±0.01	0.49±0.02	0.49±0.01	0.38±0.00	0.41±0.01	0.48±0.01	0.50±0.02	0.47±0.00	0.48±0.00	0.41±0.01	0.44±0.01	0.56±0.04	0.51±0.02	0.47±0.03	0.48±0.02	0.48±0.01	0.49±0.01	0.68±0.06	0.56±0.03	0.59±0.04	0.53±0.02
	20	0.44±0.01	0.46±0.01	0.50±0.04	0.50±0.02	0.38±0.01	0.41±0.02	0.45±0.01	0.47±0.01	0.49±0.01	0.49±0.01	0.42±0.01	0.45±0.01	0.64±0.04	0.55±0.02	0.42±0.01	0.44±0.01	0.49±0.01	0.50±0.01	0.63±0.05	0.54±0.03	0.61±0.04	0.54±0.03
C=0.4	3	0.45±0.02	0.47±0.01	0.46±0.01	0.47±0.01	0.39±0.01	0.43±0.01	0.48±0.01	0.49±0.01	0.47±0.01	0.48±0.01	0.41±0.01	0.44±0.01	0.62±0.03	0.55±0.02	0.47±0.04	0.46±0.02	0.48±0.00	0.49±0.00	0.54±0.01	0.49±0.01	0.60±0.03	0.54±0.02
	5	0.47±0.01	0.49±0.01	0.50±0.02	0.50±0.01	0.42±0.01	0.45±0.01	0.47±0.01	0.48±0.01	0.49±0.01	0.50±0.01	0.40±0.01	0.44±0.01	0.57±0.03	0.52±0.02	0.50±0.02	0.48±0.02	0.47±0.01	0.48±0.01	0.51±0.06	0.48±0.04	0.57±0.04	0.52±0.03
	10	0.46±0.01	0.48±0.01	0.47±0.02	0.48±0.01	0.38±0.01	0.42±0.01	0.48±0.01	0.49±0.01	0.47±0.01	0.48±0.01	0.41±0.01	0.44±0.01	0.58±0.05	0.52±0.03	0.43±0.01	0.45±0.01	0.47±0.01	0.48±0.01	0.63±0.05	0.54±0.02	0.60±0.02	0.53±0.01
	20	0.45±0.01	0.46±0.01	0.49±0.02	0.49±0.01	0.39±0.01	0.42±0.01	0.48±0.01	0.49±0.01	0.49±0.01	0.50±0.01	0.43±0.00	0.45±0.00	0.61±0.04	0.53±0.02	0.45±0.01	0.47±0.01	0.49±0.01	0.49±0.01	0.71±0.03	0.58±0.03	0.65±0.05	0.56±0.02
C=0.5	3	0.45±0.01	0.48±0.01	0.51±0.03	0.50±0.02	0.41±0.01	0.43±0.01	0.50±0.01	0.50±0.01	0.47±0.01	0.48±0.01	0.42±0.01	0.45±0.01	0.71±0.09	0.58±0.04	0.51±0.03	0.50±0.02	0.48±0.01	0.49±0.01	0.74±0.05	0.59±0.01	0.63±0.04	0.55±0.02
	5	0.46±0.01	0.47±0.01	0.46±0.01	0.48±0.01	0.40±0.02	0.43±0.01	0.47±0.00	0.48±0.00	0.47±0.01	0.49±0.01	0.39±0.01	0.42±0.01	0.64±0.05	0.55±0.03	0.52±0.02	0.49±0.02	0.48±0.01	0.48±0.01	0.68±0.06	0.56±0.02	0.61±0.04	0.53±0.02
	10	0.46±0.01	0.48±0.01	0.50±0.02	0.50±0.01	0.38±0.01	0.42±0.01	0.46±0.01	0.47±0.01	0.49±0.01	0.50±0.01	0.42±0.01	0.45±0.01	0.72±0.05	0.58±0.03	0.47±0.02	0.46±0.01	0.47±0.01	0.48±0.01	0.73±0.03	0.59±0.02	0.62±0.04	0.54±0.02
	20	0.46±0.01	0.47±0.01	0.49±0.01	0.49±0.01	0.35±0.01	0.40±0.01	0.48±0.01	0.48±0.01	0.49±0.01	0.50±0.01	0.44±0.01	0.46±0.01	0.64±0.08	0.55±0.03	0.45±0.02	0.46±0.01	0.48±0.01	0.49±0.01	0.61±0.01	0.54±0.02	0.58±0.04	0.53±0.02
C=0.6	3	0.47±0.01	0.49±0.01	0.46±0.02	0.48±0.01	0.36±0.01	0.40±0.01	0.48±0.01	0.49±0.01	0.49±0.01	0.50±0.01	0.42±0.01	0.45±0.01	0.69±0.05	0.57±0.02	0.56±0.03	0.51±0.02	0.48±0.00	0.49±0.00	0.63±0.05	0.54±0.02	0.59±0.04	0.53±0.02
	5	0.46±0.01	0.48±0.01	0.48±0.01	0.49±0.01	0.39±0.01	0.43±0.01	0.49±0.01	0.50±0.01	0.47±0.01	0.49±0.01	0.41±0.00	0.44±0.00	0.64±0.04	0.55±0.02	0.51±0.02	0.49±0.02	0.47±0.01	0.49±0.01	0.72±0.08	0.59±0.04	0.64±0.03	0.55±0.02
	10	0.46±0.01	0.47±0.01	0.52±0.01	0.51±0.01	0.37±0.01	0.41±0.01	0.48±0.01	0.49±0.01	0.48±0.01	0.49±0.01	0.41±0.00	0.44±0.00	0.62±0.03	0.54±0.02	0.50±0.03	0.49±0.02	0.48±0.01	0.49±0.01	0.61±0.04	0.53±0.02	0.61±0.07	0.53±0.03
	20	0.46±0.01	0.48±0.01	0.46±0.01	0.47±0.01	0.38±0.00	0.42±0.01	0.49±0.00	0.49±0.00	0.48±0.01	0.49±0.01	0.43±0.01	0.45±0.01	0.67±0.06	0.56±0.03	0.46±0.02	0.47±0.01	0.46±0.01	0.47±0.01	0.73±0.08	0.59±0.03	0.63±0.08	0.55±0.04
C=0.7	3	0.46±0.00	0.47±0.01	0.44±0.01	0.46±0.01	0.40±0.01	0.43±0.01	0.49±0.02	0.50±0.01	0.49±0.01	0.49±0.01	0.41±0.01	0.44±0.01	0.65±0.03	0.55±0.01	0.55±0.03	0.52±0.01	0.49±0.01	0.50±0.01	0.75±0.04	0.60±0.01	0.61±0.05	0.54±0.03
	5	0.46±0.01	0.47±0.01	0.48±0.02	0.49±0.01	0.39±0.01	0.43±0.01	0.46±0.01	0.48±0.01	0.48±0.00	0.49±0.00	0.41±0.00	0.44±0.01	0.66±0.04	0.55±0.02	0.54±0.03	0.51±0.02	0.47±0.00	0.48±0.00	0.61±0.03	0.53±0.02	0.58±0.04	0.52±0.03
	10	0.45±0.01	0.47±0.01	0.50±0.01	0.50±0.01	0.39±0.01	0.43±0.01	0.48±0.01	0.49±0.01	0.47±0.00	0.48±0.00	0.39±0.01	0.43±0.01	0.65±0.05	0.56±0.03	0.50±0.04	0.49±0.02	0.46±0.01	0.48±0.01	0.66±0.04	0.56±0.02	0.64±0.03	0.55±0.02
	20	0.46±0.01	0.47±0.01	0.47±0.02	0.48±0.01	0.40±0.01	0.43±0.01	0.46±0.01	0.47±0.01	0.48±0.00	0.49±0.00	0.42±0.01	0.45±0.01	0.66±0.06	0.56±0.03	0.47±0.01	0.47±0.01	0.49±0.01	0.49±0.00	0.55±0.02	0.50±0.01	0.62±0.04	0.54±0.02
C=0.8	3	0.46±0.01	0.48±0.01	0.51±0.02	0.50±0.01	0.39±0.01	0.42±0.01	0.48±0.01	0.49±0.01	0.48±0.00	0.49±0.00	0.42±0.01	0.45±0.01	0.74±0.05	0.60±0.02	0.50±0.03	0.48±0.02	0.47±0.01	0.48±0.01	0.62±0.05	0.54±0.02	0.57±0.02	0.51±0.01
	5	0.45±0.01	0.46±0.01	0.51±0.01	0.51±0.01	0.39±0.01	0.43±0.01	0.48±0.01	0.49±0.01	0.48±0.01	0.49±0.01	0.38±0.01	0.42±0.01	0.55±0.03	0.50±0.01	0.48±0.04	0.47±0.02	0.48±0.01	0.49±0.01	0.59±0.03	0.53±0.01	0.62±0.03	0.54±0.01
	10	0.45±0.01	0.47±0																				

Table 18. Forecasting performance of dataset distillation methods on the **Electricity** dataset. Each cell shows **MSE / MAE** for various S values. Our method demonstrates clear advantages over prior baselines, maintaining stable accuracy improvements through frequency-domain teacher–student label-loss alignment.

Models	EDF [2025]		MCT [2025]		DATM [2024]		FTD [2023]		PP [2023]		TESLA [2023]		IDM [2023]		FRPo [2022]		MTT [2022]		KIP [2021]		DC [2021]		
	MSE	MAE	MSE	MAE	MSE	MAE	MSE	MAE	MSE	MAE	MSE	MAE	MSE	MAE	MSE	MAE	MSE	MAE	MSE	MAE	MSE	MAE	
Electricity	3	0.86±0.04	0.74±0.02	0.90±0.03	0.76±0.01	0.86±0.02	0.75±0.01	0.81±0.02	0.73±0.01	0.88±0.02	0.77±0.01	0.98±0.05	0.79±0.03	1.07±0.08	0.83±0.03	1.02±0.06	0.81±0.03	0.80±0.01	0.72±0.01	1.04±0.05	0.81±0.02	1.08±0.14	0.83±0.06
	5	0.86±0.04	0.74±0.02	0.84±0.06	0.74±0.03	0.81±0.02	0.74±0.01	0.81±0.02	0.73±0.01	0.81±0.03	0.73±0.01	1.07±0.01	0.83±0.00	1.04±0.06	0.82±0.02	1.02±0.05	0.82±0.02	0.82±0.01	0.74±0.00	1.19±0.11	0.88±0.04	1.07±0.10	0.83±0.05
	10	1.02±0.05	0.81±0.02	0.90±0.03	0.77±0.01	0.84±0.01	0.75±0.01	0.81±0.02	0.73±0.01	0.86±0.02	0.75±0.01	1.07±0.04	0.83±0.02	1.03±0.02	0.82±0.01	0.90±0.03	0.77±0.01	0.80±0.02	0.73±0.01	1.08±0.03	0.84±0.01	1.08±0.05	0.84±0.02
	20	1.01±0.03	0.81±0.01	0.90±0.03	0.76±0.01	0.86±0.02	0.75±0.01	0.82±0.01	0.73±0.01	0.84±0.03	0.75±0.01	1.07±0.02	0.83±0.01	1.08±0.13	0.83±0.03	0.92±0.04	0.78±0.02	0.81±0.02	0.73±0.01	1.11±0.10	0.85±0.04	1.14±0.06	0.85±0.03
$\alpha = 0.1$	3	0.94±0.07	0.78±0.03	0.88±0.04	0.75±0.02	0.76±0.01	0.71±0.01	0.68±0.01	0.66±0.00	0.74±0.02	0.69±0.01	1.10±0.07	0.84±0.03	1.06±0.08	0.82±0.03	0.99±0.10	0.80±0.05	0.73±0.02	0.69±0.01	1.11±0.06	0.85±0.03	1.06±0.06	0.82±0.02
	5	0.97±0.08	0.78±0.03	0.87±0.04	0.75±0.02	0.73±0.01	0.69±0.01	0.68±0.03	0.66±0.02	0.74±0.03	0.69±0.01	1.03±0.06	0.81±0.03	1.02±0.06	0.81±0.03	1.06±0.07	0.82±0.03	0.71±0.03	0.68±0.02	1.12±0.05	0.85±0.02	1.12±0.07	0.85±0.04
	10	1.00±0.07	0.80±0.03	0.87±0.03	0.75±0.02	0.72±0.03	0.69±0.01	0.72±0.01	0.69±0.01	0.76±0.02	0.70±0.01	1.06±0.07	0.82±0.03	1.09±0.14	0.84±0.06	0.98±0.07	0.80±0.03	0.74±0.03	0.70±0.01	1.09±0.12	0.84±0.05	1.10±0.04	0.84±0.01
	20	1.06±0.13	0.82±0.05	0.88±0.05	0.75±0.03	0.73±0.03	0.69±0.01	0.72±0.03	0.68±0.02	0.75±0.03	0.70±0.01	1.02±0.04	0.80±0.02	1.11±0.12	0.84±0.05	0.94±0.06	0.78±0.03	0.74±0.01	0.69±0.01	1.06±0.04	0.83±0.02	1.10±0.08	0.84±0.03
$\alpha = 0.2$	3	0.87±0.05	0.75±0.03	0.84±0.04	0.74±0.02	0.72±0.02	0.69±0.01	0.74±0.03	0.69±0.01	0.74±0.03	0.69±0.01	1.00±0.04	0.80±0.02	1.04±0.06	0.82±0.03	1.02±0.05	0.81±0.02	0.72±0.02	0.68±0.01	1.10±0.05	0.84±0.02	1.13±0.03	0.86±0.01
	5	1.01±0.04	0.81±0.02	0.83±0.03	0.73±0.02	0.73±0.02	0.69±0.01	0.72±0.02	0.68±0.01	0.72±0.03	0.68±0.02	1.07±0.10	0.83±0.04	1.08±0.11	0.83±0.04	1.03±0.08	0.82±0.04	0.72±0.02	0.68±0.01	1.13±0.06	0.85±0.03	1.08±0.07	0.83±0.03
	10	1.03±0.04	0.81±0.02	0.91±0.04	0.77±0.02	0.73±0.02	0.69±0.01	0.71±0.01	0.68±0.00	0.77±0.03	0.71±0.02	1.04±0.04	0.81±0.02	1.06±0.05	0.83±0.02	0.96±0.09	0.78±0.04	0.71±0.03	0.67±0.01	1.03±0.08	0.81±0.03	1.10±0.12	0.84±0.06
	20	1.14±0.06	0.86±0.02	0.88±0.04	0.75±0.02	0.75±0.02	0.70±0.01	0.75±0.02	0.70±0.01	0.75±0.02	0.70±0.01	1.10±0.05	0.84±0.02	1.12±0.12	0.85±0.05	0.96±0.07	0.79±0.03	0.73±0.03	0.69±0.01	1.09±0.07	0.84±0.03	1.04±0.05	0.81±0.02
$\alpha = 0.3$	3	0.94±0.05	0.77±0.02	0.79±0.03	0.71±0.01	0.72±0.02	0.69±0.01	0.73±0.02	0.69±0.01	0.68±0.02	0.66±0.01	1.10±0.09	0.84±0.04	1.09±0.11	0.83±0.05	1.01±0.04	0.81±0.02	0.74±0.01	0.69±0.01	1.16±0.11	0.87±0.05	1.12±0.11	0.84±0.04
	5	0.98±0.06	0.80±0.03	0.87±0.04	0.75±0.02	0.76±0.01	0.71±0.01	0.71±0.04	0.68±0.02	0.75±0.02	0.70±0.01	1.16±0.07	0.87±0.03	1.09±0.04	0.84±0.02	0.93±0.07	0.77±0.03	0.74±0.02	0.70±0.01	1.15±0.06	0.86±0.03	1.09±0.10	0.84±0.04
	10	0.99±0.08	0.79±0.04	0.88±0.05	0.75±0.02	0.72±0.02	0.69±0.01	0.71±0.01	0.68±0.01	0.75±0.04	0.69±0.02	1.10±0.04	0.85±0.01	1.06±0.08	0.82±0.04	0.93±0.09	0.78±0.04	0.72±0.01	0.68±0.01	1.05±0.07	0.82±0.03	1.10±0.08	0.84±0.03
	20	1.03±0.02	0.81±0.01	0.89±0.04	0.76±0.02	0.74±0.02	0.70±0.01	0.72±0.03	0.68±0.02	0.77±0.02	0.70±0.01	1.13±0.02	0.85±0.01	1.13±0.04	0.85±0.02	0.94±0.09	0.78±0.04	0.76±0.02	0.70±0.01	1.07±0.10	0.83±0.04	1.10±0.09	0.84±0.04
$\alpha = 0.4$	3	0.90±0.06	0.76±0.03	0.87±0.04	0.75±0.02	0.76±0.02	0.70±0.01	0.72±0.02	0.69±0.01	0.74±0.01	0.69±0.01	0.97±0.04	0.79±0.02	1.16±0.08	0.87±0.04	0.92±0.08	0.77±0.04	0.73±0.01	0.69±0.01	1.06±0.05	0.82±0.02	1.10±0.11	0.84±0.05
	5	1.00±0.02	0.80±0.01	0.87±0.03	0.75±0.02	0.74±0.02	0.70±0.01	0.71±0.01	0.68±0.01	0.71±0.02	0.68±0.01	1.07±0.07	0.83±0.03	1.11±0.07	0.84±0.03	0.92±0.03	0.77±0.02	0.75±0.01	0.70±0.01	1.16±0.06	0.86±0.03	1.09±0.03	0.84±0.01
	10	1.00±0.08	0.80±0.04	0.85±0.05	0.74±0.02	0.72±0.02	0.69±0.01	0.71±0.01	0.68±0.01	0.73±0.01	0.69±0.01	1.03±0.06	0.81±0.03	1.02±0.07	0.80±0.03	0.88±0.04	0.75±0.02	0.73±0.02	0.69±0.01	1.11±0.08	0.85±0.04	1.06±0.07	0.82±0.03
	20	1.06±0.09	0.82±0.04	0.83±0.04	0.73±0.02	0.77±0.02	0.71±0.01	0.74±0.02	0.69±0.01	0.75±0.02	0.70±0.01	1.09±0.10	0.83±0.04	1.06±0.08	0.83±0.04	0.92±0.02	0.78±0.01	0.72±0.02	0.68±0.01	1.03±0.04	0.81±0.02	1.10±0.07	0.84±0.04
$\alpha = 0.5$	3	0.85±0.03	0.74±0.01	0.83±0.03	0.73±0.01	0.72±0.02	0.69±0.01	0.74±0.04	0.69±0.02	0.77±0.02	0.70±0.01	1.04±0.07	0.82±0.03	1.07±0.07	0.83±0.03	1.00±0.05	0.80±0.02	0.74±0.04	0.69±0.02	1.13±0.09	0.85±0.04	1.10±0.04	0.84±0.01
	5	1.06±0.08	0.82±0.04	0.87±0.02	0.75±0.01	0.75±0.02	0.70±0.01	0.73±0.02	0.69±0.01	0.76±0.02	0.70±0.01	1.09±0.05	0.83±0.02	1.07±0.03	0.83±0.02	0.96±0.10	0.79±0.05	0.72±0.01	0.68±0.00	1.09±0.07	0.84±0.03	1.10±0.08	0.84±0.03
	10	1.02±0.05	0.81±0.02	0.86±0.04	0.75±0.02	0.73±0.01	0.69±0.01	0.69±0.01	0.67±0.00	0.72±0.02	0.68±0.01	1.07±0.08	0.83±0.03	1.10±0.07	0.84±0.03	0.87±0.04	0.75±0.02	0.70±0.01	0.67±0.01	1.14±0.07	0.85±0.02	1.06±0.09	0.82±0.03
	20	1.05±0.03	0.82±0.01	0.89±0.05	0.76±0.02	0.74±0.01	0.70±0.01	0.72±0.02	0.68±0.01	0.76±0.01	0.70±0.01	1.08±0.04	0.83±0.02	1.06±0.09	0.82±0.04	0.92±0.05	0.78±0.02	0.74±0.02	0.70±0.01	1.12±0.07	0.85±0.02	1.12±0.03	0.85±0.01
$\alpha = 0.6$	3	1.05±0.09	0.82±0.04	0.87±0.05	0.74±0.02	0.74±0.03	0.70±0.01	0.70±0.03	0.67±0.02	0.75±0.03	0.70±0.02	1.04±0.04	0.81±0.02	1.13±0.09	0.85±0.04	1.02±0.08	0.81±0.03	0.77±0.02	0.71±0.01	1.13±0.11	0.85±0.05	1.15±0.10	0.86±0.03
	5	0.96±0.06	0.78±0.02	0.86±0.04	0.74±0.02	0.72±0.01	0.69±0.01	0.70±0.02	0.67±0.01	0.77±0.02	0.71±0.01	0.99±0.08	0.79±0.04	1.07±0.03	0.83±0.02	0.91±0.09	0.76±0.04	0.72±0.02	0.69±0.01	1.08±0.06	0.83±0.03	1.12±0.06	0.85±0.03
	10	1.07±0.07	0.83±0.03	0.87±0.03	0.75±0.01	0.70±0.02	0.68±0.01	0.71±0.02	0.68±0.01	0.73±0.01	0.69±0.01	1.07±0.05	0.83±0.03	1.02±0.07	0.80±0.03	0.85±0.02	0.74±0.01	0.71±0.01	0.68±0.00	1.15±0.12	0.86±0.05	1.11±0.06	0.85±0.03
	20	1.02±0.06	0.81±0.03	0.87±0.02	0.75±0.01	0.76±0.01	0.70±0.00	0.72±0.02	0.68±0.01	0.74±0.02	0.69±0.01	1.13±0.04	0.85±0.02	1.11±0.08	0.84±0.04	0.95±0.03	0.79±0.01	0.74±0.01	0.69±0.01	1.14±0.09	0.86±0.03	1.13±0.04	0.85±0.01
$\alpha = 0.7$	3	0.90±0.06	0.76±0.03	0.86±0.04	0.74±0.02	0.74±0.02	0.70±0.01	0.75±0.03	0.70±0.01	0.70±0.02	0.67±0.01	1.06±0.09	0.82±0.04	1.12±0.06	0.85±0.03	1.05±0.06	0.82±0.02	0.69±0.01	0.67±0.01	1.20±0.08	0.88±0.04	1.12±0.09	0.85±0.04
	5	0.95±0.05	0.78±0.02	0.83±0.05	0.73±0.03	0.74±0.03	0.70±0.01	0.70±0.02	0.67±0.01	0.77±0.03	0.71±0.02	1.09±0.05	0.84±0.02	1.13±0.07	0.85±0.03	0.96±0.03	0.79±0.01	0.70±0.02	0.68±0.01	1.03±0.05	0.81±0.02	1.11±0.06	0.85±0.03
	10	1.10±0.10	0.84±0.04	0.87±0.01	0.75±0.01	0.73±0.04	0.69±0.02	0.71±0.02	0.68±0.01	0.74±0.03	0.69±0.01	1.06±0.08	0.83±0.03	1.12±0.06	0.85±0.02	0.98±0.06	0.80±0.03	0.70±0.03	0.67±0.02	1.09±0.09	0.83±0.04	1.07±0.11	0.83±0.05
	20	1.09±0.07	0.84±0.03	0.88±0.03	0.76±0.01	0.74±0.02	0.69±0.01	0.72±0.02	0.68±0.01	0.75±0.01	0.70±0.00	1.08±0.11	0.84±0.05	1.06±0.07	0.82±0.03	0.94±0.08	0.78±0.04	0.73±0.03	0.69±0.01	1.03±0.05	0.81±0.02	1.06±0.07	0.82±0.03
$\alpha = 0.8$	3	0.91±0.02	0.76±0.01	0.92±0.05	0.77±0.02	0.72±0.02	0.69±0.01	0.73±0.01	0.69±0.00	0.71±0.02	0.67±0.01	1.00±0.05	0.80±0.02	1.01±0.09	0.80±0.04	1.02±0.06	0.81±0.02	0.73±0.03	0.69±0.01	1.20±0.09	0.88±0.03	1.08±0.08	0.83±0.03
	5	0.97±0.06	0.79±0.03	0.86±0.02	0.74±0.01	0.72±0.03	0.69±0.01	0.71±0.01	0.68±0.01	0.74±0.03	0.69±0.01	1.07±0.03	0.83±0.01	1.05±0.03	0.82±0.01	1.02±0.04	0.82±0.02	0.75±0.02	0.70±0.01	1.09±0.07	0.84±0.03	1.15±0.13	0.86±0.06</

Table 19. Comprehensive comparison on the Solar dataset. Each cell reports MSE / MAE under different synthetic sample sizes. Our approach achieves strong generalization in periodic solar generation data, demonstrating the effectiveness of frequency domain label loss matching for preserving temporal periodicity.

Models	EDF [2025]	MCT [2025]		DATM [2024]		FTD [2023]		PP [2023]		TESLA [2023]		IDM [2023]		FRPo [2022]		MTT [2022]		KIP [2021]		DC [2021]			
		MSE	MAE	MSE	MAE	MSE	MAE	MSE	MAE	MSE	MAE	MSE	MAE	MSE	MAE	MSE	MAE	MSE	MAE	MSE	MAE		
Solar	3	0.77±0.04	0.71±0.02	0.73±0.02	0.69±0.01	0.84±0.01	0.77±0.02	0.74±0.02	0.74±0.02	0.86±0.01	0.78±0.01	0.80±0.01	0.75±0.01	1.01±0.05	0.83±0.03	0.69±0.03	0.69±0.02	0.73±0.02	0.71±0.02	0.85±0.06	0.74±0.04	0.93±0.08	0.77±0.03
	5	0.78±0.01	0.75±0.02	0.72±0.01	0.69±0.01	0.81±0.02	0.76±0.01	0.84±0.01	0.76±0.01	0.80±0.01	0.76±0.02	0.74±0.01	0.73±0.01	0.94±0.04	0.78±0.02	0.67±0.04	0.66±0.03	0.79±0.02	0.75±0.01	0.90±0.04	0.76±0.03	0.85±0.04	0.76±0.01
	10	0.78±0.02	0.73±0.02	0.71±0.01	0.70±0.02	0.82±0.01	0.78±0.01	0.83±0.02	0.77±0.01	0.84±0.02	0.77±0.01	0.73±0.02	0.71±0.01	1.03±0.08	0.83±0.04	0.77±0.04	0.70±0.02	0.84±0.06	0.77±0.02	1.01±0.05	0.82±0.03	0.89±0.05	0.77±0.03
	20	0.79±0.03	0.74±0.02	0.74±0.01	0.71±0.01	0.79±0.01	0.75±0.01	0.77±0.02	0.73±0.01	0.80±0.01	0.75±0.01	0.82±0.06	0.76±0.02	0.90±0.05	0.76±0.02	0.78±0.03	0.72±0.02	0.80±0.01	0.75±0.01	0.87±0.06	0.76±0.03	0.93±0.02	0.79±0.01
C-1	3	0.64±0.01	0.67±0.01	0.65±0.01	0.65±0.02	0.68±0.01	0.68±0.02	0.67±0.01	0.68±0.01	0.72±0.01	0.69±0.02	0.74±0.02	0.70±0.02	1.05±0.15	0.82±0.06	0.93±0.06	0.77±0.03	0.66±0.06	0.67±0.01	1.05±0.05	0.81±0.03	0.90±0.04	0.78±0.01
	5	0.68±0.02	0.70±0.02	0.61±0.01	0.63±0.00	0.65±0.01	0.67±0.01	0.67±0.01	0.68±0.01	0.65±0.01	0.67±0.01	0.74±0.01	0.73±0.01	0.97±0.03	0.80±0.02	0.79±0.04	0.73±0.02	0.60±0.01	0.64±0.02	1.02±0.05	0.81±0.02	0.92±0.05	0.77±0.02
	10	0.71±0.01	0.71±0.01	0.62±0.01	0.64±0.02	0.67±0.01	0.68±0.02	0.68±0.06	0.69±0.02	0.66±0.01	0.68±0.01	0.72±0.03	0.69±0.02	0.98±0.06	0.81±0.03	0.88±0.06	0.76±0.02	0.62±0.01	0.65±0.01	0.94±0.06	0.78±0.03	0.91±0.04	0.76±0.03
	20	0.75±0.04	0.72±0.02	0.62±0.01	0.64±0.01	0.68±0.01	0.68±0.01	0.68±0.01	0.68±0.01	0.66±0.01	0.68±0.01	0.78±0.04	0.71±0.03	0.95±0.04	0.79±0.03	0.72±0.03	0.69±0.02	0.66±0.01	0.68±0.01	0.89±0.03	0.77±0.02	0.92±0.07	0.77±0.04
C-2	3	0.70±0.01	0.69±0.02	0.67±0.02	0.66±0.00	0.68±0.01	0.68±0.01	0.75±0.02	0.71±0.01	0.71±0.01	0.71±0.01	0.67±0.01	0.67±0.01	1.05±0.12	0.85±0.04	0.77±0.03	0.71±0.03	0.63±0.02	0.66±0.03	0.92±0.06	0.72±0.02	0.92±0.02	0.79±0.01
	5	0.64±0.01	0.66±0.01	0.60±0.02	0.63±0.02	0.66±0.01	0.68±0.01	0.64±0.01	0.66±0.02	0.65±0.02	0.66±0.01	0.70±0.02	0.67±0.02	0.96±0.06	0.81±0.02	0.69±0.02	0.68±0.01	0.64±0.01	0.66±0.02	1.02±0.07	0.80±0.03	0.86±0.05	0.74±0.03
	10	0.77±0.03	0.72±0.01	0.62±0.01	0.65±0.01	0.64±0.02	0.67±0.02	0.65±0.01	0.68±0.02	0.64±0.01	0.67±0.01	0.72±0.04	0.69±0.01	0.87±0.04	0.75±0.02	0.83±0.04	0.75±0.02	0.68±0.01	0.69±0.01	1.00±0.07	0.81±0.03	0.91±0.10	0.77±0.05
	20	0.67±0.01	0.66±0.01	0.65±0.01	0.66±0.01	0.67±0.00	0.69±0.01	0.67±0.01	0.69±0.01	0.67±0.01	0.68±0.01	0.74±0.04	0.69±0.02	0.92±0.07	0.76±0.03	0.77±0.05	0.73±0.04	0.68±0.01	0.69±0.02	0.93±0.06	0.77±0.03	0.93±0.07	0.78±0.03
C-3	3	0.69±0.01	0.68±0.01	0.69±0.01	0.68±0.01	0.64±0.01	0.67±0.01	0.67±0.01	0.68±0.02	0.65±0.01	0.67±0.01	0.70±0.01	0.68±0.01	0.88±0.04	0.73±0.02	0.81±0.03	0.73±0.03	0.68±0.01	0.68±0.01	0.94±0.08	0.80±0.04	0.92±0.03	0.78±0.02
	5	0.76±0.03	0.72±0.02	0.58±0.02	0.63±0.02	0.65±0.01	0.67±0.02	0.66±0.01	0.67±0.02	0.72±0.01	0.70±0.01	0.76±0.05	0.70±0.03	0.90±0.07	0.75±0.02	0.68±0.02	0.66±0.01	0.62±0.01	0.65±0.01	0.93±0.05	0.77±0.03	0.93±0.03	0.79±0.02
	10	0.70±0.02	0.69±0.02	0.63±0.01	0.65±0.01	0.68±0.01	0.68±0.01	0.67±0.01	0.67±0.01	0.66±0.00	0.68±0.02	0.77±0.03	0.73±0.01	0.97±0.07	0.79±0.03	0.75±0.03	0.71±0.03	0.61±0.01	0.64±0.01	0.90±0.04	0.75±0.03	0.89±0.02	0.76±0.01
	20	0.78±0.02	0.72±0.03	0.62±0.02	0.64±0.02	0.66±0.01	0.67±0.01	0.66±0.01	0.68±0.01	0.69±0.01	0.68±0.01	0.74±0.01	0.70±0.02	0.86±0.06	0.76±0.03	0.75±0.06	0.70±0.04	0.67±0.01	0.68±0.01	0.99±0.04	0.81±0.03	0.87±0.03	0.75±0.02
C-4	3	0.70±0.00	0.70±0.01	0.60±0.01	0.63±0.01	0.71±0.01	0.70±0.01	0.63±0.01	0.66±0.02	0.71±0.01	0.71±0.01	0.65±0.01	0.65±0.01	0.84±0.06	0.71±0.03	0.74±0.03	0.72±0.02	0.60±0.02	0.64±0.02	0.98±0.04	0.79±0.03	0.90±0.07	0.76±0.04
	5	0.67±0.01	0.68±0.01	0.66±0.02	0.66±0.02	0.67±0.01	0.69±0.02	0.66±0.01	0.67±0.01	0.66±0.01	0.68±0.01	0.75±0.01	0.70±0.01	0.87±0.05	0.76±0.03	0.77±0.03	0.72±0.02	0.62±0.01	0.64±0.01	0.95±0.03	0.79±0.02	0.91±0.06	0.78±0.03
	10	0.71±0.01	0.70±0.01	0.62±0.01	0.63±0.01	0.68±0.01	0.68±0.01	0.62±0.01	0.66±0.01	0.64±0.01	0.67±0.01	0.75±0.04	0.70±0.03	0.83±0.02	0.72±0.02	0.83±0.04	0.75±0.01	0.64±0.01	0.67±0.02	0.95±0.04	0.79±0.02	0.89±0.02	0.76±0.01
	20	0.74±0.03	0.72±0.03	0.62±0.02	0.63±0.02	0.68±0.01	0.69±0.01	0.69±0.01	0.69±0.01	0.68±0.01	0.68±0.01	0.74±0.03	0.69±0.01	0.85±0.04	0.75±0.02	0.75±0.01	0.72±0.01	0.64±0.01	0.67±0.01	0.88±0.06	0.76±0.03	0.83±0.01	0.73±0.04
C-5	3	0.68±0.02	0.69±0.01	0.65±0.01	0.65±0.02	0.70±0.01	0.70±0.02	0.64±0.02	0.66±0.01	0.64±0.01	0.65±0.01	0.79±0.03	0.72±0.01	1.03±0.04	0.81±0.02	0.77±0.04	0.71±0.03	0.64±0.01	0.65±0.01	0.94±0.03	0.79±0.01	0.93±0.06	0.77±0.02
	5	0.68±0.02	0.70±0.01	0.63±0.01	0.65±0.02	0.68±0.01	0.68±0.01	0.64±0.06	0.66±0.02	0.64±0.00	0.66±0.01	0.71±0.02	0.69±0.01	0.88±0.05	0.74±0.02	0.92±0.06	0.80±0.03	0.63±0.01	0.66±0.02	0.96±0.06	0.80±0.02	0.83±0.03	0.72±0.02
	10	0.71±0.01	0.71±0.01	0.66±0.02	0.65±0.01	0.67±0.01	0.68±0.01	0.64±0.01	0.67±0.01	0.68±0.01	0.67±0.01	0.78±0.03	0.73±0.02	0.95±0.04	0.78±0.03	0.89±0.05	0.78±0.03	0.65±0.01	0.67±0.01	0.93±0.06	0.78±0.03	0.93±0.03	0.77±0.02
	20	0.78±0.03	0.73±0.02	0.63±0.02	0.65±0.02	0.66±0.02	0.67±0.01	0.67±0.01	0.68±0.01	0.65±0.01	0.67±0.02	0.73±0.03	0.69±0.02	0.81±0.03	0.72±0.01	0.71±0.03	0.69±0.02	0.66±0.01	0.69±0.01	0.87±0.05	0.75±0.03	0.89±0.02	0.76±0.00
C-6	3	0.68±0.00	0.68±0.01	0.62±0.01	0.64±0.02	0.70±0.01	0.69±0.01	0.64±0.01	0.67±0.02	0.66±0.01	0.67±0.01	0.74±0.05	0.66±0.03	0.89±0.03	0.74±0.01	0.73±0.02	0.70±0.02	0.68±0.01	0.69±0.02	0.82±0.04	0.72±0.02	0.92±0.06	0.78±0.03
	5	0.68±0.01	0.69±0.01	0.66±0.01	0.65±0.02	0.65±0.01	0.68±0.02	0.63±0.01	0.65±0.01	0.64±0.01	0.66±0.01	0.74±0.02	0.70±0.02	1.04±0.10	0.83±0.05	0.97±0.06	0.80±0.04	0.66±0.01	0.68±0.02	1.03±0.07	0.79±0.03	0.88±0.04	0.76±0.02
	10	0.81±0.03	0.75±0.01	0.63±0.01	0.64±0.01	0.64±0.00	0.66±0.01	0.63±0.01	0.65±0.02	0.66±0.01	0.68±0.01	0.78±0.06	0.71±0.03	0.82±0.04	0.71±0.02	0.82±0.05	0.74±0.03	0.61±0.01	0.64±0.02	0.93±0.05	0.78±0.03	0.89±0.04	0.76±0.02
	20	0.74±0.04	0.70±0.02	0.63±0.01	0.66±0.01	0.67±0.01	0.67±0.01	0.68±0.01	0.69±0.00	0.68±0.01	0.68±0.02	0.78±0.02	0.73±0.01	0.96±0.01	0.80±0.02	0.78±0.05	0.72±0.02	0.66±0.01	0.67±0.01	0.88±0.05	0.76±0.04	0.91±0.05	0.77±0.03
C-7	3	0.68±0.01	0.68±0.01	0.60±0.01	0.63±0.02	0.64±0.01	0.67±0.01	0.66±0.01	0.68±0.01	0.63±0.01	0.66±0.01	0.70±0.02	0.67±0.02	0.71±0.03	0.66±0.03	0.65±0.02	0.66±0.02	0.82±0.02	0.74±0.01	1.00±0.06	0.80±0.03	0.89±0.07	0.74±0.03
	5	0.66±0.01	0.68±0.01	0.61±0.01	0.64±0.02	0.68±0.01	0.68±0.01	0.66±0.01	0.66±0.01	0.69±0.01	0.69±0.01	0.63±0.02	0.64±0.02	1.05±0.08	0.82±0.04	0.89±0.04	0.78±0.02	0.65±0.01	0.68±0.01	0.93±0.04	0.78±0.02	0.80±0.04	0.71±0.02
	10	0.69±0.02	0.69±0.01	0.63±0.01	0.65±0.01	0.63±0.01	0.66±0.01	0.67±0.01	0.68±0.01	0.64±0.00	0.66±0.01	0.77±0.04	0.72±0.02	0.84±0.04	0.75±0.04	0.89±0.08	0.77±0.06	0.63±0.01	0.65±0.02	0.84±0.06	0.73±0.03	0.87±0.03	0.75±0.02
	20	0.74±0.01	0.72±0.01	0.65±0.02	0.65±0.02	0.68±0.00	0.69±0.01	0.67±0.01	0.69±0.01	0.65±0.01	0.67±0.01	0.75±0.02	0.70±0.01	0.98±0.08	0.81±0.04	0.75±0.03	0.71±0.02	0.65±0.01	0.68±0.01	0.93±0.05	0.78±0.03	0.93±0.05	0.78±0.02
C-8	3	0.82±0.04	0.73±0.02	0.64±0.01	0.66±0.01	0.69±0.01	0.68±0.02	0.67±0.01	0.67±0.01	0.70±0.00	0.70±0.02	0.79±0.06	0.71±0.03	1.02±0.03	0.80±0.02	0.70±0.01	0.69±0.01	0.69±0.01	0.67±0.01	0.87±0.04	0.75±0.03	0.89±0.04	0.75±0.03
	5	0.67±0.01	0.68±0.01	0.60±0.02	0.63±0.02	0.64±0.01	0.66±0.02	0.64±0.01	0.65±0.02	0.62±0.01	0.65±0.01	0.63±0.01	0.64±0.01	0.91±0.07	0.75±0.03	0.95±0.06	0.79±0.02	0.67±0.01	0.68±0.02	0.96±0.06	0.79±0.02	0.93±0.03	0.78±0.03
	10	0.77±0.02	0.73±0.02	0.62±0.01	0.63±																		

Table 20. Comparison of dataset distillation methods on the **Exchange** dataset. The table reports **MSE** and **MAE** under different synthetic sample sizes ($S = 3, 5, 10, 20$). Our frequency domain label loss alignment method achieves consistently lower errors and higher proportions of top-ranked (Best/Second) results across settings, confirming its robustness in capturing financial temporal dynamics.

Models	EDF [2025]		MCT [2025]		DATM [2024]		FTD [2023]		PP [2023]		TESLA [2023]		IDM [2023]		FRPo [2022]		MTT [2022]		KIP [2021]		DC [2021]		
	MSE	MAE	MSE	MAE	MSE	MAE	MSE	MAE	MSE	MAE	MSE	MAE	MSE	MAE	MSE	MAE	MSE	MAE	MSE	MAE	MSE	MAE	
Exchange	3	0.90±0.05	0.79±0.03	1.01±0.11	0.81±0.05	0.83±0.03	0.77±0.02	0.98±0.06	0.83±0.03	0.72±0.03	0.71±0.01	0.91±0.15	0.77±0.06	1.20±0.08	0.88±0.03	1.10±0.24	0.85±0.09	0.66±0.05	0.68±0.03	0.95±0.06	0.78±0.03	1.28±0.09	0.93±0.04
	5	0.96±0.03	0.83±0.01	0.93±0.12	0.77±0.06	1.04±0.08	0.86±0.03	0.86±0.05	0.78±0.02	1.00±0.08	0.84±0.03	0.89±0.12	0.75±0.05	1.28±0.17	0.91±0.06	1.02±0.07	0.82±0.03	0.60±0.02	0.64±0.01	0.92±0.09	0.76±0.04	1.20±0.18	0.88±0.06
	10	0.74±0.03	0.72±0.01	1.10±0.12	0.85±0.05	0.71±0.03	0.71±0.01	0.72±0.06	0.71±0.03	0.66±0.04	0.68±0.03	1.01±0.07	0.82±0.03	1.32±0.09	0.91±0.03	1.00±0.12	0.82±0.05	0.72±0.04	0.71±0.02	0.90±0.09	0.75±0.04	1.16±0.13	0.87±0.04
	20	0.71±0.05	0.70±0.02	0.99±0.12	0.81±0.06	0.71±0.05	0.71±0.03	0.75±0.06	0.73±0.03	0.70±0.06	0.69±0.03	0.97±0.06	0.80±0.03	1.37±0.05	0.93±0.03	0.90±0.07	0.79±0.03	0.70±0.09	0.70±0.05	1.45±0.12	0.96±0.03	1.05±0.20	0.81±0.08
α = 0.1	3	0.82±0.02	0.76±0.01	1.03±0.12	0.81±0.06	0.79±0.06	0.74±0.03	0.59±0.05	0.64±0.03	0.65±0.06	0.67±0.03	1.07±0.09	0.85±0.03	1.54±0.28	0.98±0.10	1.11±0.12	0.86±0.05	0.87±0.08	0.78±0.04	1.33±0.18	0.93±0.07	0.90±0.04	0.74±0.02
	5	0.71±0.04	0.71±0.02	1.00±0.08	0.81±0.04	0.80±0.03	0.76±0.01	0.73±0.03	0.71±0.02	0.64±0.04	0.67±0.03	1.18±0.09	0.88±0.04	1.40±0.22	0.93±0.09	0.96±0.11	0.80±0.04	0.63±0.07	0.66±0.04	0.76±0.05	0.69±0.03	1.04±0.14	0.82±0.06
	10	0.69±0.05	0.70±0.03	1.01±0.11	0.81±0.05	0.67±0.06	0.68±0.03	0.67±0.06	0.69±0.03	0.66±0.02	0.67±0.01	1.18±0.09	0.89±0.03	1.42±0.21	0.95±0.07	0.90±0.06	0.78±0.03	0.72±0.05	0.71±0.02	1.12±0.11	0.84±0.05	1.19±0.08	0.88±0.03
	20	0.68±0.06	0.69±0.04	1.07±0.08	0.83±0.03	0.80±0.06	0.75±0.03	0.69±0.05	0.70±0.03	0.67±0.02	0.68±0.01	1.03±0.10	0.82±0.04	1.18±0.07	0.87±0.03	0.78±0.07	0.73±0.04	0.69±0.08	0.69±0.05	1.31±0.08	0.91±0.03	0.95±0.10	0.79±0.05
α = 0.2	3	0.67±0.02	0.69±0.01	1.05±0.10	0.83±0.05	0.78±0.08	0.75±0.04	0.88±0.04	0.79±0.02	0.57±0.04	0.62±0.03	1.20±0.06	0.90±0.03	0.95±0.19	0.78±0.10	0.92±0.13	0.79±0.05	0.73±0.05	0.71±0.02	1.40±0.17	0.95±0.06	1.30±0.08	0.92±0.03
	5	0.66±0.06	0.68±0.03	1.00±0.10	0.81±0.04	0.78±0.04	0.74±0.02	0.59±0.04	0.65±0.02	0.75±0.04	0.72±0.02	0.89±0.17	0.76±0.08	1.15±0.19	0.87±0.08	1.08±0.19	0.85±0.08	0.60±0.03	0.65±0.01	1.10±0.08	0.83±0.04	1.15±0.13	0.86±0.05
	10	0.68±0.03	0.69±0.01	1.03±0.17	0.83±0.07	0.66±0.04	0.68±0.02	0.59±0.02	0.64±0.01	0.69±0.03	0.70±0.02	0.97±0.13	0.79±0.06	1.00±0.04	0.80±0.03	1.02±0.12	0.82±0.05	0.63±0.05	0.66±0.02	1.35±0.13	0.94±0.06	1.19±0.15	0.87±0.04
	20	0.66±0.06	0.68±0.03	1.06±0.20	0.81±0.01	0.79±0.04	0.75±0.02	0.68±0.05	0.69±0.03	0.69±0.02	0.69±0.01	1.03±0.10	0.81±0.04	1.28±0.15	0.90±0.07	0.70±0.02	0.69±0.01	0.70±0.04	0.70±0.02	1.38±0.14	0.93±0.06	1.04±0.11	0.82±0.05
α = 0.3	3	0.63±0.05	0.66±0.03	1.03±0.13	0.83±0.05	0.75±0.06	0.73±0.03	0.78±0.07	0.74±0.04	0.68±0.07	0.68±0.04	0.87±0.10	0.74±0.04	0.98±0.09	0.80±0.04	0.96±0.16	0.79±0.07	0.69±0.07	0.70±0.03	1.43±0.21	0.97±0.08	1.15±0.19	0.85±0.07
	5	0.60±0.02	0.65±0.02	0.98±0.11	0.81±0.04	0.63±0.05	0.66±0.03	0.60±0.05	0.65±0.03	0.71±0.05	0.71±0.03	1.01±0.11	0.82±0.04	1.19±0.22	0.87±0.09	0.95±0.10	0.80±0.04	0.78±0.06	0.74±0.03	1.26±0.14	0.90±0.06	1.20±0.16	0.89±0.07
	10	0.64±0.02	0.67±0.01	1.06±0.06	0.83±0.02	0.70±0.05	0.70±0.03	0.58±0.03	0.64±0.01	0.68±0.02	0.69±0.01	0.99±0.05	0.80±0.03	1.09±0.15	0.84±0.07	0.97±0.06	0.80±0.02	0.59±0.05	0.64±0.03	1.23±0.13	0.88±0.05	1.20±0.17	0.88±0.06
	20	0.70±0.03	0.70±0.01	1.13±0.09	0.85±0.03	0.76±0.03	0.73±0.02	0.65±0.06	0.67±0.03	0.67±0.02	0.69±0.01	1.03±0.17	0.82±0.07	1.21±0.26	0.88±0.11	0.77±0.07	0.74±0.03	0.69±0.02	0.69±0.01	1.18±0.14	0.87±0.06	1.11±0.17	0.84±0.07
α = 0.4	3	0.77±0.07	0.73±0.03	0.92±0.05	0.77±0.02	0.62±0.01	0.66±0.01	0.67±0.01	0.69±0.01	0.76±0.05	0.73±0.02	0.96±0.17	0.79±0.07	0.87±0.03	0.75±0.02	1.11±0.13	0.86±0.06	0.81±0.03	0.76±0.02	1.09±0.13	0.84±0.06	1.07±0.10	0.83±0.05
	5	0.73±0.03	0.72±0.02	1.01±0.08	0.82±0.04	0.77±0.03	0.74±0.02	0.64±0.05	0.67±0.03	0.62±0.04	0.65±0.03	0.93±0.12	0.78±0.05	1.11±0.18	0.84±0.09	1.15±0.14	0.87±0.05	0.67±0.03	0.69±0.01	0.96±0.11	0.77±0.04	1.30±0.28	0.92±0.09
	10	0.68±0.01	0.69±0.01	1.02±0.09	0.82±0.03	0.72±0.04	0.71±0.02	0.59±0.03	0.64±0.02	0.72±0.03	0.71±0.02	0.94±0.13	0.79±0.06	1.33±0.15	0.92±0.06	1.12±0.09	0.85±0.04	0.66±0.02	0.68±0.02	1.11±0.12	0.84±0.04	1.25±0.08	0.90±0.03
	20	0.69±0.02	0.69±0.01	1.12±0.09	0.86±0.03	0.72±0.09	0.71±0.04	0.65±0.03	0.68±0.02	0.67±0.05	0.68±0.04	1.14±0.08	0.87±0.04	1.37±0.13	0.94±0.03	0.77±0.06	0.73±0.04	0.68±0.06	0.69±0.03	1.19±0.17	0.88±0.06	1.22±0.09	0.89±0.03
α = 0.5	3	0.74±0.04	0.72±0.02	1.08±0.12	0.85±0.04	0.71±0.04	0.71±0.02	0.74±0.05	0.72±0.02	0.77±0.04	0.73±0.02	1.07±0.11	0.86±0.04	1.27±0.14	0.89±0.04	0.74±0.04	0.70±0.01	0.63±0.03	0.67±0.01	0.81±0.06	0.72±0.03	1.22±0.21	0.88±0.08
	5	0.61±0.06	0.65±0.03	1.22±0.06	0.90±0.02	0.68±0.04	0.69±0.02	0.66±0.03	0.68±0.02	0.79±0.07	0.74±0.04	0.88±0.17	0.74±0.07	1.20±0.13	0.88±0.05	1.15±0.09	0.86±0.03	0.69±0.05	0.70±0.03	1.00±0.13	0.80±0.07	1.21±0.15	0.88±0.06
	10	0.72±0.05	0.71±0.03	1.15±0.11	0.85±0.05	0.72±0.02	0.71±0.01	0.74±0.05	0.72±0.02	0.62±0.04	0.65±0.02	1.03±0.07	0.82±0.04	1.00±0.13	0.79±0.05	1.03±0.09	0.82±0.04	0.69±0.04	0.69±0.02	1.13±0.13	0.84±0.05	1.26±0.21	0.90±0.07
	20	0.66±0.04	0.68±0.03	1.23±0.23	0.89±0.05	0.75±0.04	0.73±0.02	0.68±0.05	0.69±0.03	0.73±0.08	0.71±0.04	0.98±0.14	0.81±0.06	1.26±0.13	0.89±0.05	0.80±0.07	0.74±0.03	0.71±0.05	0.71±0.03	1.33±0.18	0.92±0.06	1.21±0.10	0.89±0.04
α = 0.6	3	0.75±0.05	0.73±0.02	0.96±0.17	0.78±0.07	0.75±0.04	0.73±0.02	0.66±0.02	0.68±0.01	0.78±0.05	0.74±0.02	1.07±0.06	0.85±0.02	1.37±0.15	0.92±0.05	1.23±0.06	0.90±0.03	0.81±0.05	0.75±0.02	1.13±0.08	0.85±0.03	0.79±0.06	0.69±0.04
	5	0.63±0.03	0.67±0.02	1.21±0.20	0.89±0.05	0.75±0.04	0.73±0.02	0.66±0.03	0.68±0.02	0.63±0.04	0.66±0.03	0.93±0.11	0.76±0.06	1.07±0.12	0.82±0.05	1.25±0.14	0.91±0.05	0.71±0.06	0.70±0.03	1.14±0.14	0.85±0.05	1.13±0.14	0.86±0.06
	10	0.71±0.04	0.71±0.02	1.02±0.13	0.82±0.06	0.70±0.07	0.70±0.04	0.54±0.02	0.62±0.01	0.85±0.10	0.77±0.05	1.06±0.11	0.84±0.04	1.15±0.07	0.85±0.03	0.92±0.18	0.78±0.09	0.68±0.03	0.69±0.02	1.01±0.08	0.79±0.04	1.13±0.15	0.85±0.07
	20	0.70±0.05	0.70±0.02	1.17±0.12	0.88±0.05	0.80±0.04	0.75±0.02	0.67±0.07	0.69±0.04	0.71±0.02	0.70±0.01	1.10±0.15	0.85±0.06	1.36±0.18	0.94±0.06	0.90±0.06	0.78±0.03	0.64±0.02	0.67±0.01	1.10±0.10	0.83±0.05	1.21±0.23	0.87±0.08
α = 0.7	3	0.65±0.06	0.67±0.03	1.27±0.10	0.92±0.04	0.68±0.04	0.68±0.02	0.66±0.02	0.68±0.01	0.70±0.04	0.69±0.02	0.94±0.14	0.78±0.05	0.92±0.13	0.75±0.07	0.98±0.12	0.81±0.05	0.78±0.07	0.74±0.04	1.15±0.10	0.86±0.05	1.16±0.03	0.87±0.01
	5	0.83±0.06	0.77±0.03	1.07±0.10	0.83±0.05	0.82±0.06	0.76±0.03	0.72±0.06	0.71±0.03	0.70±0.02	0.70±0.01	1.04±0.14	0.82±0.06	1.22±0.06	0.89±0.03	1.05±0.16	0.82±0.06	0.58±0.06	0.63±0.03	1.15±0.07	0.86±0.03	1.25±0.10	0.90±0.03
	10	0.68±0.05	0.69±0.03	1.01±0.07	0.80±0.03	0.81±0.03	0.76±0.01	0.61±0.04	0.65±0.02	0.70±0.06	0.69±0.03	0.94±0.18	0.78±0.08	1.21±0.13	0.88±0.05	1.10±0.19	0.84±0.07	0.66±0.06	0.68±0.03	0.90±0.07	0.76±0.03	0.94±0.12	0.77±0.06
	20	0.68±0.02	0.69±0.01	1.01±0.12	0.81±0.05	0.71±0.03	0.71±0.02	0.65±0.05	0.68±0.03	0.71±0.04	0.70±0.02	1.09±0.09	0.84±0.03	1.44±0.11	0.95±0.04	0.84±0.04	0.76±0.01	0.65±0.02	0.68±0.01	1.16±0.21	0.86±0.09	1.21±0.15	0.88±0.06
α = 0.8	3	0.67±0.05	0.68±0.03	1.00±0.12	0.80±0.06	0.73±0.03	0.72±0.01	0.69±0.06	0.70±0.03	0.65±0.04	0.68±0.02	0.90±0.10	0.76±0.05	1.44±0.16	0.96±0.06	1.08±0.14	0.84±0.05	0.66±0.03	0.69±0.01	1.33±0.13	0.93±0.04	1.18±0.09	0.88±0.03
	5	0.69±0.03	0.70±0.02	1.02±0.05	0.82±0.03	0.78±0.03	0.75±0.02	0.60±0.03	0.65±0.02	0.72±0.03	0.71±0.01	0.96±0.11	0.78±0.04	1.09±0.13	0.83±0.05	0.83±0.06	0.74±0.03	0.66±0.05	0.68±0.03	1.51±0.17	0.96±0.04	1.24±0.08	0.89±0.03

Table 21. Ablation results of our method on multiple datasets using different distillation baselines.

Models	Metric	EDF [2025]		MCT [2025]		DATM [2024]		FTD [2023]		PP [2023]		MTT [2022]	
		MSE	MAE	MSE	MAE	MSE	MAE	MSE	MAE	MSE	MAE	MSE	MAE
Weather	3	0.50±0.01	0.50±0.01	0.64±0.05	0.57±0.03	0.51±0.01	0.50±0.01	0.53±0.02	0.52±0.02	0.49±0.01	0.49±0.01	0.56±0.01	0.54±0.01
	5	0.59±0.01	0.55±0.01	0.51±0.03	0.49±0.01	0.48±0.02	0.47±0.01	0.55±0.01	0.53±0.01	0.57±0.00	0.54±0.00	0.56±0.01	0.53±0.01
	10	0.51±0.00	0.50±0.00	0.57±0.04	0.53±0.02	0.57±0.01	0.54±0.01	0.52±0.01	0.51±0.01	0.56±0.01	0.53±0.01	0.58±0.01	0.54±0.01
	20	0.50±0.01	0.49±0.01	0.48±0.01	0.48±0.01	0.56±0.01	0.53±0.01	0.52±0.01	0.51±0.01	0.52±0.01	0.51±0.01	0.50±0.01	0.50±0.01
+TFA	3	0.46±0.01	0.48±0.01	0.51±0.02	0.50±0.01	0.39±0.01	0.42±0.01	0.48±0.01	0.49±0.01	0.48±0.00	0.49±0.00	0.47±0.01	0.48±0.01
	5	0.45±0.01	0.46±0.01	0.51±0.01	0.51±0.01	0.39±0.01	0.43±0.01	0.48±0.01	0.49±0.01	0.48±0.01	0.49±0.01	0.48±0.01	0.49±0.01
	10	0.45±0.01	0.47±0.01	0.49±0.02	0.49±0.01	0.38±0.01	0.42±0.01	0.47±0.01	0.48±0.01	0.47±0.00	0.49±0.00	0.48±0.01	0.49±0.01
	20	0.45±0.01	0.47±0.01	0.47±0.02	0.48±0.01	0.37±0.00	0.41±0.01	0.49±0.01	0.50±0.01	0.48±0.01	0.49±0.00	0.47±0.01	0.48±0.01
+ISIB	3	0.43±0.01	0.46±0.01	0.38±0.01	0.42±0.01	0.33±0.01	0.36±0.01	0.41±0.01	0.45±0.01	0.41±0.01	0.44±0.01	0.43±0.01	0.46±0.01
	5	0.45±0.01	0.47±0.01	0.37±0.01	0.41±0.01	0.33±0.01	0.38±0.01	0.37±0.01	0.41±0.01	0.34±0.01	0.39±0.01	0.38±0.01	0.42±0.01
	10	0.45±0.01	0.47±0.01	0.40±0.02	0.44±0.02	0.33±0.01	0.37±0.01	0.39±0.00	0.43±0.01	0.37±0.00	0.41±0.01	0.39±0.01	0.43±0.01
	20	0.46±0.01	0.48±0.01	0.40±0.01	0.43±0.01	0.33±0.01	0.38±0.01	0.37±0.00	0.42±0.00	0.39±0.01	0.43±0.01	0.40±0.00	0.44±0.00
Electricity	3	0.86±0.04	0.74±0.02	0.90±0.03	0.76±0.01	0.86±0.02	0.75±0.01	0.81±0.02	0.73±0.01	0.88±0.02	0.77±0.01	0.80±0.01	0.72±0.01
	5	0.86±0.04	0.74±0.02	0.84±0.06	0.74±0.03	0.81±0.02	0.74±0.01	0.81±0.02	0.73±0.01	0.81±0.03	0.73±0.01	0.82±0.01	0.74±0.00
	10	1.02±0.05	0.81±0.02	0.90±0.03	0.77±0.01	0.84±0.01	0.75±0.01	0.81±0.02	0.73±0.01	0.86±0.02	0.75±0.01	0.80±0.02	0.73±0.01
	20	1.01±0.03	0.81±0.01	0.90±0.03	0.76±0.01	0.86±0.02	0.75±0.01	0.82±0.01	0.73±0.01	0.84±0.03	0.75±0.01	0.81±0.02	0.73±0.01
+TFA	3	0.91±0.02	0.76±0.01	0.92±0.05	0.77±0.02	0.72±0.02	0.69±0.01	0.73±0.01	0.69±0.00	0.71±0.02	0.67±0.01	0.73±0.03	0.69±0.01
	5	0.97±0.06	0.79±0.03	0.86±0.02	0.74±0.01	0.72±0.03	0.69±0.01	0.71±0.01	0.68±0.01	0.74±0.03	0.69±0.01	0.75±0.02	0.70±0.01
	10	1.04±0.08	0.81±0.04	0.83±0.02	0.73±0.01	0.69±0.01	0.67±0.01	0.71±0.02	0.68±0.01	0.75±0.04	0.69±0.02	0.71±0.02	0.68±0.01
	20	1.08±0.04	0.83±0.02	0.86±0.02	0.74±0.01	0.76±0.03	0.71±0.01	0.73±0.03	0.68±0.02	0.76±0.04	0.70±0.02	0.75±0.02	0.70±0.01
-ISIB	3	1.11±0.07	0.84±0.02	0.89±0.05	0.76±0.02	0.73±0.02	0.69±0.01	0.70±0.02	0.67±0.01	0.71±0.02	0.68±0.01	0.70±0.02	0.67±0.01
	5	1.08±0.11	0.83±0.05	0.84±0.03	0.74±0.02	0.73±0.02	0.69±0.01	0.72±0.02	0.69±0.01	0.73±0.02	0.69±0.01	0.70±0.02	0.68±0.01
	10	1.08±0.04	0.83±0.02	0.85±0.03	0.74±0.01	0.71±0.03	0.68±0.01	0.73±0.02	0.69±0.01	0.73±0.03	0.69±0.02	0.71±0.01	0.68±0.01
	20	1.10±0.06	0.84±0.02	0.90±0.06	0.76±0.03	0.72±0.02	0.69±0.01	0.73±0.02	0.69±0.01	0.76±0.03	0.70±0.01	0.77±0.04	0.71±0.02
Solar	3	0.77±0.04	0.71±0.02	0.73±0.02	0.69±0.01	0.84±0.01	0.77±0.02	0.74±0.02	0.74±0.02	0.86±0.01	0.78±0.01	0.73±0.02	0.71±0.02
	5	0.78±0.01	0.75±0.02	0.72±0.01	0.69±0.01	0.81±0.02	0.76±0.01	0.84±0.01	0.76±0.01	0.80±0.01	0.76±0.02	0.79±0.02	0.75±0.01
	10	0.78±0.02	0.73±0.02	0.71±0.01	0.70±0.02	0.82±0.01	0.78±0.01	0.83±0.02	0.77±0.01	0.84±0.02	0.77±0.01	0.84±0.01	0.77±0.01
	20	0.79±0.03	0.74±0.02	0.74±0.01	0.71±0.01	0.79±0.01	0.75±0.01	0.77±0.02	0.73±0.01	0.80±0.01	0.75±0.01	0.80±0.01	0.75±0.01
+TFA	3	0.82±0.04	0.73±0.02	0.64±0.01	0.66±0.01	0.69±0.01	0.68±0.02	0.67±0.01	0.67±0.01	0.70±0.00	0.70±0.02	0.69±0.01	0.67±0.01
	5	0.67±0.01	0.68±0.01	0.60±0.02	0.63±0.02	0.64±0.01	0.66±0.02	0.64±0.01	0.65±0.02	0.62±0.01	0.65±0.01	0.67±0.01	0.68±0.02
	10	0.77±0.02	0.73±0.02	0.62±0.01	0.63±0.01	0.64±0.01	0.67±0.02	0.65±0.01	0.67±0.01	0.64±0.00	0.66±0.01	0.63±0.01	0.66±0.01
	20	0.75±0.03	0.72±0.02	0.68±0.01	0.67±0.01	0.67±0.01	0.69±0.01	0.64±0.01	0.66±0.01	0.66±0.01	0.68±0.01	0.65±0.01	0.67±0.01
+ISIB	3	0.82±0.03	0.75±0.01	0.64±0.01	0.64±0.01	0.56±0.01	0.61±0.01	0.50±0.01	0.58±0.02	0.60±0.01	0.63±0.02	0.65±0.00	0.66±0.01
	5	0.81±0.02	0.73±0.01	0.60±0.01	0.61±0.01	0.52±0.01	0.58±0.01	0.49±0.01	0.57±0.01	0.53±0.01	0.59±0.01	0.57±0.01	0.61±0.01
	10	0.77±0.04	0.71±0.02	0.58±0.00	0.60±0.01	0.57±0.01	0.62±0.02	0.48±0.01	0.55±0.02	0.58±0.00	0.61±0.02	0.53±0.01	0.59±0.01
	20	0.82±0.05	0.72±0.01	0.64±0.01	0.63±0.01	0.56±0.01	0.60±0.01	0.58±0.00	0.62±0.01	0.56±0.01	0.61±0.01	0.59±0.01	0.62±0.01
Exchange	3	0.90±0.05	0.79±0.03	1.01±0.11	0.81±0.05	0.83±0.03	0.77±0.02	0.98±0.06	0.83±0.03	0.72±0.03	0.71±0.01	0.66±0.05	0.68±0.03
	5	0.96±0.03	0.83±0.01	0.93±0.12	0.77±0.06	1.04±0.08	0.86±0.03	0.86±0.05	0.78±0.02	1.00±0.08	0.84±0.03	0.92±0.09	0.76±0.04
	10	0.74±0.03	0.72±0.01	1.10±0.12	0.85±0.05	0.71±0.03	0.71±0.01	0.72±0.06	0.71±0.03	0.66±0.04	0.68±0.03	0.90±0.09	0.75±0.04
	20	0.71±0.05	0.70±0.02	0.99±0.12	0.81±0.06	0.71±0.05	0.71±0.03	0.75±0.06	0.73±0.03	0.70±0.06	0.69±0.03	0.95±0.06	0.78±0.03
+TFA	3	0.67±0.05	0.68±0.03	1.00±0.12	0.80±0.06	0.73±0.03	0.72±0.01	0.69±0.06	0.70±0.03	0.65±0.04	0.68±0.02	0.68±0.03	0.69±0.01
	5	0.69±0.03	0.70±0.02	1.02±0.05	0.82±0.03	0.78±0.03	0.75±0.02	0.60±0.03	0.65±0.02	0.72±0.03	0.71±0.01	0.66±0.05	0.68±0.03
	10	0.68±0.04	0.69±0.02	0.95±0.16	0.78±0.07	0.79±0.04	0.75±0.02	0.61±0.07	0.65±0.04	0.72±0.06	0.71±0.03	0.63±0.06	0.66±0.03
	20	0.71±0.08	0.70±0.04	1.14±0.08	0.86±0.04	0.75±0.05	0.73±0.02	0.67±0.03	0.68±0.02	0.78±0.08	0.74±0.04	0.77±0.04	0.70±0.02
+ISIB	3	0.60±0.06	0.64±0.04	0.93±0.11	0.78±0.05	0.40±0.05	0.52±0.04	0.39±0.04	0.51±0.03	0.30±0.02	0.45±0.01	0.37±0.02	0.51±0.02
	5	0.62±0.03	0.66±0.02	1.09±0.18	0.84±0.08	0.49±0.02	0.58±0.02	0.56±0.04	0.62±0.02	0.61±0.04	0.64±0.02	0.54±0.03	0.60±0.02
	10	0.79±0.06	0.73±0.05	0.95±0.09	0.80±0.04	0.18±0.01	0.35±0.01	0.24±0.02	0.40±0.02	0.44±0.06	0.55±0.05	0.40±0.03	0.52±0.02
	20	0.84±0.08	0.75±0.04	1.13±0.04	0.86±0.02	0.42±0.02	0.54±0.01	0.38±0.05	0.50±0.04	0.46±0.02	0.56±0.01	0.47±0.04	0.56±0.02

Table 22. Runtime and GPU memory comparison of baseline and ours across all frameworks and datasets.

Dataset	Framework	Num_Samples	Mode	Runtime (s)	Max GPU Memory (MB)
ETTh1	EDF	5	baseline	73	637
ETTh1	EDF	5	ours	76	645
ETTh1	MCT	5	baseline	63	637
ETTh1	MCT	5	ours	70	645
ETTh1	DC	5	baseline	257	637
ETTh1	DC	5	ours	228	645
ETTh1	MTT	5	baseline	77	637
ETTh1	MTT	5	ours	77	645
ETTh1	FTD	5	baseline	74	637
ETTh1	FTD	5	ours	77	645
ETTh1	DATM	5	baseline	77	637
ETTh1	DATM	5	ours	73	645
ETTh1	IDM	5	baseline	56	659
ETTh1	IDM	5	ours	59	669
ETTh1	KIP	5	baseline	35	703
ETTh1	KIP	5	ours	45	711
ETTh1	FRPo	5	baseline	264	703
ETTh1	FRPo	5	ours	231	711
ETTh1	TESLA	5	baseline	75	637
ETTh1	TESLA	5	ours	77	645
ETTh1	PP	5	baseline	71	637
ETTh1	PP	5	ours	73	645
ETTm1	EDF	5	baseline	72	657
ETTm1	EDF	5	ours	77	665
ETTm1	MCT	5	baseline	65	657
ETTm1	MCT	5	ours	59	665
ETTm1	DC	5	baseline	356	657
ETTm1	DC	5	ours	300	665
ETTm1	MTT	5	baseline	71	657
ETTm1	MTT	5	ours	78	665
ETTm1	FTD	5	baseline	74	657
ETTm1	FTD	5	ours	77	665
ETTm1	DATM	5	baseline	73	657
ETTm1	DATM	5	ours	77	665
ETTm1	IDM	5	baseline	87	683
ETTm1	IDM	5	ours	85	691
ETTm1	KIP	5	baseline	36	723
ETTm1	KIP	5	ours	48	731
ETTm1	FRPo	5	baseline	363	723
ETTm1	FRPo	5	ours	312	731
ETTm1	TESLA	5	baseline	75	657
ETTm1	TESLA	5	ours	69	665
ETTm1	PP	5	baseline	70	657
ETTm1	PP	5	ours	59	665
Electricity	EDF	5	baseline	73	965
Electricity	EDF	5	ours	77	989
Electricity	MCT	5	baseline	62	965
Electricity	MCT	5	ours	69	991
Electricity	DC	5	baseline	292	965
Electricity	DC	5	ours	250	991
Electricity	MTT	5	baseline	75	965
Electricity	MTT	5	ours	81	991
Electricity	FTD	5	baseline	77	965
Electricity	FTD	5	ours	81	989
Electricity	DATM	5	baseline	78	965
Electricity	DATM	5	ours	82	991
Electricity	IDM	5	baseline	63	2205
Electricity	IDM	5	ours	66	2231
Electricity	KIP	5	baseline	36	1031
Electricity	KIP	5	ours	51	1057
Electricity	FRPo	5	baseline	300	1031
Electricity	FRPo	5	ours	270	1057
Electricity	TESLA	5	baseline	80	965
Electricity	TESLA	5	ours	82	989
Electricity	PP	5	baseline	75	965
Electricity	PP	5	ours	78	991
Global_Temp	EDF	5	baseline	77	973
Global_Temp	EDF	5	ours	80	1037
Global_Temp	MCT	5	baseline	59	973
Global_Temp	MCT	5	ours	72	1035
Global_Temp	DC	5	baseline	219	997
Global_Temp	DC	5	ours	189	1055
Global_Temp	MTT	5	baseline	76	973
Global_Temp	MTT	5	ours	82	1035
Global_Temp	FTD	5	baseline	81	973
Global_Temp	FTD	5	ours	76	1035

Dataset	Framework	Num_Samples	Mode	Runtime (s)	Max GPU Memory (MB)
Global_Temp	DATM	5	baseline	78	973
Global_Temp	DATM	5	ours	66	1035
Global_Temp	IDM	5	baseline	48	4453
Global_Temp	IDM	5	ours	62	4489
Global_Temp	KIP	5	baseline	35	1041
Global_Temp	KIP	5	ours	51	1101
Global_Temp	FRePo	5	baseline	230	1039
Global_Temp	FRePo	5	ours	199	1099
Global_Temp	TESLA	5	baseline	82	973
Global_Temp	TESLA	5	ours	82	1035
Global_Temp	PP	5	baseline	73	973
Global_Temp	PP	5	ours	74	1035
PEMS03	EDF	5	baseline	77	993
PEMS03	EDF	5	ours	79	1023
PEMS03	MCT	5	baseline	65	993
PEMS03	MCT	5	ours	66	1023
PEMS03	DC	5	baseline	297	993
PEMS03	DC	5	ours	258	1023
PEMS03	MTT	5	baseline	73	993
PEMS03	MTT	5	ours	80	1023
PEMS03	FTD	5	baseline	77	993
PEMS03	FTD	5	ours	81	1023
PEMS03	DATM	5	baseline	74	993
PEMS03	DATM	5	ours	77	1023
PEMS03	IDM	5	baseline	64	2399
PEMS03	IDM	5	ours	68	2403
PEMS03	KIP	5	baseline	35	1059
PEMS03	KIP	5	ours	48	1089
PEMS03	FRePo	5	baseline	299	1059
PEMS03	FRePo	5	ours	263	1089
PEMS03	TESLA	5	baseline	79	993
PEMS03	TESLA	5	ours	81	1023
PEMS03	PP	5	baseline	73	993
PEMS03	PP	5	ours	77	1023
PEMS07	EDF	5	baseline	77	1575
PEMS07	EDF	5	ours	82	1639
PEMS07	MCT	5	baseline	68	1575
PEMS07	MCT	5	ours	71	1637
PEMS07	DC	5	baseline	300	1575
PEMS07	DC	5	ours	262	1637
PEMS07	MTT	5	baseline	78	1577
PEMS07	MTT	5	ours	80	1637
PEMS07	FTD	5	baseline	79	1577
PEMS07	FTD	5	ours	81	1637
PEMS07	DATM	5	baseline	78	1577
PEMS07	DATM	5	ours	80	1637
PEMS07	IDM	5	baseline	65	5673
PEMS07	IDM	5	ours	73	5657
PEMS07	KIP	5	baseline	36	1639
PEMS07	KIP	5	ours	50	1701
PEMS07	FRePo	5	baseline	284	1641
PEMS07	FRePo	5	ours	265	1703
PEMS07	TESLA	5	baseline	77	1577
PEMS07	TESLA	5	ours	82	1637
PEMS07	PP	5	baseline	76	1577
PEMS07	PP	5	ours	80	1637
Solar	EDF	5	baseline	76	875
Solar	EDF	5	ours	79	889
Solar	MCT	5	baseline	64	875
Solar	MCT	5	ours	72	889
Solar	DC	5	baseline	351	879
Solar	DC	5	ours	299	897
Solar	MTT	5	baseline	76	875
Solar	MTT	5	ours	82	889
Solar	FTD	5	baseline	70	875
Solar	FTD	5	ours	79	889
Solar	DATM	5	baseline	77	875
Solar	DATM	5	ours	80	889
Solar	IDM	5	baseline	83	1491
Solar	IDM	5	ours	84	1503
Solar	KIP	5	baseline	35	941
Solar	KIP	5	ours	51	957
Solar	FRePo	5	baseline	358	941
Solar	FRePo	5	ours	311	957
Solar	TESLA	5	baseline	78	875
Solar	TESLA	5	ours	81	891
Solar	PP	5	baseline	75	875
Solar	PP	5	ours	77	889

Dataset	Framework	Num_Samples	Mode	Runtime (s)	Max GPU Memory (MB)
Weather	EDF	5	baseline	78	677
Weather	EDF	5	ours	83	685
Weather	MCT	5	baseline	67	677
Weather	MCT	5	ours	76	685
Weather	DC	5	baseline	349	677
Weather	DC	5	ours	300	687
Weather	MTT	5	baseline	79	677
Weather	MTT	5	ours	81	685
Weather	FTD	5	baseline	76	677
Weather	FTD	5	ours	80	685
Weather	DATM	5	baseline	78	677
Weather	DATM	5	ours	84	685
Weather	IDM	5	baseline	84	755
Weather	IDM	5	ours	86	765
Weather	KIP	5	baseline	37	743
Weather	KIP	5	ours	54	751
Weather	FRPo	5	baseline	360	743
Weather	FRPo	5	ours	312	751
Weather	TESLA	5	baseline	80	677
Weather	TESLA	5	ours	81	685
Weather	PP	5	baseline	91	677
Weather	PP	5	ours	91	685
WindL1	EDF	5	baseline	70	657
WindL1	EDF	5	ours	77	665
WindL1	MCT	5	baseline	65	659
WindL1	MCT	5	ours	66	665
WindL1	DC	5	baseline	335	659
WindL1	DC	5	ours	291	667
WindL1	MTT	5	baseline	76	659
WindL1	MTT	5	ours	74	665
WindL1	FTD	5	baseline	70	659
WindL1	FTD	5	ours	81	665
WindL1	DATM	5	baseline	77	659
WindL1	DATM	5	ours	81	665
WindL1	IDM	5	baseline	76	691
WindL1	IDM	5	ours	77	699
WindL1	KIP	5	baseline	36	723
WindL1	KIP	5	ours	51	731
WindL1	FRPo	5	baseline	347	725
WindL1	FRPo	5	ours	304	731
WindL1	TESLA	5	baseline	80	659
WindL1	TESLA	5	ours	76	665
WindL1	PP	5	baseline	74	659
WindL1	PP	5	ours	79	665
WindL3	EDF	5	baseline	77	657
WindL3	EDF	5	ours	75	665
WindL3	MCT	5	baseline	59	659
WindL3	MCT	5	ours	71	665
WindL3	DC	5	baseline	331	659
WindL3	DC	5	ours	287	667
WindL3	MTT	5	baseline	76	659
WindL3	MTT	5	ours	80	665
WindL3	FTD	5	baseline	76	659
WindL3	FTD	5	ours	82	665
WindL3	DATM	5	baseline	69	659
WindL3	DATM	5	ours	80	665
WindL3	IDM	5	baseline	75	691
WindL3	IDM	5	ours	77	699
WindL3	KIP	5	baseline	36	725
WindL3	KIP	5	ours	50	731
WindL3	FRPo	5	baseline	352	723
WindL3	FRPo	5	ours	289	731
WindL3	TESLA	5	baseline	72	659
WindL3	TESLA	5	ours	78	665
WindL3	PP	5	baseline	75	659
WindL3	PP	5	ours	79	665
ETTh2	EDF	5	baseline	76	637
ETTh2	EDF	5	ours	78	645
ETTh2	MCT	5	baseline	61	637
ETTh2	MCT	5	ours	72	645
ETTh2	DC	5	baseline	265	637
ETTh2	DC	5	ours	223	645
ETTh2	MTT	5	baseline	77	637
ETTh2	MTT	5	ours	83	645
ETTh2	FTD	5	baseline	75	637
ETTh2	FTD	5	ours	82	645
ETTh2	DATM	5	baseline	74	637
ETTh2	DATM	5	ours	81	645

Dataset	Framework	Num_Samples	Mode	Runtime (s)	Max GPU Memory (MB)
ETTh2	IDM	5	baseline	54	661
ETTh2	IDM	5	ours	53	669
ETTh2	KIP	5	baseline	35	703
ETTh2	KIP	5	ours	48	711
ETTh2	FRePo	5	baseline	262	703
ETTh2	FRePo	5	ours	237	711
ETTh2	TESLA	5	baseline	72	637
ETTh2	TESLA	5	ours	81	645
ETTh2	PP	5	baseline	75	637
ETTh2	PP	5	ours	79	645
ETTm2	EDF	5	baseline	77	657
ETTm2	EDF	5	ours	81	665
ETTm2	MCT	5	baseline	65	657
ETTm2	MCT	5	ours	73	665
ETTm2	DC	5	baseline	360	657
ETTm2	DC	5	ours	302	665
ETTm2	MTT	5	baseline	76	657
ETTm2	MTT	5	ours	79	665
ETTm2	FTD	5	baseline	77	657
ETTm2	FTD	5	ours	77	665
ETTm2	DATM	5	baseline	76	657
ETTm2	DATM	5	ours	80	665
ETTm2	IDM	5	baseline	87	683
ETTm2	IDM	5	ours	84	691
ETTm2	KIP	5	baseline	36	723
ETTm2	KIP	5	ours	51	731
ETTm2	FRePo	5	baseline	364	723
ETTm2	FRePo	5	ours	319	731
ETTm2	TESLA	5	baseline	77	657
ETTm2	TESLA	5	ours	81	665
ETTm2	PP	5	baseline	70	657
ETTm2	PP	5	ours	79	665
ExchangeRate	EDF	5	baseline	73	635
ExchangeRate	EDF	5	ours	78	643
ExchangeRate	MCT	5	baseline	69	635
ExchangeRate	MCT	5	ours	72	643
ExchangeRate	DC	5	baseline	240	635
ExchangeRate	DC	5	ours	207	643
ExchangeRate	MTT	5	baseline	80	635
ExchangeRate	MTT	5	ours	79	643
ExchangeRate	FTD	5	baseline	77	635
ExchangeRate	FTD	5	ours	82	643
ExchangeRate	DATM	5	baseline	76	635
ExchangeRate	DATM	5	ours	80	643
ExchangeRate	IDM	5	baseline	54	665
ExchangeRate	IDM	5	ours	55	673
ExchangeRate	KIP	5	baseline	35	701
ExchangeRate	KIP	5	ours	51	709
ExchangeRate	FRePo	5	baseline	233	701
ExchangeRate	FRePo	5	ours	210	709
ExchangeRate	TESLA	5	baseline	75	635
ExchangeRate	TESLA	5	ours	80	643
ExchangeRate	PP	5	baseline	73	635
ExchangeRate	PP	5	ours	75	643
ILI	EDF	5	baseline	74	633
ILI	EDF	5	ours	79	641
ILI	MCT	5	baseline	62	633
ILI	MCT	5	ours	69	641
ILI	DC	5	baseline	199	635
ILI	DC	5	ours	178	641
ILI	MTT	5	baseline	77	633
ILI	MTT	5	ours	77	641
ILI	FTD	5	baseline	76	633
ILI	FTD	5	ours	80	641
ILI	DATM	5	baseline	74	633
ILI	DATM	5	ours	77	641
ILI	IDM	5	baseline	48	655
ILI	IDM	5	ours	50	663
ILI	KIP	5	baseline	5	631
ILI	KIP	5	ours	4	641
ILI	FRePo	5	baseline	5	631
ILI	FRePo	5	ours	6	641
ILI	TESLA	5	baseline	76	633
ILI	TESLA	5	ours	79	641
ILI	PP	5	baseline	70	633
ILI	PP	5	ours	74	641
PEMS04	EDF	5	baseline	74	831
PEMS04	EDF	5	ours	78	859

Dataset	Framework	Num_Samples	Mode	Runtime (s)	Max GPU Memory (MB)
PEMS04	MCT	5	baseline	56	831
PEMS04	MCT	5	ours	72	859
PEMS04	DC	5	baseline	267	841
PEMS04	DC	5	ours	235	881
PEMS04	MTT	5	baseline	77	831
PEMS04	MTT	5	ours	80	859
PEMS04	FTD	5	baseline	65	831
PEMS04	FTD	5	ours	69	859
PEMS04	DATM	5	baseline	77	831
PEMS04	DATM	5	ours	79	859
PEMS04	IDM	5	baseline	58	1987
PEMS04	IDM	5	ours	62	1983
PEMS04	KIP	5	baseline	36	897
PEMS04	KIP	5	ours	52	925
PEMS04	FRePo	5	baseline	275	897
PEMS04	FRePo	5	ours	238	925
PEMS04	TESLA	5	baseline	77	831
PEMS04	TESLA	5	ours	79	859
PEMS04	PP	5	baseline	73	831
PEMS04	PP	5	ours	78	859
PEMS08	EDF	5	baseline	73	785
PEMS08	EDF	5	ours	81	799
PEMS08	MCT	5	baseline	54	785
PEMS08	MCT	5	ours	65	799
PEMS08	DC	5	baseline	266	787
PEMS08	DC	5	ours	215	803
PEMS08	MTT	5	baseline	76	785
PEMS08	MTT	5	ours	82	799
PEMS08	FTD	5	baseline	74	785
PEMS08	FTD	5	ours	67	799
PEMS08	DATM	5	baseline	77	785
PEMS08	DATM	5	ours	81	799
PEMS08	IDM	5	baseline	51	1383
PEMS08	IDM	5	ours	66	1403
PEMS08	KIP	5	baseline	33	851
PEMS08	KIP	5	ours	52	863
PEMS08	FRePo	5	baseline	284	851
PEMS08	FRePo	5	ours	251	867
PEMS08	TESLA	5	baseline	77	785
PEMS08	TESLA	5	ours	81	799
PEMS08	PP	5	baseline	73	785
PEMS08	PP	5	ours	80	799
Traffic	EDF	5	baseline	78	1275
Traffic	EDF	5	ours	81	1331
Traffic	MCT	5	baseline	66	1273
Traffic	MCT	5	ours	62	1331
Traffic	DC	5	baseline	260	1273
Traffic	DC	5	ours	231	1329
Traffic	MTT	5	baseline	76	1273
Traffic	MTT	5	ours	83	1331
Traffic	FTD	5	baseline	79	1273
Traffic	FTD	5	ours	85	1331
Traffic	DATM	5	baseline	66	1273
Traffic	DATM	5	ours	83	1331
Traffic	IDM	5	baseline	60	5315
Traffic	IDM	5	ours	72	5209
Traffic	KIP	5	baseline	36	1339
Traffic	KIP	5	ours	54	1397
Traffic	FRePo	5	baseline	271	1339
Traffic	FRePo	5	ours	229	1395
Traffic	TESLA	5	baseline	80	1273
Traffic	TESLA	5	ours	82	1329
Traffic	PP	5	baseline	92	1273
Traffic	PP	5	ours	92	1331
Wike2000	EDF	5	baseline	79	1029
Wike2000	EDF	5	ours	83	1147
Wike2000	MCT	5	baseline	67	1023
Wike2000	MCT	5	ours	74	1147
Wike2000	DC	5	baseline	194	1103
Wike2000	DC	5	ours	178	1227
Wike2000	MTT	5	baseline	81	1027
Wike2000	MTT	5	ours	80	1147
Wike2000	FTD	5	baseline	81	1027
Wike2000	FTD	5	ours	84	1147
Wike2000	DATM	5	baseline	76	1027
Wike2000	DATM	5	ours	85	1147
Wike2000	IDM	5	baseline	53	7443
Wike2000	IDM	5	ours	66	7567

Dataset	Framework	Num_Samples	Mode	Runtime (s)	Max GPU Memory (MB)
Wike2000	KIP	5	baseline	36	1086
Wike2000	KIP	5	ours	53	1213
Wike2000	FRePo	5	baseline	219	1089
Wike2000	FRePo	5	ours	191	1213
Wike2000	TESLA	5	baseline	81	1027
Wike2000	TESLA	5	ours	84	1147
Wike2000	PP	5	baseline	95	1027
Wike2000	PP	5	ours	88	1147
WindL2	EDF	5	baseline	75	657
WindL2	EDF	5	ours	70	665
WindL2	MCT	5	baseline	54	659
WindL2	MCT	5	ours	63	665
WindL2	DC	5	baseline	335	659
WindL2	DC	5	ours	288	667
WindL2	MTT	5	baseline	77	659
WindL2	MTT	5	ours	79	665
WindL2	FTD	5	baseline	76	659
WindL2	FTD	5	ours	78	665
WindL2	DATM	5	baseline	76	659
WindL2	DATM	5	ours	76	665
WindL2	IDM	5	baseline	75	691
WindL2	IDM	5	ours	77	699
WindL2	KIP	5	baseline	35	725
WindL2	KIP	5	ours	46	731
WindL2	FRePo	5	baseline	344	723
WindL2	FRePo	5	ours	297	731
WindL2	TESLA	5	baseline	76	659
WindL2	TESLA	5	ours	80	665
WindL2	PP	5	baseline	74	659
WindL2	PP	5	ours	75	665
WindL4	EDF	5	baseline	77	657
WindL4	EDF	5	ours	79	665
WindL4	MCT	5	baseline	64	659
WindL4	MCT	5	ours	68	665
WindL4	DC	5	baseline	300	659
WindL4	DC	5	ours	283	667
WindL4	MTT	5	baseline	74	659
WindL4	MTT	5	ours	78	665
WindL4	FTD	5	baseline	75	659
WindL4	FTD	5	ours	79	665
WindL4	DATM	5	baseline	78	659
WindL4	DATM	5	ours	77	665
WindL4	IDM	5	baseline	74	693
WindL4	IDM	5	ours	77	699
WindL4	KIP	5	baseline	35	725
WindL4	KIP	5	ours	54	731
WindL4	FRePo	5	baseline	341	723
WindL4	FRePo	5	ours	301	731
WindL4	TESLA	5	baseline	69	659
WindL4	TESLA	5	ours	80	665
WindL4	PP	5	baseline	73	659
WindL4	PP	5	ours	78	665
Total			ours/baseline total ratio	-2.59%	+2.49%